Title

Parthenolide Covalently Targets and Inhibits Focal Adhesion Kinase in Breast Cancer Cells

Journal

Cell Chemical Biology, 26(7)

ISSN

2451-9456

Authors

Berdan, Charles A

Ho, Raymond

Lehtola, Haley S

et al.

Publication Date

2019-07-01

DOI

10.1016/j.chembiol.2019.03.016

Peer reviewed

HHS Public Access

Author manuscript

Cell Chem Biol. Author manuscript; available in PMC 2020 July 18.

Published in final edited form as:

Cell Chem Biol. 2019 July 18; 26(7): 1027–1035.e22. doi:10.1016/j.chembiol.2019.03.016.

Parthenolide Covalently Targets and Inhibits Focal Adhesion Kinase in Breast Cancer Cells

Charles A. Berdan[1,4], **Raymond Ho**[3], **Haley S. Lehtola**[1], **Milton To**[1], **Xirui Hu**[2], **Tucker R. Huffman**[2], **Yana Petri**[2,4], **Chad R. Altobelli**[2], **Sasha G. Demeulenaere**[2], **James A. Olzmann**[1], **Thomas J. Maimone**[2,4,*], **Daniel K. Nomura**[1,2,3,4,5,*]

[1]Department of Nutritional Sciences and Toxicology, University of California, Berkeley, Berkeley, CA 94720, USA

[2]Department of Chemistry, University of California, Berkeley, Berkeley, CA 94720, USA

[3]Department of Molecular and Cell Biology, University of California, Berkeley, Berkeley, CA 94720, USA

[4]Novartis-Berkeley Center for Proteomics and Chemistry Technologies, University of California, Berkeley, Berkeley, CA 94720, USA

[5]Lead Contact

SUMMARY

Parthenolide, a natural product from the feverfew plant and member of the large family of sesquiterpene lactones, exerts multiple biological and therapeutic activities including anti-inflammatory and anti-cancer effects. Here, we further study the parthenolide mechanism of action using activity-based protein profiling-based chemoproteomic platforms to map additional covalent targets engaged by parthenolide in human breast cancer cells. We find that parthenolide, as well as other related exocyclic methylene lactone-containing sesquiterpenes, covalently modify cysteine 427 of focal adhesion kinase 1 (FAK1), leading to impairment of FAK1-dependent signaling pathways and breast cancer cell proliferation, survival, and motility. These studies reveal a functional target exploited by members of a large family of anti-cancer natural products.

In Brief

We find that parthenolide, as well as other related exocyclic methylene lactone-containing sesquiterpenes, covalently modify cysteine 427 of focal adhesion kinase 1 (FAK1), leading to

*Correspondence: maimone@berkeley.edu (T.J.M.), dnomura@berkeley.edu (D.K.N.).

AUTHOR CONTRIBUTIONS

D.K.N. and C.A.B. conceived the project, contributed intellectually to the project, performed, analyzed, and interpreted experiments and data, and wrote the paper; R.H., H.S.L., M.T., C.R.A., and S.G.D. performed, analyzed, and interpreted experiments and data; X.H., T.R.H., and Y.P. synthesized small molecules described in this project; T.J.M. and J.A.O. analyzed and interpreted experiments and data, contributed intellectually to the project, and assisted in writing the paper.

DECLARATION OF INTERESTS

D.K.N. is a co-founder and scientific adviser for Artris Therapeutics and Frontier Medicines. This study was partially funded by the Novartis Institutes for BioMedical Research and the Novartis-Berkeley Center for Proteomics and Chemistry Technologies.

SUPPLEMENTAL INFORMATION

Supplemental Information can be found online at https://doi.org/10.1016/j.chembiol.2019.03.016.

impairment of FAK1-dependent signaling pathways and breast cancer cell proliferation, survival, and motility.

Graphical Abstract

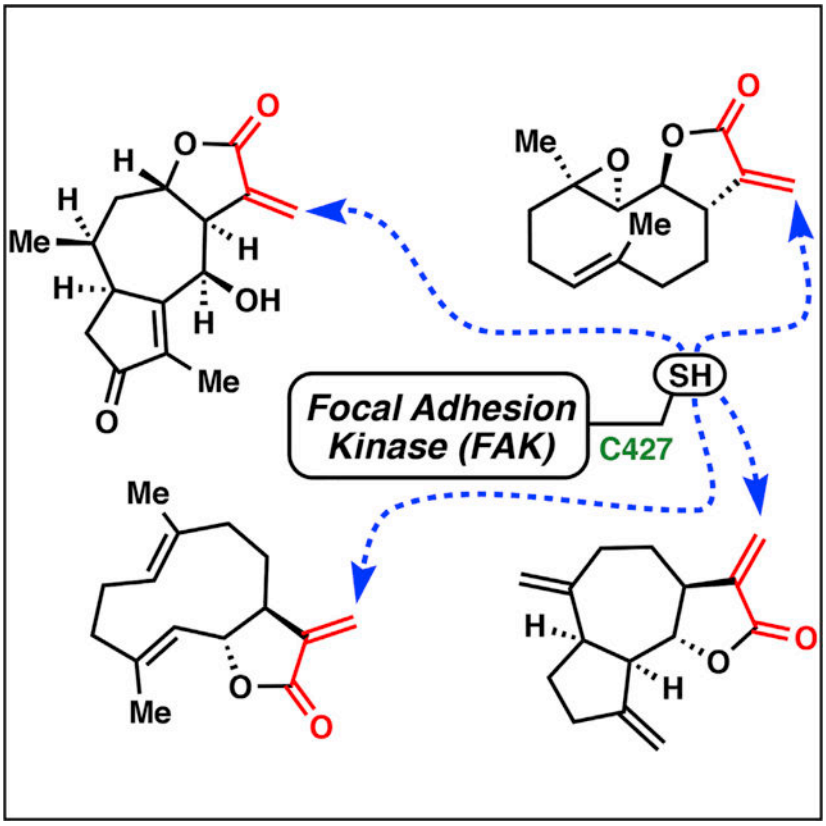

Parthenolide, a natural product found in the feverfew plant (*Tana-cetum parthenium*), possesses myriad therapeutic activities, including anti-inflammatory and anti-cancer effects. Through covalent bond formation between its reactive α-methylene-γ-butyrolactone moiety and various protein targets, multiple cellular signaling pathways are affected (Ghantous et al., 2013; Kwok et al., 2001; Liu et al., 2018a; Mathema et al., 2012; Shin et al., 2017). Moreover, this natural product belongs to the broader family of sesquiterpene lactones (estimated at >5,000 members), many members of which are also cytotoxic and have been hypothesized or shown to act through covalent mechanisms (Coricello et al., 2018; Quintana and Estévez, 2019). Parthenolide impairs cancer pathogenicity or confers chemotherapy or radiation sensitivity across a wide range of cancer types, including leukemia, colorectal, glioblastoma, cervical, liver, prostate, lung, pancreatic, skin, and breast cancers (Anderson and Bejcek, 2008; Carlisi et al., 2016; Diamanti et al., 2013; Jeyamohan et al., 2016; Kim et al., 2012, 2017; Lesiak et al., 2010; Lin et al., 2017; Liu et al., 2017; Morel et al., 2017; Ralstin et al., 2006; Sun et al., 2007; Sweeney et al., 2005). Despite possessing multi-target activity and exhibiting cytotoxicity across a wide range of human cancers, parthenolide is remarkably well tolerated in humans (Curry et al., 2004).

Using a biotinylated parthenolide analog, previous studies by the lab of Crews established that one of the primary targets that drives the anti-inflammatory and anti-cancer activity of parthenolide is IκB kinase β (IKK-β) wherein cysteine 179 (C179) is modified, thus impairing IKK-β and nuclear factor κB (NF-κB) signaling (Kwok et al., 2001). Additional studies have revealed other direct targets of parthenolide that may help to explain the therapeutic properties of this natural product, including targeting of specific cysteines within heat-shock protein Hsp72 and STAT3 downstream signaling targets such as Janus kinases JAK2 (Liu et al., 2018a; Shin et al., 2017). Moreover, this natural product has also been shown to affect additional cell signaling pathways including induction of oxidative stress and apoptosis, focal adhesion kinase 1 (FAK1) signaling, hypoxia-inducible factor 1α signaling, epithelial-to-mesenchymal transition, Wnt/β-catenin signaling, mitogen-activated protein kinase signaling, and mitochondrial function (Carlisi et al., 2011, 2016; Jafari et al., 2018; Kim et al., 2017; Kwok et al., 2001; Lin et al., 2017; Zhang et al., 2017). Based on the broader scope of influence on these biological pathways and systems, parthenolide likely still possesses additional targets that are not yet fully elucidated. In previous works investigating the direct targets of parthenolide, multiple studies have revealed unique ligandable and functional cysteines within their respective proteins that could be targeted to influence cellular signaling and pathogenicity. Recent studies have shown that activity-based protein profiling (ABPP)-based chemoproteomic platforms can be utilized to uncover unique and functional druggable hotspots and modalities, which can be accessed by covalently acting small molecules and natural products that may not be obvious using standard drug-discovery paradigms (Backus et al., 2016; Banerjee et al., 2013; Bateman et al., 2017; Grossman et al., 2017; Hacker et al., 2017; Spradlin et al., 2018; Ward et al., 2018; Weerapana et al., 2010). ABPP uses reactivity-based chemical probes to profile proteome-wide reactive, ligandable, and functional sites directly in complex proteomes. When used in a competitive manner, covalently acting small molecules can be competed against binding of reactivity-based probes to map the proteome-wide targets of these compounds (Backus et al., 2016; Bateman et al., 2017; Grossman et al., 2017; Hacker et al., 2017; Roberts et al., 2017a; Wang et al., 2014). Importantly, this technology allows for the interrogation of natural products in their unmodified form.

In this study, we used ABPP chemoproteomic platforms to map additional targets of parthenolide in breast cancer cells, uncovering additional druggable hotspots that may contribute to the cell signaling and anti-cancer effects of parthenolide (Figure 1A). Parthenolide impaired cell proliferation and serum-free cell motility, and significantly attenuated *in vivo* tumor xenograft growth in estrogen receptor, progesterone receptor, and HER2 receptor-negative breast cancer (triple-negative breast cancer [TNBC]) cells—231MFP or HCC38 cells—in a time-dependent and dose-responsive manner (Figures 1B–1F and S1). The impairment in cell viability induced by parthenolide, evidenced by pro-pidium iodide-positive and annexin-V-positive cells, may be due to various forms of cell death, including apoptosis, necrosis, or ferroptosis. We show that parthenolide leads to the activation of caspase-3/7 and that this cell death is significantly attenuated by the pan-caspase inhibitor Q-VD-OPh, indicating that parthenolide impairs cell viability in a caspase-dependent manner (Figure S1) and suggesting that a portion of the cell death is apoptotic. We note that we are observing anti-tumorigenic effects at a relatively low dose of 30 mg/kg,

despite observing cell-viability impairments at 50-μM concentrations. This may be because of the covalent nature of parthenolide and accumulating target engagement over time. Since parthenolide irreversibly binds to their targets, the targets will stay bound to parthenolide until the protein turns over. TNBCs show the worst prognoses due to the lack of key druggable targets, and there are few targeted therapies (Dawson et al., 2009). Our data suggested that parthenolide may be effective at attenuating TNBC pathogenicity.

We next used ABPP methods to identify additional targets of parthenolide in breast cancer cells. To confirm that parthenolide was not completely non-specific, we first performed a competitive gel-based ABPP experiment in which we competed parthenolide against labeling of 231MFP breast cancer cell proteomes with a rhodamine-functionalized cysteine-reactive iodoacetamide (lA-rhodamine) probe. While this method is imprecise, we observed that parthenolide did not broadly inhibit global proteome-wide cysteine reactivity (Figure S1). Using a more specific, previously reported alkyne-functionalized parthenolide probe (parthenolide-alkyne) (Shin et al., 2017), we observed multiple labeled proteins in 231MFP proteomes, of which some, but not all, targets were competed by parthenolide (Figure S1). Collectively, these results indicated that parthenolide does possess multiple protein targets in 231MFP proteomes but that this natural product is not completely promiscuous in its reactivity.

While the parthenolide-alkyne probe could be used to identify additional targets of this natural product, we sought to map the specific amino acids within these targets that were engaged by unfunctionalized parthenolide. Thus, we next used isotopic tandem orthogonal proteolysis-enabled ABPP (isoTOP-ABPP) to identify specific ligandable sites targeted by parthenolide in 231MFP breast cancer proteomes. We competed parthenolide binding against the broadly cysteine-reactive alkyne-functionalized iodoacetamide probe (iodoacetamide-alkyne [IA-alkyne]) directly in 231MFP TNBC proteomes using previously established methods (Figure 2A and Table S1) (Backus et al., 2016; Bateman et al., 2017; Grossman et al., 2017; Roberts et al., 2017a; Weerapana et al., 2010). This analysis revealed three highly engaged targets of parthenolide that showed isotopically light vehicle-treated to heavy parthenolide-treated probe-modified peptide ratios of greater than 10, indicating >90% engagement of these sites—focal adhesion kinase 1 (FAK1) C427, paraoxonase 3 (PON3) C240, and DNA-protein kinase (DNA-PK or PRKDC) C729. FAK1 C427 was the top target showing the highest ratio, and thus we placed subsequent focus on investigating the role of FAK1-dependent effects of parthenolide in breast cancer cells (Figure 2A and Table S1). While the role of PON3 in cancer cells is unclear, FAK1 and PRKDC are known to be important drivers of cancer cell signaling and DNA repair, respectively. Notably, FAK1 and DNA-PK inhibitors have been shown to impair both cell survival and cell proliferation in cancer cells and are being pursued in the clinic (Helleday et al., 2008; Sulzmaier et al., 2014). Since C427 of FAK1 was the most highly engaged target in this study, we focused our attention on investigating the FAK1-dependent effects of parthenolide in TNBC cells.

We validated the interaction of parthenolide with C427 of FAK1 using several complementary approaches. We first validated the interaction of parthenolide with FAK1, whereby we showed parthenolide prevention of pure human FAK1 kinase domain cysteine reactivity with a rhodamine-functionalized iodoacetamide probe (lA-rhodamine) by gel-

based ABPP (Figure 2A). Based on previous studies, we conjectured that parthenolide reacted covalently with C427 of FAK1 through a homo-Michael addition involving the α/β unsaturated lactone (Figure 2B) (Kwok et al., 2001). Second, we demonstrated that parthenolide covalently reacts with C427 of FAK1 by identifying this parthenolide adduct on human FAK1 kinase domain by liquid chromatography-tandem mass spectrometry (LC-MS/MS) (Figure 2C). We also demonstrated that lA-rhodamine labeling of pure human FAK1 was abrogated in the C427A mutant and that no additional inhibition of remaining lA-rhodamine labeling of FAK1 was observed with parthenolide treatment (Figure 2D). Using a parthenolide-alkyne probe, we further showed that this probe labeled wild-type FAK1 protein, and that this labeling was prevented by parthenolide or in the C427A mutant FAK1 protein (Figure 2E).

Previous studies have shown that FAK1 is amplified or overexpressed across a large fraction of breast tumors wherein FAK1 activity and expression is correlated with poor prognosis. FAK1 has been shown to be important in breast cancer cell survival, proliferation, and migration (Luo and Guan, 2010; Sulzmaier et al., 2014). To determine whether any of the observed parthenolide-mediated proliferative, survival, or migration impairments were dependent on FAK1, we assessed parthenolide effects on these phenotypes under FAK1 knockdown in 231MFP breast cancer cells (Figures 2F and 2G). FAK1 knockdown confers significant resistance to parthenolide-mediated impairments in cell proliferation, serum-free cell survival, and cell migration, particularly at early time points, compared with control cells (Figures 2F and 2G), demonstrating that FAK1 contributes to the anti-cancer effects of parthenolide. Because parthenolide rapidly impairs cell proliferation and survival, we note that the migration phenotypes shown here are likely confounded by reduced cell viability from parthenolide treatment. Interestingly, FAK1 knockdown by small interfering RNA (siRNA) did not impair basal cell proliferation, survival, or migration. We postulate that this lack of effect may be due to either the multi-target polypharmacological nature of parthenolide, or potential adaptation to FAK1 knockdown during the inherently slower process of siRNA-mediated knockdown compared with acute inhibition of FAK1. We later show evidence for the latter hypothesis.

We next sought to determine whether parthenolide functionally inhibits FAK1 activity and signaling. On the basis of previously reported crystal structures of FAK1, C427 resided in a loop region proximal to the ATP site, indicating that covalent modification of this site may be inhibitory (Iwatani et al., 2013). Consistent with this premise, we showed that FAK1 activity was inhibited by parthenolide *in vitro* with pure human FAK1 kinase domain in a substrate activity assay (Figure 2H). While this paper was under revision, an elegant study describing the first structure-guided design, synthesis, and characterization of a FAK1 inhibitor that also covalently targeted C427 of FAK1 and inhibited its function was reported (Yen-Pon et al., 2018). Importantly, this report gives further credence to our hypothesis of the functional relevance of this cysteine and its effects on cancer cell proliferation.

FAK1 is activated through membrane recruitment by growth factors, extracellular matrix, and integrin signaling followed by subsequent autophosphorylation at Y397. This produces an SH2-binding domain, which in turn recruits Src and promotes semi-autophosphorylation of Y576/577 of FAK1. The fully active FAK1/Src complex can now recruit, phosphorylate,

and activate numerous targets including p130Cas/Bcar1 and paxillin (PXN)to drive cell motility and cytoskeletal modifications (Frame et al., 2010; Sulzmaier et al., 2014) (Figure 2I). We show that parthenolide, but not the analog dimethylaminoparthenolide, which lacks a reactive Michael acceptor, impaired multiple components of the FAK1 signaling pathway, including phosphorylation of FAK1 itself, as well as p130Cas and PXN phosphorylation *in situ* in 231MFP breast cancer cells (Figures 2J–2K). While FAK1 knockdown itself did not affect p130Cas and PXN phosphorylation, FAK1 knockdown conferred total resistance to parthenolide-mediated inhibition of p130Cas and PXN phosphorylation observed in siControl 231MFP cells (Figure 2L). These results suggest that the slower or longer knockdown of FAK1 by siRNA leads to a rewiring of FAK1 signaling to maintain p130Cas and PXN activity, but that the acute parthenolide-mediated inhibition of FAK1 signaling is still FAK1 dependent and contributes to the viability and motility impairments observed (Figures 2F and 2G).

Activation of FAK1 has also been shown to recruit phosphatidylinositol 3-kinase (PI3K) to activate AKT/PKC-mediated cell survival pathways (Figure 2F) (Frame et al., 2010; Sulzmaier et al., 2014). While we observed inhibition of AKT phosphorylation with parthenolide treatment, this inhibition was not attenuated in siFAK1 cells and was thus not mediated by parthenolide interactions with FAK1, but rather through interactions with other targets (Figure S2). Consistent with known interaction of parthenolide with IKK-β to inhibit IKK-β and NF-κB signaling (Kwok et al., 2001), NF-κB phosphorylation was inhibited by parthenolide, and this inhibition was also not driven through FAK1 (Figure S1). Nonetheless, our data demonstrate that C427 of FAK1 is both a covalent and functional target of parthenolide that contributes to acute inhibition of specific arms of the FAK1 signaling pathway and the overall anti-cancer effects of parthenolide.

Parthenolide, which belongs to the germacrene family of sesquiterpenes, is just one natural product among hundreds of known sesquiterpene lactones containing the reactive α-methylene-γ-butyrolactone motif (Jackson et al., 2017). Many of these plant metabolites possess notable anti-cancer properties and have been employed in traditional medicine regimes (Ren et al., 2016; Silva Castro et al., 2017). Given the accessibility of C427, we wondered whether other related sesquiterpene lactones can also target this residue. The related germacranolide costunolide and the guaianolide natural product dehydrocostus lactone, which both contain α-methylene-γ-butyrolactone pharmacophores, impaired 231MFP breast cancer cell survival (Figure 3A). On the other hand, the eudesmane-type sesquiterpene natural product α-santonin, which does not contain this reactive functional group, did not impair 231MFP cell survival (Figure 3A). Consistent with these results, parthenolide, costunolide, and dehydrocostus lactone, but not α-santonin, exhibited FAK1 cysteine reactivity as shown by competitive IA-rhodamine labeling of FAK1 (Figure 3B). Moreover, the more highly oxidized guaianolide sesquiterpene mikanokryptin (Hu et al., 2017), which also possesses differing stereochemistry relative to dehydrocostus lactone, also showed FAK1 cysteine reactivity and impaired 231MFP breast cancer cell proliferation and survival (Figures 3C–3E). Taken together, these findings indicate some flexibility in targeting this druggable hotspot with sesquiterpene natural products harboring reactive α-methylene-β-butyrolactone homo-Michael acceptors. We do note, however, that this reactive

cysteine has not been pinpointed in previous target identification studies employing related natural products (Tian et al., 2017).

In accordance with previous findings (Yen-Pon et al., 2018), we also discovered small, fully synthetic covalent binders of FAK C427 via a cysteine-reactive covalent ligand screen using gel-based ABPP against the pure human FAK1 kinase domain (Figure S2 and Table S2). After screening 149 covalent ligands, we found 15 potential hits that impaired IA-rhodamine labeling of FAK1 (Figure S2). We then evaluated these 15 compounds for 231MFP survival and proliferation impairment to identify compounds that gave similar responses to parthenolide. This led us to three promising leads, namely TRH 1–191, TRH 1–23, and TRH 1–171 (Figure S2). We then tested these compounds for FAK1 signaling impairment. While all three impaired Y397 FAK1 phosphorylation in 231MFP cells, TRH 1–191 was superior (Figure S2). We further confirmed that TRH 1–191 impaired FAK1 IA-rhodamine labeling at concentrations comparable with those of parthenolide without causing any artifactual protein precipitation that may arise from non-specific reactivity (Figure S2). While TRH 1–191 is a simple chloroacetamide fragment, we showed that a structurally similar negative control compound TRH 1–189 did not react with FAK1 and had no impact on FAK1 signaling (Figure S2). We also showed the corresponding TRH 1–191 covalent adduct on C427 of FAK1 by LC-MS/MS (Figure S3). TRH 1–191 also inhibited FAK1 activity *in vitro,* with pure FAK1 kinase domain protein and impaired FAK1 signaling *in situ* in 231MFP breast cancer cells (Figure S3). TRH 1–191 may thus represent an additional scaffold for targeting C427 of FAK1 to inhibit FAK1 signaling in cancer cells.

Here, we have used ABPP-based chemoproteomic platforms to identify C427 of FAK1 as a ligandable and functional site targeted by the anti-cancer natural product parthenolide. This target adds further complexity to the polypharmacological landscape of parthenolide, which also includes IKK-β, heat-shock protein Hsp72, and thioredoxin reductase as targets (Duan et al., 2016; Kwok et al., 2001; Shin et al., 2017). Moreover, these findings also implicate a broad array of widely examined natural products as potential FAK impairment agents. Previous studies have shown that parthenolide and other sesquiterpene lactone natural products inhibit the FAK1 signaling pathway, but the mechanism through which parthenolide inhibited this pathway was poorly understood (Kwak et al., 2014; Liu et al., 2018b). Our study indicates that these natural products inhibit FAK1 signaling through targeting C427 of FAK1 to inhibit FAK1 activity and downstream signaling. Our study highlights the utility of using chemoproteomic platforms for discovering unique druggable modalities that are accessed by covalently acting natural products.

STAR★METHODS

CONTACT FOR REAGENT AND RESOURCE SHARING

Further information and requests for resources and reagents should be directed to and will be fulfilled by the Lead Contact, Daniel K. Nomura (dnomura@berkeley.edu).

EXPERIMENTAL MODEL AND SUBJECT DETAILS

Cell Culture—Professor Benjamin Cravatt's group provided the 231MFP cells. The generation of these cells have been described previously (Jessani et al., 2004). HCC38 and HEK293T cells were obtained from American Type Culture Collection (ATCC). These cell lines have not been authenticated. 231MFP cells were cultured in L-15 (HyClone) media supplemented with 10% fetal bovine serum (FBS) (Gibco) and 2 mM glutamine at 37°C and 0% CO_2. HCC38 cells were cultured in RPMI (Gibco) supplemented with 10 % FBS and 2 mM glutamine at 37°C and 5% CO_2. HEK293T cells were cultured in DMEM (Gibco) supplemented with 10 % FBS and 2 mM glutamine at 37°C and 5% CO_2. 231MFP, HCC38, and HEK293T cells are all female in origin.

In Vivo Animal Studies—Animal experiments were conducted in accordance with the guidelines of the Institutional Animal Care and Use Committee (IACUC) of the University of California, Berkeley. Female immune-deficient SCID mice (6–8 weeks old, 20–30 g body weight) purchased from Taconic laboratories were used for tumor xenograft studies. Mice were group housed and fed a standard chow diet. Mice were randomly assigned to experimental groups.

METHOD DETAILS

Chemicals—Parthenolide and dimethylaminoparthenolide were obtained from Cayman Chemicals. Synthesis of the parthenolide-alkyne probe was performed as previously reported (Shin et al., 2017). All other chemicals were obtained from Millipore-Sigma unless otherwise noted. Antibodies were obtained from Cell Signaling Technologies unless otherwise noted. Mikanokryptin was synthesized as previously described (Hu et al., 2017). Synthesis and characterization of cysteine-reactive covalent ligands screened against FAK1 were either described previously or described in Supporting Methods (Bateman et al., 2017; Grossman et al., 2017; Roberts et al., 2017b).

Cell Proliferation and Survival and Migration—Serum-containing cell proliferation and serum-free cell survival were assessed by Hoechst stain as previously described (Grossman et al., 2017; Louie et al., 2016). Briefly, we seeded cells at 1×10^4 and 2×10^4 cells/well, respectively, in 150 μL serum-containing or serum-free media in 96-well plates overnight. The next day, cells were treated with an additional 50 mL of DMSO vehicle or compound-containing media for 24 or 48 h before fixation and staining with 10 % formalin and Hoechst 33342 (Invitrogen) according to manufacturer's protocol. Wells were washed with PBS, and fluorescence was measured using a fluorescent plate reader with an excitation and emission of 350 nm and 461 nm, respectively.

For migration assays, cells (5×10^4) were placed in collagen-coated Transwell chambers (Corning) and incubated in DMSO vehicle or compound-containing serum-free media for 6 h. Migrated cells were fixed and stained with Diff-Quik solution (Dade Behring) and non-migrated cells were removed using a cotton swab. Migrated cells were imaged and counted at 200 x magnification. An average of cells in three fields for one migration chamber represents n=1.

Flow Cytometry Studies—Apoptotic analyses were performed following cell exposure (6 cm plates, 1×10^6 cells) to DMSO vehicle or compound-containing serum-free media using flow cytometry. Briefly, media and trypsinized cells were pelleted by centrifugation at 500 × g for 5 min, washed once in PBS, resuspended in binding buffer (10 mM HEPES/NaOH at pH 7.4, 140 nM NaCl, 2.5 mM $CaCl_2$) containing propidium iodide (BD) and FITC-conjugated Annexin V (BD) and incubated for 15 min. Cells were then diluted with additional binding buffer to a final volume of 0.5 mL and the fluorescence measured using a BD Biosciences LSR Fortessa cytometer. Annexin-V positive, propidium iodide negative cells were considered early apoptotic and Annexin-V positive, propidium iodide positive cells were considered late apoptotic, as previously described (Anderson et al., 2017). Data analysis was performed using FlowJo software and quantified for three biological replicates per condition.

Caspase 3/7 activity was performed using the CellEvent Caspase-3/7 Green Flow Cytometry Assay Kit (Thermo) according to manufacturer's specifications. Cells (1×10^6) were pretreated with DMSO vehicle or 20 μM caspase inhibitor Q-VD-OPh for 1 h and then with DMSO vehicle or compound-containing serum-free media for an additional 4 h. Cells were then harvested and pelleted as described above and then resuspended in 0.5 mL PBS containing 500 nM CellEvent Reagent before incubating for 30 min at 37°C. For the final 5 minutes of incubation, SYTOX AADvanced was added to a final concentration of 1 mM. FlowJo Software was used for data analysis, and the percentage of cells exhibiting active caspase-3/7 was quantified for three biological replicates per condition. A t-test was employed for all statistical analyses.

Tumor Xenograft Studies—C.B17 SCID female mice (6–8 weeks old) were injected subcutaneously in the flank with 231MFP cells (1×10^6 cells) suspended in serum-free media. Mice were exposed via intraperitoneal injection with either vehicle (18:1:1 PBS/ethanol/PEG40) or 30 mg/kg parthenolide once per day starting 2 weeks, respectively, after injection of cancer cells. Tumor size was assessed weekly by caliper measurements.

FAK1 Knockdown—Cells were plated in 6-well plates overnight (2×10^5 cells/well). Cells were then treated with Dharmafect1 reagent (GE) and either nontargeting siRNA oligonucleotide (siControl, D-001810–10-05, GE) or siFAK1 oligonucleotides (L-003164–00, GE) were transfected for 48 h according to manufacturer instructions. Cells were then reseeded for survival and proliferation as described above. Knockdown was confirmed by Western blotting.

Vectors for FAK1 Kinase Expression—The full length FAK1 expression vector was purchased from VectorBuilder (FAK1 sequence NM_005607.4). To express just the kinase domain (AA393–698) Gibson Assembly was performed using the pCMV6-Entry (C-term FLAG + Myc tag) using the primers CTGCCGCCGCGATCGCCatggaaacagatgattatgctgagattataga, TCGAGCGGCCGCGTACGCGTtcttctggactccatcctcatgcgctcttcttgct to amplify the FAK1 kinase domain ORF with desired overlaps, and ACGCGTACGCGGCCG, GGCGATCGCGGCGG to linearize the pCMV6-Entry backbone using a Gibson Assembly Cloning Kit (New England Biolabs) according to manufacturer protocol. To achieve the

C427A mutant, site-directed mutagenesis was performed using Q5 Site-Directed Mutagenesis Kit (New England BioLabs) using the primers ACTTGGACGAGCTATTGGAGAAGGC, TCTATTCTTTCTCTTTGAATCTC according to manufacturer protocol.

Expression of FAK1 C427A Mutant—HEK293T cells were seeded at 30% confluency in 15 cm dishes in 10%. On the day of transfection media was replaced with DMEM containing 2.5 % FBS and 500mL0pti-MEM (Thermo) containing 10mg pCMV6-Entry-FAK1 either control or C427A vector and 50 mg polyethylenimine was added to the plate. 48 h later cells were scraped into 1 mL PBS and pelleted at 2,000 g for 5 min at 4°C and the supernatant removed before freezing at −80°C to achieve cell lysis. Pellets were then resuspended in 500 μL PBS and further lysed by probe tip sonication at 15 % amplitude for 2 × 10 s on ice. Lysates were cleared by centrifugation at 21,000 g for 20 min at 4°C and the resulting supernatant was mixed with 30 mL anti-FLAG resin (Genescript) and rotated at 4°C for 2 h before washing 3 × with 500 μL PBS and subsequent elution of FLAG-tagged proteins with 100 μL of 250 ng/μL 3 × FLAG peptide (APExBIO) in PBS. Resultant peptides were further concentrated and 3 × FLAG peptide removed using Amicon centrifugal filtration devices (Millipore).

Western Blotting—Cells (1×10^6 cells) were plated in 6 cm dishes in complete media the night before experiment. Cells were washed with PBS and placed in DMSO vehicle or compound-containing serum-free media for 2 h before being washed and collected into a lysis buffer containing protease and phosphatase inhibitors. Proteins were separated on a 4–20% Tris-Glycine precast Midi-PROTEAN TGX SDS/PAGE gel (BioRad). Proteins were then transferred to a PVDF membrane using the iBlot system (Invitrogen). Membranes were blocked in 5 % nonfat milk in TBST and incubated in primary antibodies overnight according to manufacturer instructions. Membranes were then washed in TBST and probed with secondary antibody (Li-Cor) and visualized using a fluorescent scanner (Li-Cor). Quantitation was performed using ImageJ.

FAK1 Activity Assay—FAK1 kinase domain (0.1 mg) was preincubated with DMSO vehicle or compound (100 μM) for 30 minutes at room temperature in 5 μL buffer containing 40 mM Tris, 20 mM $MgCl_2$, 2 mM $MnCl_2$, 4% DMSO, pH 7.4. ATP solution (5 μL of a 100 μM solution containing 0.1 μg 4:1 glycine:tyrosine peptide substrate (Promega)) was added and incubated at 37°C for 20 min before the addition of ADP-Glo reagent (5μL) (Promega) for an additional 20 min incubation at room temperature. Kinase detection solution (10 μL) (Promega) was added and incubated for 15 minutes at room temperature and luminescence was measured on a plate reader.

Gel-Based ABPP—Recombinant FAK1 kinase domain was diluted to .002 μg/μL in PBS and 50 μL protein solution was treated with DMSO vehicle or compound for 30 min at room temperature. Samples were then incubated with IA-rhodmaine (1 μM) (Thermo) for 1 h at room temperature in the dark before separating proteins by SDS/PAGE. Probe-labeled proteins were analyzed by in-gel fluorescence using a Bio-Rad gel scanner and fluorescent bands were quantified using Image J.

IsoTOP-ABPP Analysis of Parthenolide Targets—Cell lysate was collected and probe sonicated in PBS before diluting to 4 mg proteome per biological replicate. Samples were then preincubated with DMSO vehicle or parthenolide (50 μM) for 30 minutes at room temperature before labeling of proteomes with iodoacetamide (IA)-alkyne (10 μM) (Chess Organics) for 1 h at room temperature. Isotopically light (control) or heavy (treated) TEV-biotin handles (100 μM) were appended to probe-labeled proteins using CuAAC through sequential addition of tris(2-carboxyethyl) phosphine (1 mM, Sigma), tris[(1-benzyl-1H-1,2,3-triazol-4-yl)methyl]amine (34 mM, Sigma), copper (II), sulfate (1 mM, Sigma), and finally the linker functionalized with a TEV protease recognition sequence along with an isotopically light or heavy valine, and incubated for 1 h at room temperature. Probe-labeled proteins were subsequently mixed in a 1:1 ratio and precipitated by centrifugation at 6500 × g and washed in ice cold methanol, resuspended and washed again and then denatured and resolubilized by heating in 1.2 % SDS/PBS to 80°C for 5 min. Insoluble components were precipitated by centrifugation at 6500 × g and soluble proteome was diluted in 5 mL 0.2 % SDS/PBS before overnight incubation at 4°C with an additional 170 μL resuspended avadin-agarose beads. Bead-linked proteins were then washed three times in PBS and water and then resuspended in 6 M urea/PBS before being reduced in DTT (1 mM, Sigma) and heated to 65C for 20 min, alkylated with iodoacetamide (18 mM, Sigma) and heated to 37°C for 30 min, then washed and resuspended in 2 M urea and trypsinized overnight with 0.5 mg/mL sequencing grade trypsin (Promega) at 37°C. Tryptic peptides were then eluted and the remaining beads were washed three times in PBS and water, once in TEV buffer solution (water, TEV buffer, 100 mM DTT), and resuspended in TEV buffer with Ac-TEV protease and incubated overnight at 29°C. TEV-digested peptides were then isolated, acidified with formic acid (1.2 M, Spectrum), and prepared for LC-MS/MS analysis, as previously described (Grossman et al., 2017; Roberts et al., 2017b).

Proteomic Profiling to Determine Sites of Modification of Parthenolide and TRH 1–191—FAK1 kinase domain (AA393–698) (Promega) (25 μg) was pre-incubated with DMSO vehicle or compound (parthenolide or TRH 1–191) (100 μM) for 30 min at room temperature. Samples were then treated with isotopically light (control) or heavy (treated) iodoacetamide (Iodoacetamide-$^{13}C_2$, 2-d_2, #721328, Millipore-Sigma) for 1 h at room temperature before combination of control and treated samples and subsequent precipitation with 20% trichloroacetic acid for 2 h at −80°C. Proteins were pelleted at 20,000 × *g* and washed with ice cold 10 mM HCl / 90% acetone before resuspension in 60 μL 4 M Urea and 0.5 × ProteaseMax (Promega), vortexed, and then subsequently diluted with an additional 40 μL 100 mM ammonium bicarbonate. Samples were incubated at 60°C for 30 min following the addition of 10 μL 110 mM TCEP, before dilution with 120 μL 0.04 × ProteaseMax and 5 μg/μL sequencing grade trypsin (Promega) in PBS. Samples were digested overnight at 37°C in a rocking incubator before acidification with 12 μL formic acid and storage at −80°C until MS analysis.

MS Analysis—Total peptides from TEV protease digestion for isoTOP-ABPP or tryptic peptides for shotgun proteomics were pressure loaded onto 250 mm tubing packed with Aqua C18 reverse phase resin (Phenomenex) and previously equilibrated using an Agilent 600 series HPLC using gradient from 100% buffer A to 100% buffer B over 10 min,

followed by a 5 min wash with 100% buffer B and a 5 min wash with 100% buffer A. Samples were then attached to an equilibrated 13 cm laser pulled column packed with 10 cm Aqua C18 reverse-phase resin and 3 cm of strong-cation exchange resin using a MicroTee PEEK 360 mm fitting (Thermo Fisher Scientific #p-888), and then analyzed using a Q-Exactive Plus mass spectrometer (Thermo Fisher Scientific) using a Multidimenstional Protein Identification Technology (MudPIT), using 0 %, 25 %, 50 %, 80 %, and 100 % salt bumps of 500 mM aqueous ammonium acetate and a gradient of 5–55 % buffer B in buffer A (buffer A: 95:5 water:acetonitrile, 0.1 % formic acid; buffer B 80:20 acetonitrile:water, 0.1 % formic acid). Data was collected in data-dependent acquisition mode with dynamic exclusion enabled (60 s). One full MS (MS1) scan (400–1800 m/z) was followed by 15 MS2 scans (ITMS) of the nth most abundant ions. Heated capillary temperature was set to 200 C and the nanospray voltage was set to 2.75 kV, as previously described (Grossman et al., 2017; Roberts et al., 2017b).

Data was extracted using Raw Extractor 1.9.9.2 (Scripps Research Institute) in the form of MS1 and MS2 files and was subsequently searched against the Uniprot human database using ProLuCID search methodology in IP2 v.3 (Integrated Proteomics Applications, Inc.) (Xu et al., 2015). For isoTOP-ABPP, peptides were analyzed with a static modification for cysteine carboxyaminomethylation (+57.02146) and differential modifications for light or heavy TEV tags (+464.28596 and +470.29977, respectively) for cysteine, and methionine oxidation, with up to two total modifications per peptide. For proteomic analysis of while FAK1 tryptic digests, peptides were searched with differential modifications for light or heavy iodoacetamide (+57.02146 and +61.04073, respectively) on cysteines, for parthenolide or TRH 1–191 addition (+248.14125 or + 259.04001, respectively) on cysteines, and methionine oxidation, with up to two total modifications per peptide fragment. In both analyses, peptides were required to have at least one tryptic end and in isoTOP-ABPP all fragments must contain the TEV modification. To ensure a peptide false-positive of less than 5% ProLuCID data were filtered through DTASelect prior to downstream analyses (Tabb et al., 2002). Only peptides that were present in at least two out of four biological replicates were interpreted for final quantification and only those peptides with light to heavy ratios >10 that appeared in three out of four biological replicates were considered as targets of parthenolide.

General Synthetic Methods—Chemicals and reagents were purchased from major commercial suppliers and used without further purification. Reactions were performed under a nitrogen atmosphere unless otherwise noted. Silica gel flash column chromatography was performed using EMD or Sigma Aldrich silica gel 60 (230–400 mesh). Proton and carbon nuclear magnetic resonance (^{1}H NMR and ^{13}C NMR) data was acquired on a Bruker AVB 400, AVQ 400, or AV 600 spectrometer at the University of California, Berkeley. High resolution mass spectrum were obtained from the QB3 mass spectrometry facility at the University of California, Berkeley using positive or negative electrospray ionization (+ESI or -ESI). Yields are reported as a single run.

General Procedure A—The amine (1 eq.) was dissolved in DCM (5 mL/mmol) and cooled to 0°C. To the solution was added acryloyl chloride (1.2 eq.) followed by

triethylamine (1.2 eq.). The solution was warmed to room temperature and stirred overnight. The solution was then washed with brine and the crude product was purified by silica gel chromatography (and recrystallization if necessary) to afford the corresponding acrylamide.

General Procedure B—The amine (1 eq.) was dissolved in DCM (5 mL/mmol) and cooled to 0°C. To the solution was added chloroacetyl chloride (1.2 eq.) followed by triethylamine (1.2 eq.). The solution was warmed to room temperature and stirred overnight. The solution was then washed with brine and the crude product was purified by silica gel chromatography (and recrystallization if necessary) to afford the corresponding chloroacetamide.

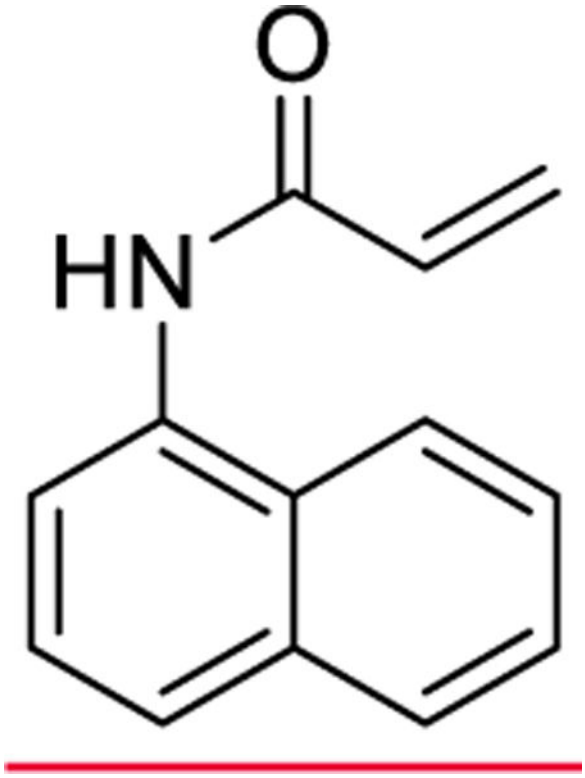

N-(naphthalene-1-yl)acrylamide (TRH-1–57): To a solution of 1-naphthylamine (294 mg, 2.0 mmol) in dichloromethane (10 mL) was added acryloyl chloride (0.20 mL, 2.4 mmol) followed by triethylamine (248 mg, 2.4 mmol) at 0°C under N_2 atmosphere. The reaction mixture was allowed to warm to room temperature and was stirred for 16 hours. The solution was washed twice with brine, and the resulting crude was purified by silica gel chromatography (30% to 40% ethyl acetate in hexanes) and recrystallized from toluene to yield 173 mg of white solid (44% yield).

^{1}HNMR (400MHz, MeOD). δ 7.96–7.94 (m, 1H), 7.88–7.86 (m, 1H), 7.76 (d, *J* = 8.1 Hz, 1H), 7.64 (d, *J* = 7.3 Hz, 1H), 7.52–7.44 (m, 3H), 6.43 (dd, *J* =16.9, 10.4 Hz, 1H), 6.41 (dd, *J* =16.9, 1.5 Hz, 1H), 5.82 (dd, *J* =10.1, 1.0 Hz, 1H).

^{13}C NMR (100MHz, MeOD). δ 167.3, 135.7, 133.9, 132.1, 129.9, 129.4, 128.2, 127.7, 127.3, 127.2, 126.4, 123.8, 123.3.

HRMS (+ESI). Calculated: 198.0913 ($C_{13}H_{12}NO$). Observed: 198.0912.

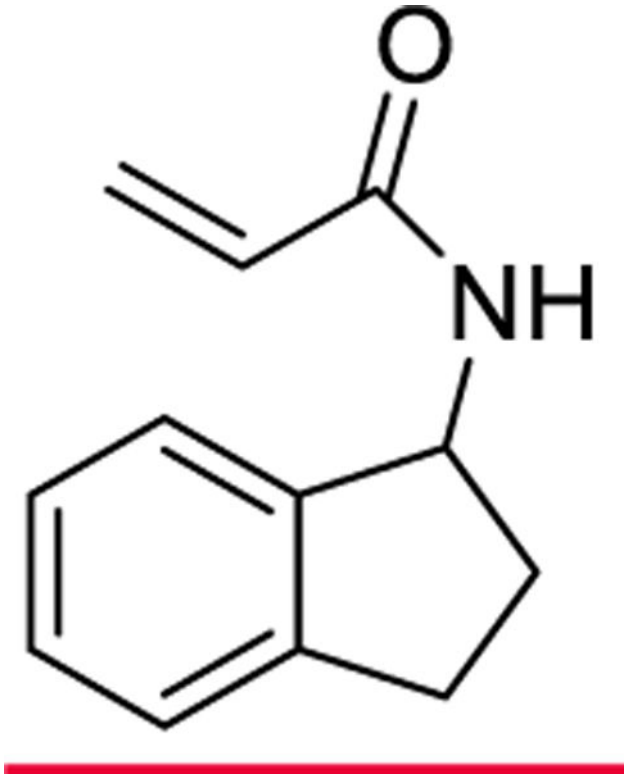

N-(2,3-dihydro-1 H-inden-1-yl)acrylamide (TRH-1–58): To a solution of 1-aminoindan (274 mg, 2.0 mmol) in dichloromethane (10 mL) was added acryloyl chloride (0.20 mL, 2.4 mmol) followed by triethylamine (276 mg, 2.4 mmol) at 0°C under N_2 atmosphere. After stirring for 20 minutes, the reaction mixture was allowed to warm to room temperature and was stirred for 28 hours. The solution was washed twice with brine, and the resulting crude was purified by silica gel chromatography (20%−40% ethyl acetate in hexanes) to yield 238 mg of white solid (62% yield).

^{1}H NMR (400MHz, $CDCI_3$). δ 7.22–7.11 (m, 4H), 6.76 (d, *J* = 7.8 Hz, 1H), 6.23–6.13 (m, 2H), 5.56 (dd, *J* = 3.5, 8.1 Hz, 1H), 5.40 (q, *J* = 7.9 Hz, 1H), 2.95–2.88 (m, 1H), 2.84–2.76 (m, 1H), 2.51–2.43 (m, 1H), 1.83–1.74 (m, 1H).

^{13}C NMR (100MHz, $CDCI_3$). 5 165.5, 143.2, 143.1, 130.9, 127.8,126.6, 126.3, 124.6, 124.0, 54.5, 33.7, 30.2.

HRMS (+ESI). Calculated: 188.1070 (ĈĤNO). Observed: 188.1068.

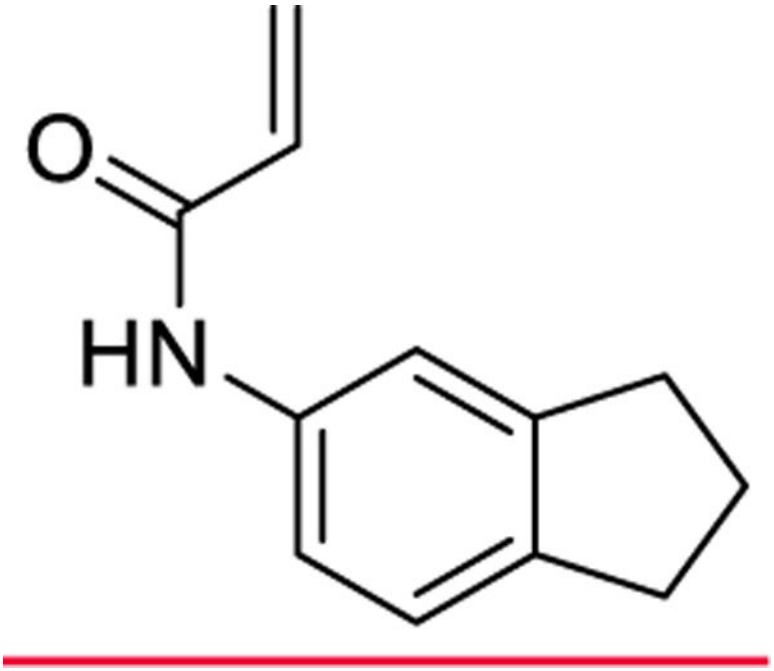

N-(2,3-dihydro-1H-inden-5-yl)acrylamide (TRH-1–59): To a solution of 5-aminoindan (269 mg, 2.0 mmol) in dichloromethane (10 mL) was added acryloyl chloride (0.20 mL, 2.4 mmol) followed by triethylamine (270 mg, 2.4 mmol) at 0°C under N_2 atmosphere. The reaction mixture was allowed to warm to room temperature and was stirred for 20 hours. The solution was washed twice with brine, and the resulting crude was purified by silica gel chromatography (40% ethyl acetate in hexanes) to yield 129 mg of white solid (34% yield).

^{1}H NMR (400MHz, CDCI3). δ 8.87 (s, 1H), 7.54 (s, 1H), 7.31 (d, *J* = 7.6 Hz, 1H), 7.11 (d, *J* = 7.8 Hz, 1H), 6.40 (d, *J* = 5.6 Hz, 2H), 5.66 (t, *J* = 5.6 Hz, 1H), 2.87–2.80 (m, 4H), 2.04 (t, *J* = 7.2 Hz, 2H).

^{13}C NMR (100MHz, $CDCl_3$). 5 164.4, 144.9, 140.4, 136.0, 131.6, 127.0, 124.3, 118.8, 117.0, 32.9, 32.4, 25.6.

HRMS (+ESI). Calculated: 188.1070 ($C_{12}H_{12}NO$). Observed: 188.1068.

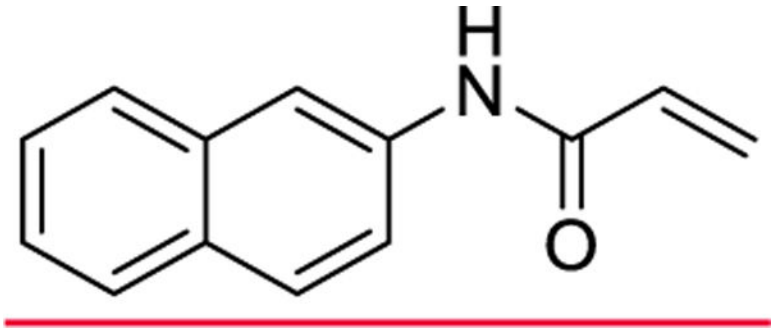

N-(naphthalene-2-yl)acrylamide (TRH-1–60): To a solution of 2-naphthylamine (289 mg, 2.0 mmol) in dichloromethane (10 mL) was added acryloyl chloride (0.20 mL, 2.4 mmol) followed by triethylamine (269 mg, 2.4 mmol) at 0°C under N_2 atmosphere. After 15 minutes, the reaction mixture was allowed to warm to room temperature and was stirred for 16 hours. The solution was washed twice with 5% citric acid and once with brine, and the resulting crude was purified by silica gel chromatography (30% ethyl acetate in hexanes) to yield 266 mg of an off-white solid (67% yield).

^{1}H NMR (400MHz, MeOD). δ 8.25 (d, *J* = 1.8 Hz, 1H), 7.73–7.69 (m, 3H), 5.54 (dd, *J* = 2.1, 8.8 Hz, 1H), 7.39–7.34 (m, 1H), 7.33–7.29 (m, 1H), 6.44 (dd, *J* =9.7, 17.0 Hz, 1H), 6.36 (dd, *J* = 2.2, 17.0 Hz, 1H), 5.72 (dd, *J* = 2.2, 9.7 Hz, 1H).

^{13}C NMR (100MHz, MeOD). 5 166.2, 137.1, 135.1, 132.4, 132.1, 129.5, 128.6, 128.5, 127.9, 127.4, 126.1, 121.1, 118.1.

HRMS (+ESI). Calculated: 198.0913 ($C_{13}H_{12}NO$). Observed: 198.0912.

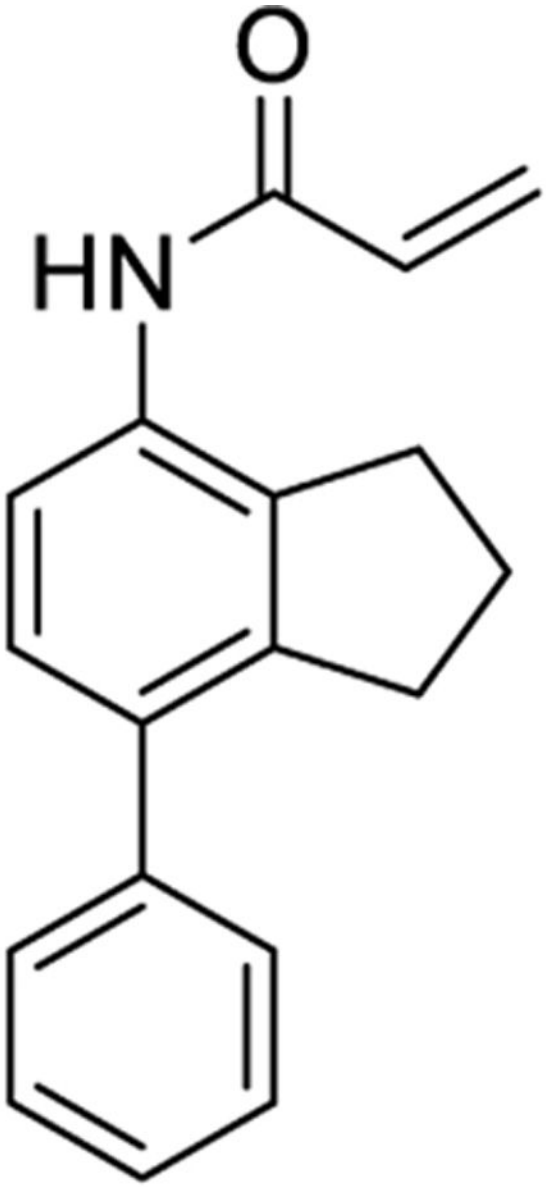

N-(7-phenyl-2,3-dihydro-1H-inden-4-yl)acrylamide (TRH-1–68): To a solution of *N*-(7-bromo-2,3-dihydro-1*H*-inden-4yl)acrylamide (**TRH-1–65**, 56 mg, 0.2 mmol) in a solution of dioxane and water (4:1 dioxane:water, 2.1 mL) was added sequentially phenylboronic acid (55 mg, 0.4 mmol), potassium carbonate (78 mg, 0.5 mmol), and tetrakis(triphenylphosphine)palladium(0) (26 mg, 10 mol%). The reaction mixture was heated to a reflux and was stirred overnight. The reaction was diluted with water (20 mL) and extracted with DCM (3×20 mL). The combined organics were evaporated and the resulting crude was purified by silica gel chromatography (10% to 50% ethyl acetate in hexanes) then recrystallized from toluene to give 11 mg of white solid (20% yield).

^{1}HNMR (400MHz, MeOD). δ 7.48 (d, *J* = 8.2 Hz, 1H), 7.40–7.39 (m, 4H), 7.33–7.27 (m, 1H), 7.16 (d, *J* = 8.2 Hz, 1H), 6.53 (dd, *J* = 10.2, 17.0 Hz, 1H), 6.36 (dd, *J* = 1.7, 17.0 Hz,

1H), 5.77 (dd, *J* =1.7,10.2 Hz, 1H), 2.96 (t, J= 7.3 Hz, 2H), 2.91 (t, *J* = 7.3 Hz, 2H), 2.04 (quint, *J* =7.3 Hz, 2H).

^{13}C NMR (100MHz, MeOD). δ 166.3, 144.2, 142.4, 139.2, 133.8, 132.2, 129., 129.3, 128.2, 127.9, 127.8, 123.0, 34.3, 32.1, 26.6.

HRMS (+ESI). Calculated: 264.1383 ($C_{18}H_{18}NO$). Observed: 264.1381.

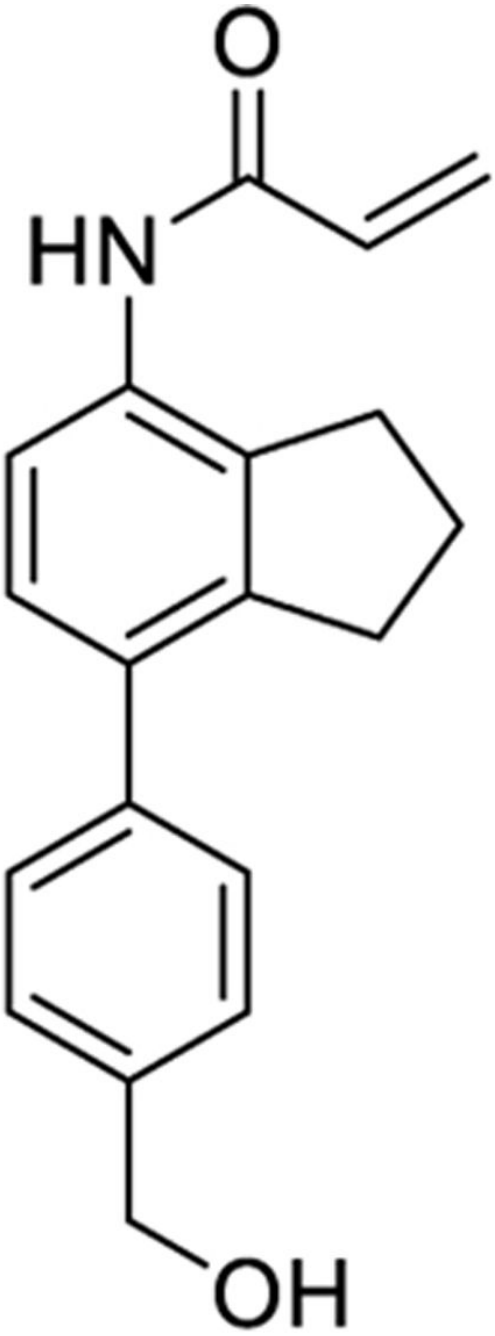

N-(7-(4-(hydroxymethyl)phenyl)-2,3-dihydro-1 H-4-yl)acrylamide (TRH-1–70): To a solution of *N*-(7-bromo-2,3-dihydro-1*H*-inden-4yl)acrylamide (**TRH-1–65**, 56 mg, 0.2 mmol) in a solution of dioxane and water (4:1 dioxane:water, 2.1 mL) under nitrogen atmosphere was added sequentially 4-(hydroxymethyl)phenylboronic acid (66 mg, 0.4 mmol), potassium carbonate (78 mg, 0.5 mmol), and tetrakis(triphenylphosphine)palladium(0) (26 mg, 10 mol%). The reaction mixture was heated to a reflux and stirred overnight. The reaction was diluted with water (20 mL) and extracted with DCM (3×20 mL). The combined organics were dried with magnesium sulfate, filtered, and evaporated, and the resulting crude was purified by silica gel chromatography (20% to 50% ethyl acetate in hexanes) to give 16 mg of white solid (26% yield).

^{1}HNMR (400MHz, MeOD). δ 7.47 (d, *J* = 8.1 Hz, 1H), 7.41–7.38 (m, 4H), 7.15 (d, *J* = 8.2 Hz, 1H), 6.52 (dd, *J* = 10.2,16.9 Hz, 1H), 6.36 (d, *J* = 17.0 Hz, 1H), 5.77 (d, *J* =10.5 Hz, 1H), 4.63 (s, 2H), 2.95 (t, *J* = 7.1 Hz, 2H), 2.90 (t, *J* =7.2 Hz, 2H), 2.03 (t, *J* = 7.3 Hz, 2H).

^{13}C NMR (100MHz, MeOD). δ 166.3, 144.1, 141.4, 139.2, 136.9, 133.8, 132.2, 129.5, 128.5,128.2, 128.0, 127.9, 123.0, 65.0, 34.3, 32.0, 26.6.

HRMS (+ESI). Calculated: 294.1489 ($C_{19}H_{20}NO_2$). Observed: 294.1486.

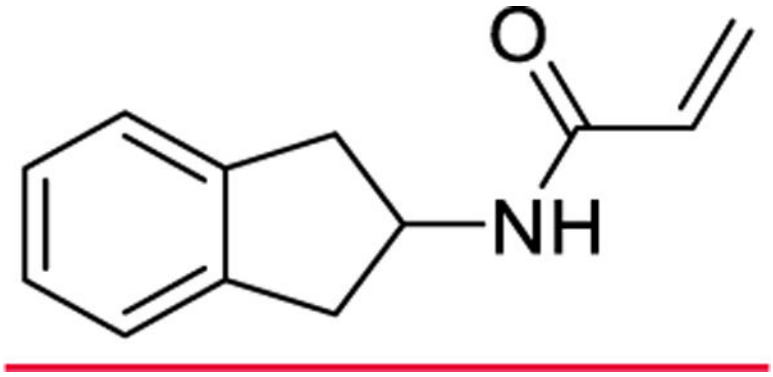

N-(2,3-dihydro-1 H-inden-2-yl)acrylamide (TRH-1–74): To a solution of 2-aminoindan (253 mg, 2.0 mmol) in dichloromethane (10 mL) was added acryloyl chloride (0.19 mL, 2.4 mmol) followed by triethylamine (222 mg, 2.4 mmol) at 0°C under N_2 atmosphere. The reaction mixture was allowed to warm to room temperature after 15 minutes and was stirred for 23 hours. The solution was washed twice with brine, and the resulting crude was purified by silica gel chromatography (40% ethyl acetate in hexanes) to yield 126 mg of an off-white solid (35% yield).

^{1}H NMR (400MHz, $CDCl_3$). δ 7.23–7.16 (m, 4H), 6.27 (dd, *J* =1.3, 17.0 Hz, 1H), 6.10 (s, 1H), 6.04 (dd, *J* =10.3, 17.0 Hz, 1H), 5.60 (dd, *J* = 1.3, 10.3 Hz, 1H), 4.82–4.75 (m, 1H), 3.32 (dd, *J* =7.1, 16.2 Hz, 2H), 2.84 (dd, *J* = 4.4, 16.1 Hz, 2H).

^{13}C NMR (100MHz, $CDCl_3$). δ 165.4 ,140.9, 130.9, 126.8, 126.5, 124.9, 50.7, 40.1.

HRMS (+ESI). Calculated: 188.1070 ($C_{12}H_{14}NO$). Observed: 188.1068.

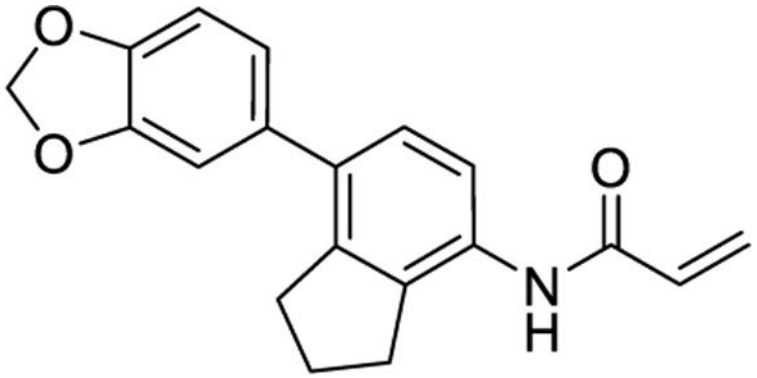

N-(7-(benzo[d][1,3]dioxol-5-yl)-2,3-dihydro-1H-inden-4-yl)acrylamide (TRH-1–78): To a solution of *N*-(7-bromo-2,3-dihydro-1H-inden-4yl)acrylamide (**TRH-1–65**, 55 mg, 0.2 mmol) in a mixture of dioxane and water (4:1 dioxane:water, 2.1 mL) under nitrogen atmosphere was added sequentially 3,4-(methylenedioxy)phenylboronic acid (70 mg, 0.4 mmol), potassium carbonate (74 mg, 0.5 mmol), and tetrakis(triphenylphosphine)palladium(0) (24 mg, 10 mol%). The reaction mixture was heated to a reflux and stirred overnight. The reaction was diluted with water (20 mL) and extracted with DCM (3×20 mL). The combined organics were dried with magnesium sulfate, filtered, and evaporated, and the resulting crude was purified by silica gel chromatography (0% to 25% ethyl acetate in hexanes) to give 7 mg of white solid (11% yield).

^{1}H NMR (600 MHz, $CDCl_3$). δ 7.93 (d, *J* = 7.0 Hz, 1H), 7.18 (d, *J* = 8.2 Hz, 1H), 7.10 (s, 1H), 6.90 (s, 1H), 6.86 (t, *J* = 8.1 Hz, 2H), 6.45 (d, *J* =16.8 Hz, 1H), 6.30 (dd, *J* = 10.3,16.8 Hz, 1H), 5.79 (d, *J* =10.2 Hz, 1H), 3.00 (t, *J* = 7.3 Hz, 2H), 2.88 (t, *J* = 7.3 Hz, 2H), 2.10 (quint, 7.3 Hz, 2H).

^{13}C NMR (150 MHz, $CDCl_3$). 5 147.7, 146.7, 142.84, 142.81, 135.2, 134.9, 132.8, 131.3, 127.9, 127.8, 122.1, 119.8, 109.2, 108.3, 101.2, 36.8, 33.5, 30.5, 25.4.

HRMS (-ESI). Calculated: 306.1136 ($C_{19}H_{16}NO_3$). Observed: 306.1130.

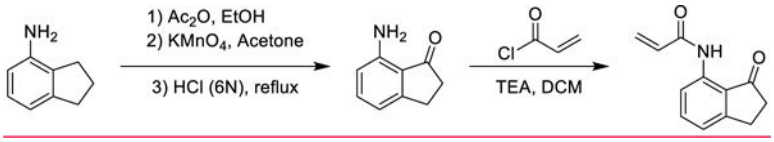

N-(3-oxo-2,3-dihydro-1 H-inden-4-yl)acrylamide (TRH-1–129): To a solution of 4-aminoindan (1.0 g, 7.5 mmol) in ethanol (20 mL) at 0°C was added acetic anhydride (1.4 mL, 15.0 mmol). The solution was raised to room temperature and stirred overnight, after which the solvent was evaporated. The residue was then dissolved in acetone (50 mL) to which was added 15% aqueous magnesium sulfate (1.2 g in 6.75 mL of water) followed by potassium permanganate (3.4 g, 17.0 mmol), and the resulting solution was stirred for 24 hours. The reaction filtered through a pad of celite, eluting with chloroform and then water. The eluent was separated, and the aqueous layer was extracted several times with additional

chloroform. The combined organics were dried over magnesium sulfate, filtered and evaporated. The residue was then dissolved in a 6N HCl solution (20 mL) and heated to 90°C. After stirring for 5 hours, the solution was cooled, neutralized with small portions of potassium carbonate, and extracted with ethyl acetate. The combined organics were dried with magnesium sulfate, filtered, and evaporated to give 610 mg (55% over 3 steps) of crude **7-aminoindan-1-one** which was used without further purification.

To a solution of 7-aminoindan-1-one in dichloromethane (15 mL) was added acryloyl chloride (0.39 mL, 4.8 mmol) followed by triethylamine (0.67 mL, 4.8 mmol) at 0°C under N_2 atmosphere. The reaction mixture was allowed to warm to room temperature and was stirred overnight. The solution was washed 1M HCl solution (2x) and brine, and the resulting crude was purified by silica gel chromatography (10% to 20% ethyl acetate in hexanes) to yield 390 mg of white solid (47% yield, 26% combined over 4 steps).

^{1}H NMR (400MHz, $CDCl_3$). δ 10.64 (s, 1H), 8.45 (d, *J* = 8.2 Hz, 1H), 7.55 (t, *J* = 7.9 Hz, 1H), 7.12 (d, *J* = 7.6 Hz, 1H), 6.45 (dd, *J* =1.0, 17.0 Hz, 1H), 6.33 (dd, *J* =10.1, 17.0 Hz, 1H), 5.82 (dd, *J* =1.0, 10.1 Hz, 1H), 3.11 (t, *J* =11.5 Hz, 2H), 2.74–2.71 (m, 2H).

^{13}C NMR (100MHz, $CDCl_3$). δ 209.3, 164.4, 155.9, 138.7, 137.0, 131.7, 128.0, 123.1, 120.8, 116.9, 36.5, 25.5.

HRMS (+ESI). Calculated: 202.0863 ($C_{12}H_{12}NO_2$). Observed: 202.0860.

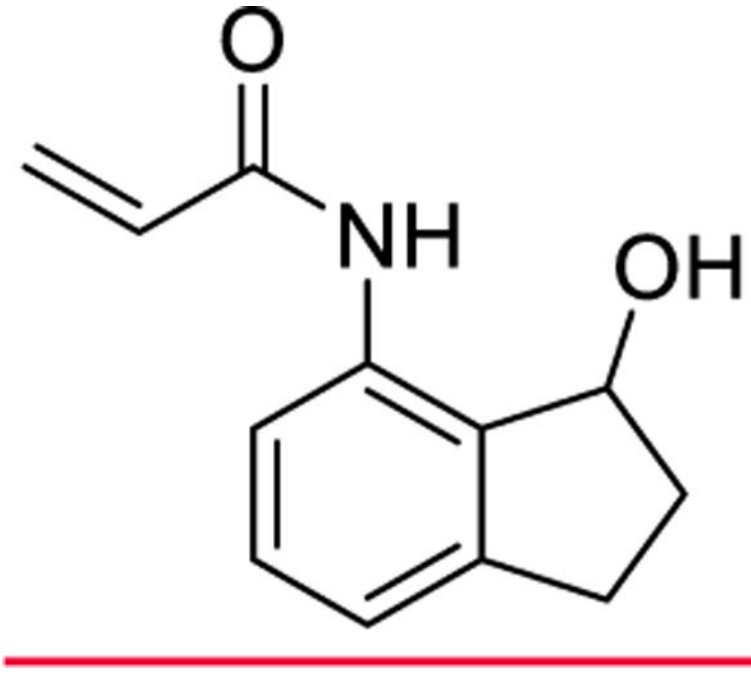

N-(3-hydroxy-2,3-dihydro-1 H-inden-4-yl)acrylamide (TRH-1–133): To a solution of N-(3-oxo-2,3-dihydro-1H-inden-4-yl)acrylamide (**TRH-1–129**,201 mg, 1.0 mmol) in anhydrous methanol (7 mL) under nitrogen atmosphere was added sodium borohydride (46.1 mg, 1.2 mmol). After 30 minutes of stirring, the reaction was quenched with saturated

sodium bicarbonate solution and extracted three times with DCM. The combined organics were dried with magnesium sulfate, filtered, and concentrated. Crude was purified by silica gel chromatography (30 to 50% ethyl acetate in hexanes) to give 190 mg of the product as a white solid (94% yield).

^{1}HNMR (400MHz, $CDCl_3$). δ 8.93 (s, 1H), 7.98 (d, *J* = 7.8 Hz, 1H), 7.19 (t, *J* = 7.9 Hz, 1H), 6.95 (d, *J* = 7.4 Hz, 1H), 6.29 (d, *J* =16.8 Hz, 1H), 6.15 (dd, *J* =10.2,16.9 Hz, 1H), 5.66 (d, *J* =10.2 Hz, 1H), 5.32 (q, *J* = 6.9 Hz, 1H), 3.60 (d, *J* = 6.7 Hz, 1H), 2.96 (ddd, *J* = 2.4, 9.0,

15.7 Hz), 2.73 (quint, *J* = 8.1 Hz, 1H), 2.56–2.48 (m, 1H), 1.96–1.86 (m, 1H).

^{13}C NMR (100 MHz, $CDCl_3$). δ 164.1, 143,7 ,135.6, 132.8, 131.6, 129.5, 127.3, 121.0, 118.5, 76.2, 36.0, 29.8.

HRMS (-ESI). Calculated: 202.0874 ($C_{12}H_{12}NO_2$). Observed: 202.0874.

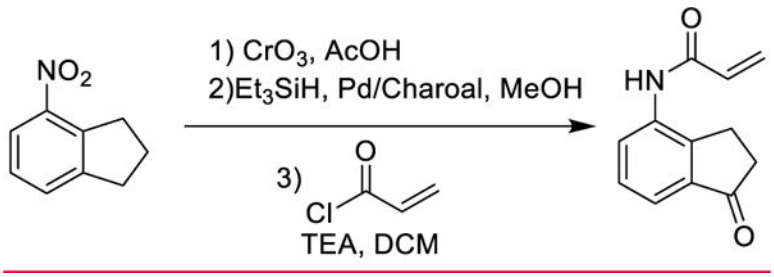

N-(1-oxo-2,3-dihydro-1 H-inden-4-yl)acrylamide (TRH-1–134): To a solution of 4-nitroindan (5.38 g, 33 mmol) in acetic acid (250 mL) was slowly added chromium trioxide (8.95 g, 90 mmol). After stirring for 24 hours, the reaction was neutralized with 2M NaOH and extracted five times with ethyl acetate. The combined organics were washed with a saturated sodium bicarbonate solution and brine, then dried over magnesium sulfate, filtered, and concentrated. The crude material was purified by silica gel chromatography (10–20% ethyl acetate in hexanes) to give 1.26 g (ca. 7.1 mmol) of 4-nitroindanone as a white solid.

This intermediate was combined with palladium on activated charcoal (125 mg, 10 wt%) dissolved in anhydrous methanol (21 mL) under the atmosphere of a nitrogen balloon. Triethylsilane (11.3 mL, 71 mmol) was slowly added by addition funnel over the course of 10 minutes while the reaction was stirred under the cooling of a room temperature water bath. After an additional 20 minutes of stirring, the reaction mixture was filtered through a pad of celite and subsequently concentrated to give crude 4-aminoindanone which was used without further purification.

This final intermediate was then dissolved in DCM (21 mL) under N_2 atmosphere and cooled to 0°C, after which acryloyl chloride (0.77 mL, 9.5 mmol) and triethylamine (1.19 mL, 8.5 mmol) were slowly added. The reaction was allowed to warm to room temperature while stirring overnight, at which point the reaction was washed twice with brine, dried with magnesium sulfate, filtered, and concentrated. The crude was purified by silica gel

chromatography (30–50% ethyl acetate in hexanes) to give 989 mg of a white solid (15% yield over 3 steps).

[1]HNMR(400MHz, CDCl3). δ 8.20 (d, *J* = 5.8 Hz, 1H), 7.63 (s, 1H), 7.56 (d, *J* = 7.5 Hz, 1H), 7.39 (t, *J* = 7.7 Hz, 1H), 6.48 (d, *J* =16.7 Hz, 1H), 6.37 (dd, *J* =10.0 Hz, 16.8 Hz, 1H), 5.83 (d, *J* = 10.1 Hz, 1H), 3.04 (t, *J* =5.6 Hz, 2H), 2.70 (t, *J* = 5.7 Hz, 2H).

^{13}C NMR (100 MHz, $CDCl_3$) δ 206.3, 163.9, 146.0, 138.0, 135.4, 130.7, 128.8, 128.7, 127.6, 120.4, 36.1, 23.4.

HRMS (-ESI). Calculated: 200.0717 ($C_{12}H_{10}NO_2$). Observed: 200.0715.

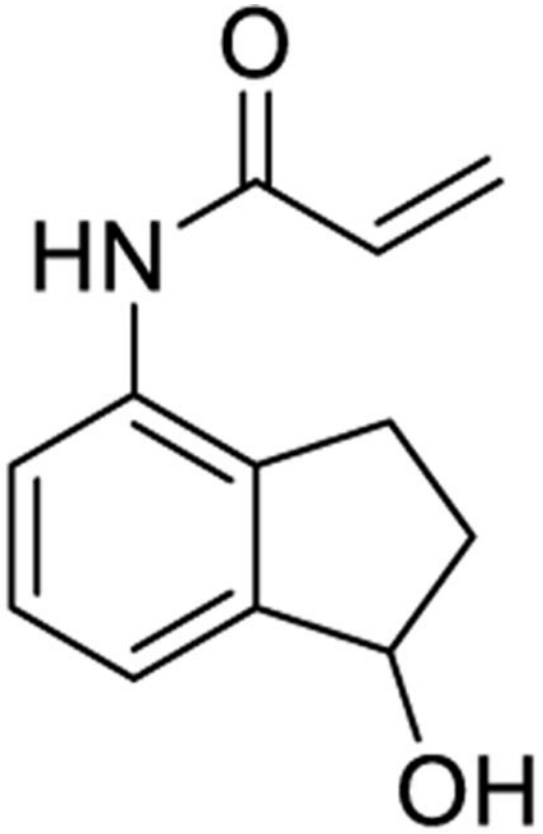

N-(1-hydroxy-2,3-dihydro-1 H-inden-4-yl)acrylamide (TRH-1–135): To a solution of *N*-(1-oxo-2,3-dihydro-1H-inden-4-yl)acrylamide (**TRH-1–134**,1.26 g, 6.25 mmol) in anhydrous methanol (50 mL) under nitrogen atmosphere was added sodium borohydride (292.7 mg, 7.7 mmol). After 30 minutes of stirring, the reaction was quenched with water and the methanol was removed *in vacuo.* The residue was saturated with NaCl and extracted five times with a 2:1 chloroform:methanol solution. The combined organics were dried over 3 angstrom molecular sieves, filtered, and concentrated. The crude material was purified by silica gel chromatography (40 to 70% ethyl acetate in hexanes) to give 1.05 g of the product as a white solid (83% yield).

^{1}H NMR (400 MHz, MeOD). δ 7.50 (dd, *J*=2.3, 6.3 Hz, 1H), 7.25–7.20 (m, 2H), 6.51 (dd, *J*=10.2, 17.0 Hz, 1H), 6.35 (dd, *J*= 1.7, 17.0 Hz, 1H), 5.77 (dd, *J*=1.7, 10.2 Hz, 1H), 5.17 (t, *J*=6.3 Hz, 1H), 2.97 (ddd, *J*= 4.5, 8.6, 16.2, 1H), 2.74 (quint, *J*= 7.8 Hz, 1H), 2.47–2.39 (m, 1H), 1.95–1.86 (m, 1H).

^{13}C NMR (100 MHz, MeOD). δ 166.3, 148.0, 137.8, 134.8, 132.1, 128.3, 127.9, 124.0, 122.7, 76.9, 36.1, 28.6.

HRMS (-ESI). Calculated: 202.0874 ($C_{12}H_{12}NO_2$). Observed: 202.0872.

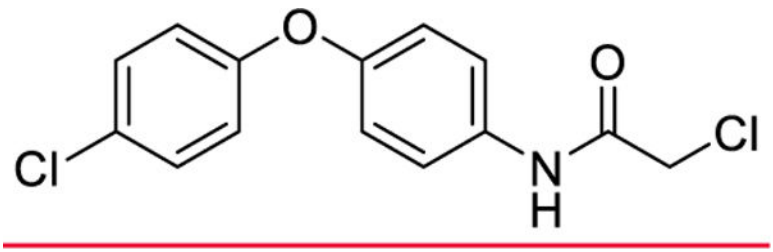

2-Chloro-N-(4-(4-chlorophenoxy)phenyl)acetamide (TRH-1–140): To a solution 4-(4-chlorophenoxy)aniline (446 mg, 2.0 mmol) in dichloromethane (10 mL) was added chloroacetyl chloride (0.39 mL, 4.8 mmol) followed by triethylamine (0.67 mL, 4.8 mmol) at 0°C under N_2 atmosphere. After stirring for 35 minutes, the reaction mixture was allowed to warm to room temperature and was stirred for 27 hours. The solution was washed twice with brine, dried with magnesium sulfate, and the resulting crude was purified by silica gel chromatography (30% to 50% ethyl acetate in hexanes) to yield 533 mg of an off-white solid (89% yield).

^{1}H NMR (400 MHz, $CDCl_3$). δ 8.33 (s, 1H), 7.52–7.48 (m, 2H), 7.29–7.25 (m, 2H), 6.99–6.96 (m, 2H), 6.93–6.89 (m, 2H), 4.17 (s, 2H)

^{13}C NMR (100 MHz, $CDCl_3$). δ 164.1, 156.0, 154.0, 132.5, 129.8, 128.4, 122.2, 119.9, 119.6, 42.9.

HRMS (-ESI). Calculated: 294.0094 ($C_{14}H_{10}NO_2Cl_2$). Observed: 294.0094.

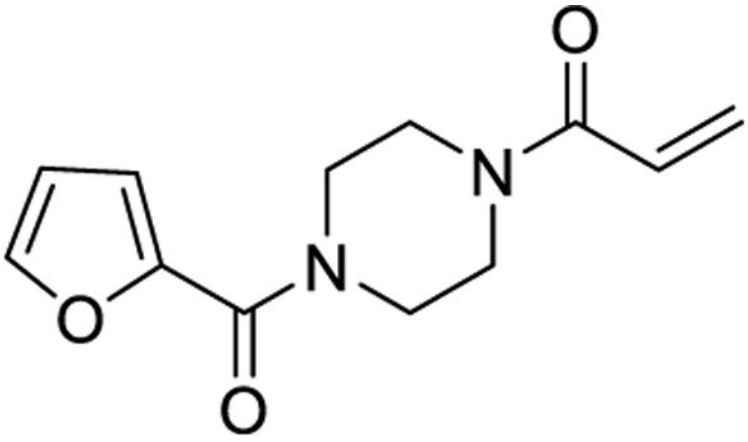

1-(4-(furan-2-carbonyl)piperazin-1-yl)prop-2-en-1-one (TRH-1–145): To a solution 1-(2-furoyl)piperazine (362 mg, 2.0 mmol) in dichloromethane (10 mL) was added acryloyl chloride (0.20 mL, 2.4 mmol) followed by triethylamine (0.34 mL, 2.4 mmol) at 0°C under N_2 atmosphere. After stirring for 20 minutes, the reaction mixture was allowed to warm to room temperature and was stirred for 24 hours. The solution was washed twice with brine, dried with magnesium sulfate, and the resulting crude was purified by silica gel chromatography (70% to 100% ethyl acetate in hexanes) to yield 446 mg of yellow solid (95% yield).

^{1}H NMR (400 MHz, $CDCl_3$). δ 7.53 (m, 1H), 7.06 (dd, *J* = 0.7,3.5 Hz, 1H), 6.61 (dd, *J* = 10.5,16.8 Hz, 1H), 6.52 (dd, *J* =1.8, 3.5 Hz, 1H), 6.33 (dd, *J* =1.9, 16.8 Hz, 1H), 5.75 (dd, *J* =1.9, 10.5 Hz, 1H), 3.84–3.67 (m, 8H).

^{13}C NMR (100 MHz, $CDCl_3$). δ 165.5, 159.1, 147.5, 144.0, 128.5, 127.1, 117.0, 111.5, 45.6, 41.9.

HRMS (+ESI). Calculated: 235.1077 ($C_{12}H_{15}O_2$). Observed: 235.1075.

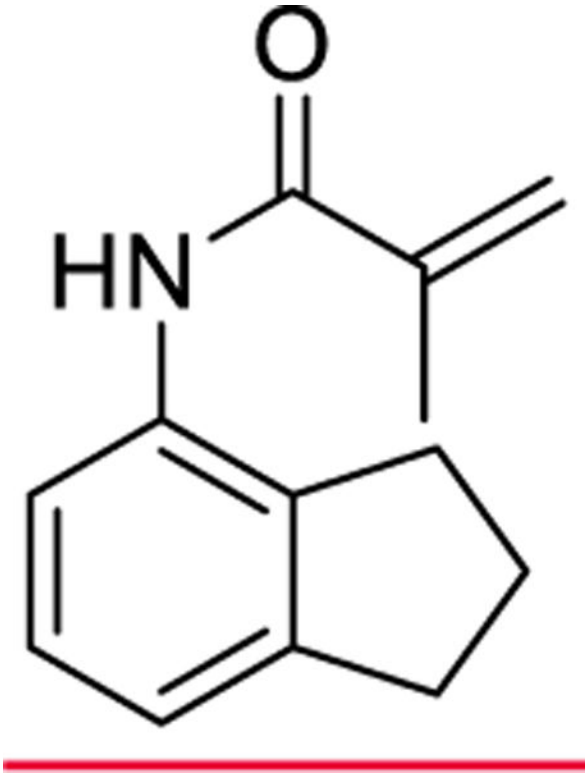

N-(2,3-dihydro-1 H-inden-4-yl)methacrylamide (TRH-1–149): To a solution 4-aminoindan (0.24 mL, 2.0 mmol) in dichloromethane (10 mL) was added methacryloyl chloride (0.23 mL, 2.4 mmol) followed by triethylamine (0.34 mL, 2.4 mmol) at 0°C under N_2 atmosphere. After stirring for 20 minutes, the reaction mixture was allowed to warm to room temperature and was stirred for 3.5 hours. The solution was washed twice with brine, dried with magnesium sulfate, and the resulting crude was purified by silica gel chromatography (35% to 40% ethyl acetate in hexanes) to yield 378 mg of off-white solid (94% yield).

^{1}H NMR (400 MHz, $CDCl_3$). δ 7.72 (d, *J* = 8.0 Hz, 1H), 7.55 (s, 1H), 7.12 (t, *J* =7.7 Hz, 1H), 7.01 (d, *J* = 7.4 Hz, 1H), 5.79 (s, 1H), 5.42 (s, 1H), 2.93 (t, *J* =7.5 Hz, 2H), 2.79 (t, *J* =7.4 Hz, 2H), 7.12–2.06 (m, 2H), 2.04 (s, 3H).

^{13}C NMR (100 MHz, $CDCl_3$). δ 166.3, 145.1, 140.6, 134.5, 133.7, 127.0, 120.7, 119.8, 118.9, 33.1, 29.9, 24.7, 18.6.

HRMS (+ESI). Calculated: 202.1226 ($C_{13}H_{16}NO$). Observed: 202.1224.

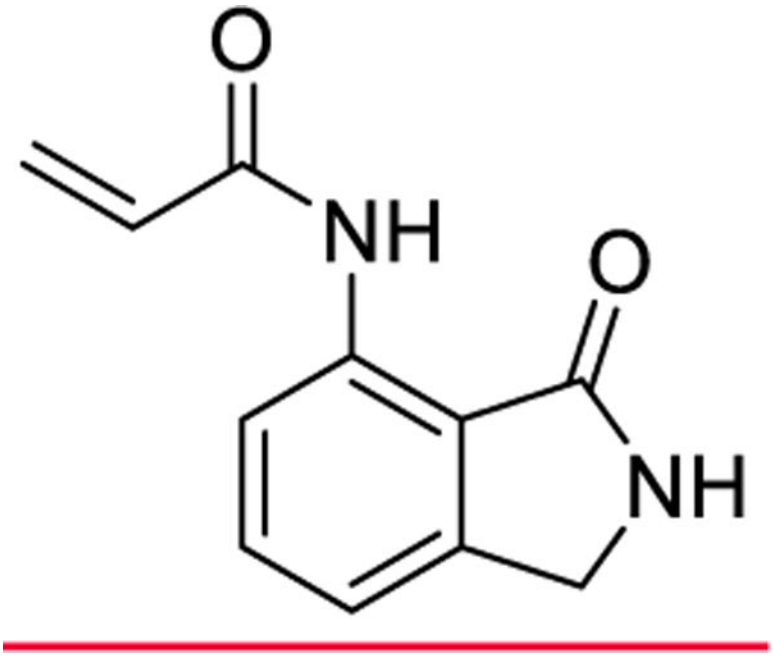

N-(3-oxoisoindolin-4-yl)acrylamide (TRH-1–152): To a solution of 7-aminoisoindolin-1-one (99 mg, 0.67 mmol) in dichloromethane (4 mL) was added acryloyl chloride (0.07 mL, 0.8 mmol) followed by triethylamine (0.11 mL, 0.8 mmol) at 0°C under N_2 atmosphere. After stirring for 20 minutes, the reaction mixture was allowed to warm to room temperature and was stirred overnight. The solution was washed twice with brine, dried with magnesium sulfate, and the resulting crude was purified by silica gel chromatography (50 to 60% ethyl acetate in hexanes) to yield 58 mg of a white solid (43% yield).

^{1}H NMR (400 MHz, $CDCl_3$). δ 10.50 (s, 1H), 8.58 (d, *J* = 8.2 Hz, 1H), 7.55 (t, *J* = 7.9 Hz, 1H), 7.15 (d, *J* = 7.5 Hz, 1H), 6.82 (s, 1H), 6.46 (dd, *J* =1.3, 17.0 Hz, 1H), 6.36 (dd, *J* =10.0, 17.0 Hz, 1H), 5.81 (dd, *J* =1.3, 10.0 Hz, 1H), 4.46 (s, 2H).

^{13}C NMR (100 MHz, $CDCl_3$). δ 172.9, 164.2, 143.9, 138.2, 133.8, 131.8, 127.8, 118.0, 117.7, 117.6, 45.6.

HRMS (+ESI). Calculated: 203.0815 ($C_{11}H_{11}N_2O_2$). Observed: 203.0814.

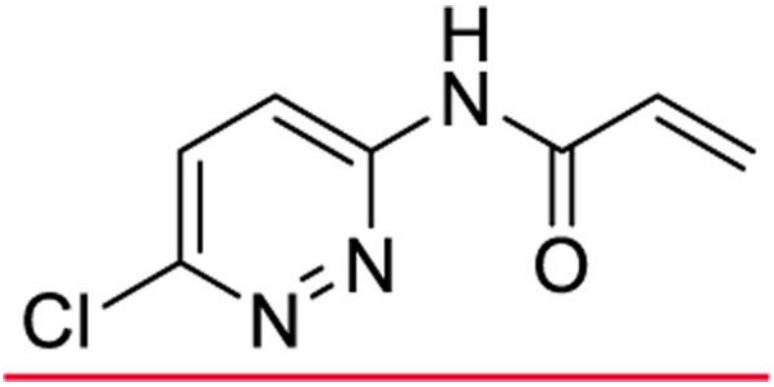

N-(6-chloropyridazin-3-yl)acrylamide (TRH-1–155): To a solution 3-amino-6-chloropyridazine (261 mg, 2.0 mmol) in dichloromethane (10 mL) was added acryloyl chloride (0.20 mL, 2.4 mmol) followed by triethylamine (0.34 mL, 2.4 mmol) at 0°C under N_2 atmosphere. After stirring for 20 minutes, the reaction mixture was allowed to warm to room temperature and was stirred overnight. The solution was washed twice with brine, dried with magnesium sulfate, and the resulting crude was purified by silica gel chromatography (40% to 50% ethyl acetate in hexanes) to yield 23 mg of a pale-yellow solid (6% yield).

^{1}H NMR (400 MHz, $CDCl_3$). δ 10.06 (s, 1H), 8.70 (d, *J* = 9.4 Hz, 1H), 7.57 (d, *J* = 9.4 Hz, 1H), 6.73 (dd, *J* =10.2, 16.8 Hz, 1H) 6.56 (dd, *J* =1.2, 16.8, 1H), 5.94 (dd, *J* =1.2, 10.2 Hz, 1H).

^{13}C NMR (100 MHz, CDCl3). δ 164.8, 155.2, 152.3, 130.7, 130.4, 130.3, 122.0.

HRMS (+ESI). Calculated: 182.0127 ($C_7H_5N_3OCl$). Observed: 182.0126.

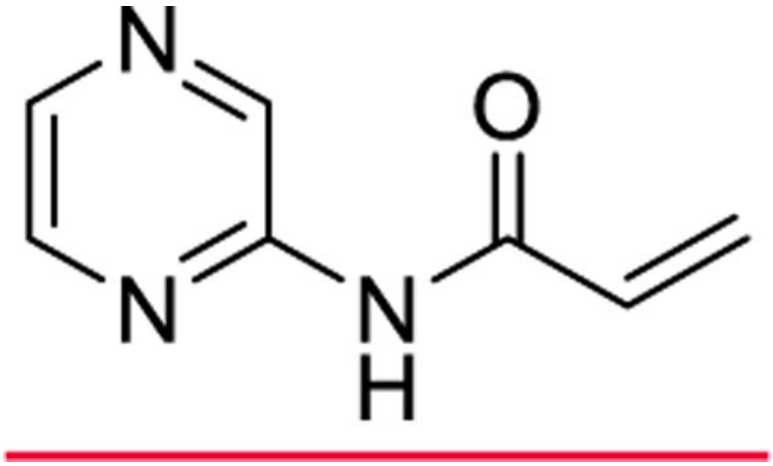

N-(Pyrazin-2-yl)acrylamide (TRH-1–156): To a solution of aminopyrazine (192 mg, 2.0 mmol) in dichloromethane (10 mL) was added acryloyl chloride (0.20 mL, 2.4 mmol) followed by triethylamine (0.34 mL, 2.4 mmol) at 0°C under N_2 atmosphere. After stirring for 20 minutes, the reaction mixture was allowed to warm to room temperature and was stirred overnight. The solution was washed twice with brine, dried with magnesium sulfate, and the resulting crude was purified by silica gel chromatography (50% to 70% ethyl acetate in hexanes) to yield 22 mg of white solid (7% yield).

^{1}H NMR(600 MHz, CDCl3). δ 9.65 (d, *J* =1.3 Hz, 1H), 8.38 (d, *J* =2.5 Hz, 1H), 8.27 (dd, *J* =1.6, 2.5 Hz, 1H), 8.19 (s, 1H), 6.54 (dd, *J* = 0.8, 16.9 Hz, 1H), 6.33 (dd, *J* = 10.3, 16.9 Hz, 1H), 5.90 (dd, *J* = 0.8, 10.3 Hz, 1H).

^{13}C NMR (150 MHz, $CDCl_3$). δ 163.5, 148.2, 142.2, 140.6, 137.4, 130.2, 129.8.

HRMS (+ESI). Calculated: 150.0662 ($C_7H_8N_3O$). Observed: 150.0660.

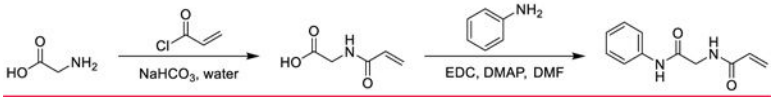

N-(2-oxo-2-(phenylamino)ethyl)acrylamide (TRH-1–160): To a solution of glycine (1.50 g, 20.0 mmol) and sodium bicarbonate (1.70 g, 20.2 mmol) in water (30 mL) at 0°C was slowly added acryloyl chloride (2.45 mL, 30.2 mmol). After stirring for 3.5 hours, the reaction was extracted 3 times with ethyl acetate. The combined organics were dried over magnesium sulfate, filtered, and concentrated to give an oil. The oil was treated with hexanes causing a white solid to crash out which was collected by gravity filtration to give 124 mg of crude acryloylglycine of which 58 mg (47% of the crude material) was used immediately without further purification.

This solid (ca. 0.45 mmol) was dissolved in DMF (2.5 mL) and a solution of N-(3-dimethylaminopropyl)-N′-ethylcarbodiimide hydro-chloride (104 mg, 0.54 mmol) and 4-dimethylaminopyridine (68 mg, 0.56 mmol) in DMF (2.5 mL) was added followed by aniline (0.050 mL, 0.54 mmol). The solution was stirred overnight, diluted with ethyl acetate, and washed with both a saturated solution of sodium bicarbonate and brine. The organics were then dried over magnesium sulfate, filtered, and concentrated, and the resulting crude was purified by silica gel chromatography (30–60% ethyl acetate in hexanes) to give 19 mg of the title compound as a white solid (1% yield over two steps).

^{1}H NMR (400 MHz, MeOD). δ 7.56–7.53 (m, 2H), 7.30 (t, *J*=8.0 Hz, 2H), 7.08 (t, *J*=7.4 Hz, 1H), 6.35 (dd, *J* = 9.9, 17.1 Hz, 1H), 6.26 (dd, *J* = 2.0, 17.1 Hz, 1H), 5.71 (dd, *J* = 2.0, 9.9 Hz, 1H), 4.08 (s, 2H).

^{13}C NMR (100 MHz, MeOD). δ 169.4, 168.6, 139.5, 131.7, 129.8, 127.2, 125.3, 121.2, 44.0.

HRMS (-ESI). Calculated: 203.0826 ($C_{11}H_{11}N_2O_2$). Observed: 203.0825.

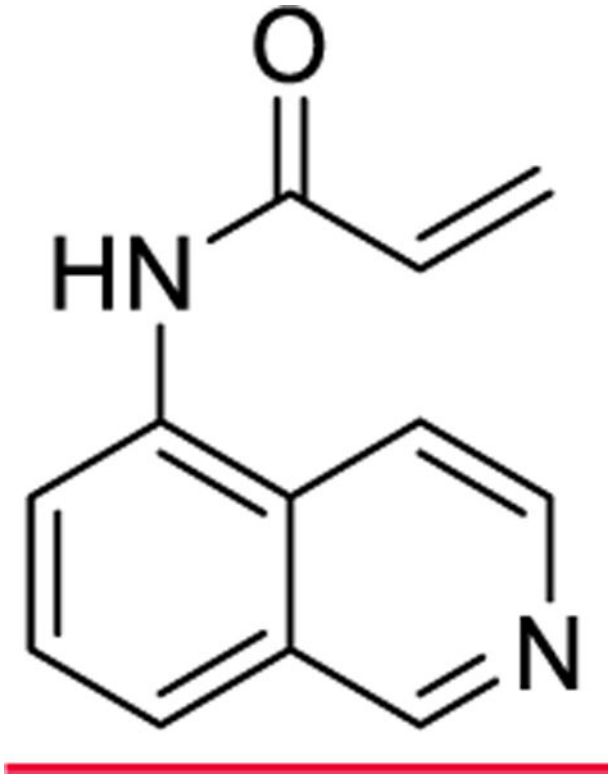

N-(isoquinolin-5-yl)acrylamide (TRH-1–162): To a solution of 5-aminoisoquinoline (287 mg, 2.0 mmol) in dichloromethane (10 mL) was added acryloyl chloride (0.20 mL, 2.4 mmol) followed by triethylamine (0.34 mL, 2.4 mmol) at 0°C under N_2 atmosphere. After stirring for 20 minutes, the reaction mixture was allowed to warm to room temperature and was stirred overnight. The solution was washed with brine, and the resulting aqueous layer was extracted with a 2:1 chloroform:methanol solution. The resulting crude was purified by chromatography on basic alumina (50% ethyl acetate in hexanes to 4% ethanol in ethyl acetate) to yield 43 mg of a yellow solid (11% yield).

^{1}HNMR (400 MHz, MeOD). δ 9.23 (s, 1H), 8.45 (d, *J* = 6.1 Hz, 1H), 8.03 (d, *J* = 7.5 Hz, 1H), 7.97 (d, *J* = 8.2 Hz, 1H), 7.88 (d, *J* =6.1 Hz, 1H), 7.68 (t, *J* = 7.9 Hz, 1H), 6.66 (dd, *J* =10.2, 17.0 Hz, 1H), 6.47 (dd, *J* =1.5, 17.0 Hz, 1H), 5.88 (dd, *J* = 1.7, 10.2 Hz, 1H).

^{13}C NMR (100 MHz, MeOD). δ 167.1, 153.5, 143.0, 133.6, 132.4, 131.9, 130.6, 128.7, 127.9, 127.1, 117.2.

HRMS (+ESI). Calculated: 199.0866 ($C_{12}H_{11}N_2O$). Observed: 199.0863.

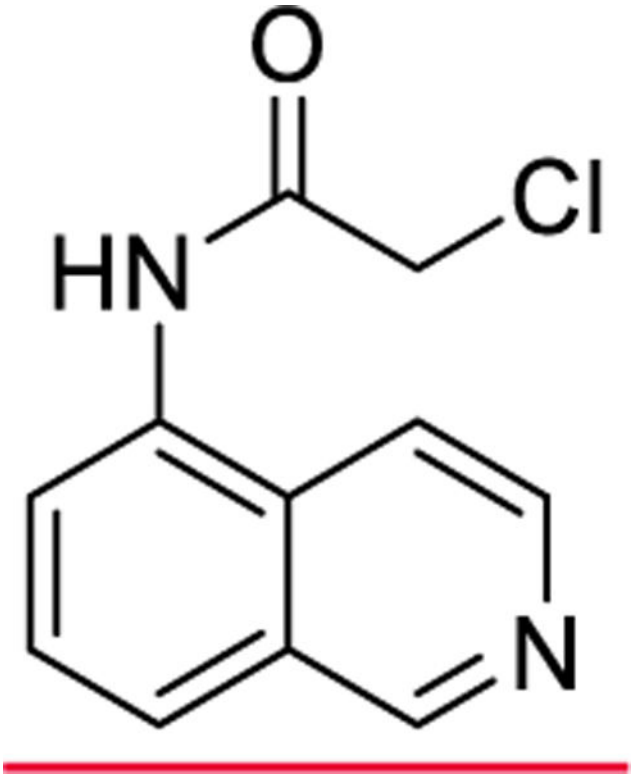

2-Chloro-N-(isoquinolin-5-yl)acetamide (TRH-1–163): To a solution 5-aminoisoquinoline (289 mg, 2.0 mmol) in dichloromethane (10 mL) was added chloroacetyl chloride (0.19 mL, 2.4 mmol) followed by triethylamine (0.34 mL, 2.4 mmol) at 0°C under N_2 atmosphere. After stirring for 20 minutes, the reaction mixture was allowed to warm to room temperature and was stirred overnight. The solution was washed with saturated sodium bicarbonate solution and brine, dried with magnesium sulfate, and the resulting crude was purified by chromatography on basic alumina (30% ethyl acetate in hexanes to 4% ethanol in ethyl acetate) to yield 157 mg of yellow solid (36% yield).

^{1}H NMR(600MHz, MeOD). δ 9.26 (s, 1H), 8.48 (d, *J* = 6.1 Hz, 1H), 8.03 (d, *J* = 8.2 Hz, 1H), 7.98 (d, *J* = 7.4 Hz, 1H), 7.91 (d, *J* =6.1 Hz, 1H), 7.71 (t, *J* = 7.9 Hz, 1H), 4.39, (s, 2H).

^{13}C NMR (150 MHz, MeOD). δ 167.4, 152.1, 141.7, 131.8, 131.2, 129.2, 127.3, 127.0, 126.1, 115.7, 42.3.

HRMS (+ESI). Calculated: 221.0476 ($C_{11}H_{10}N_2O$). Observed: 221.0473.

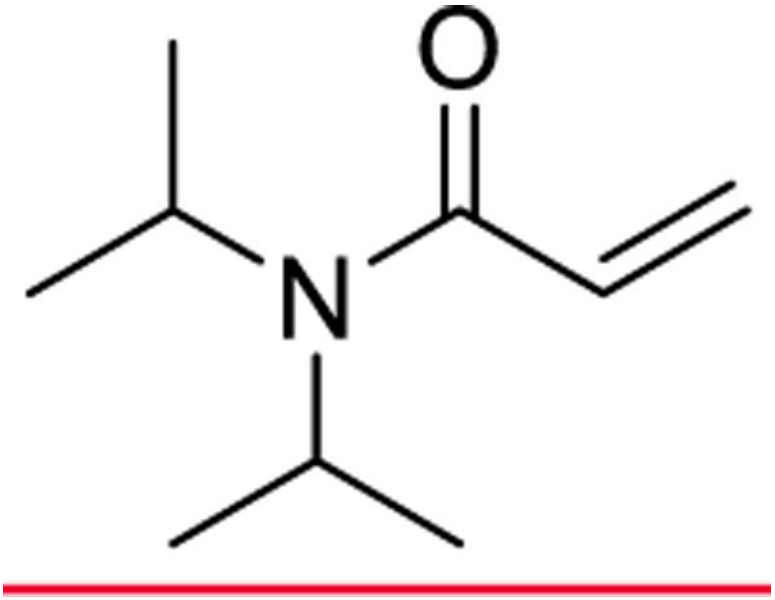

N,N-diisopropylacrylamide (TRH-1–167): To a solution of diisopropylamine (0.42 mL, 3.0 mmol) in dichloromethane (10 mL) was added acryloyl chloride (0.29 mL, 3.6 mmol) followed by triethylamine (0.50 mL, 3.6 mmol) at 0°C under N_2 atmosphere. After stirring for 20 minutes, the reaction mixture was allowed to warm to room temperature and was stirred for 19 hours. The solution was washed with a saturated solution of sodium bicarbonate followed by brine, dried with magnesium sulfate, and the resulting crude was purified by silica gel chromatography (0% to 30% ethyl acetate in hexanes) to yield 392 mg of a pale-yellow oil (84% yield).

^{1}H NMR (400 MHz, $CDCl_3$). δ 6.35 (dd, *J* =10.6, 16.8 Hz, 1H), 5.98 (dd, *J* =1.7, 16.8 Hz, 1H), 5.36 (dd, *J* =1.7, 10.6 Hz, 1H), 3.85 (s, 1H), 3.56 (s, 1H), 1.18 (s, 6H), 1.06 (s, 6H).

^{13}C NMR (100 MHz, $CDCl_3$). δ 165.9, 130.5, 125.3, 47.9, 45.4, 21.1, 20.3.

HRMS (+ESI). Calculated: 178.1202 ($C_9H_{17}NONa$). Observed: 178.1201.

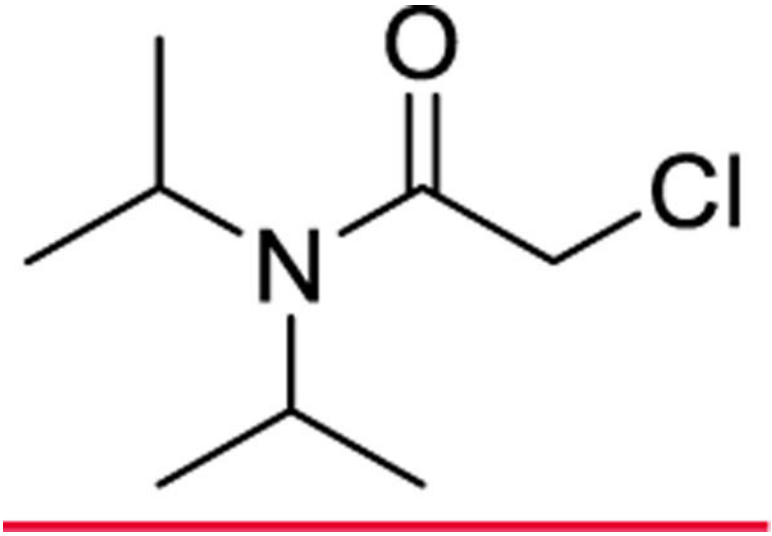

2-Chloro-N,N-diisopropylacetamide (TRH-1–168): To a solution diisopropylamine (0.42 mL, 3.0 mmol) in dichloromethane (10 mL) was added chloroacetyl chloride (0.29 mL, 3.6 mmol) followed by triethylamine (0.50 mL, 3.6 mmol) at 0°C under N_2 atmosphere. After stirring for 20 minutes, the reaction mixture was allowed to warm to room temperature and was stirred overnight. The solution was washed with saturated sodium bicarbonate solution and brine, dried with magnesium sulfate, and the resulting crude was purified by silica gel chromatography (0 to 20% ethyl acetate in hexanes) to yield 376 mg of white solid (70% yield).

^{1}H NMR (400 MHz, $CDCl_3$). δ 3.93 (s, 2H), 3.88–3.82 (m, 1H), 3.38–3.31 (m, 1H), 1.29 (d, J = 6.5 Hz, 6H), 1.14 (d, J = 6.4 Hz, 6H).

^{13}C NMR (100 MHz, $CDCl_3$). δ 165.0, 49.7, 46.1, 43.2, 20.7, 20.0.

HRMS (+ESI). Calculated: 200.0813 ($C_8H_{16}NOClNa$). Observed: 200.0811.

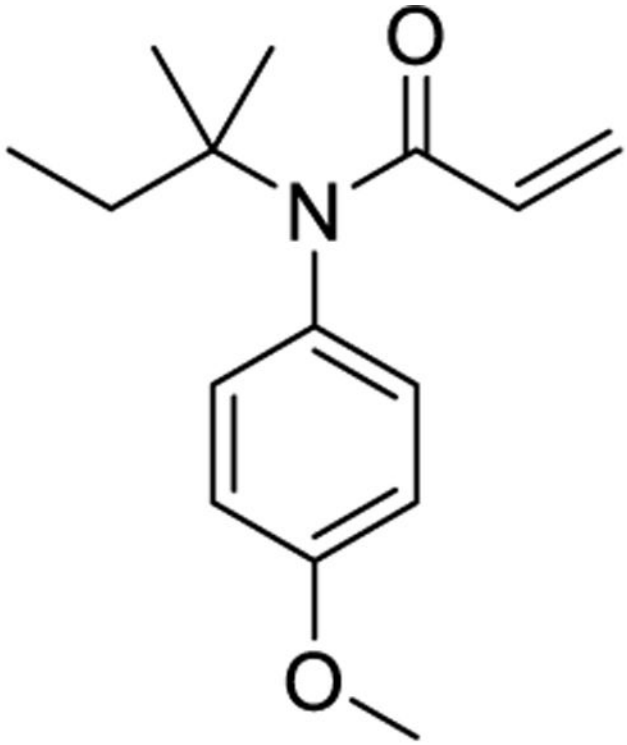

N-(4-methoxyphenyl)-N-(tert-pentyl)acrylamide (TRH-1–170): To a solution of 4-methoxy-*N*-(ferf-pentyl)aniline (94 mg, 0.49 mmol) in dichloromethane (5 mL) was added acryloyl chloride (0.05 mL, 0.6 mmol) followed by triethylamine (0.09 mL, 0.6 mmol) at 0°C under N_2 atmosphere. After stirring for 15 minutes, the reaction mixture was allowed to warm to room temperature and was stirred for 18 hours. The solution was washed with a saturated solution of sodium bicarbonate followed by brine, dried with magnesium sulfate, and the resulting crude was purified by silica gel chromatography (0% to 20% ethyl acetate in hexanes) to yield 82 mg of a pale-yellow oil (68% yield).

^{1}H NMR (400 MHz, $CDCl_3$). 5 6.99 (d, *J* = 8.7 Hz, 2H), 6.85 (d, *J* =8.7 Hz, 2H), 6.17 (dd, *J* =1.9, 16.7 Hz, 1H), 5.76 (dd, *J* = 10.3, 16.7 Hz, 1H), 5.28 (dd, *J* =1.9, 10.3 Hz, 1H), 3.81 (s, 3H), 2.11 (q, *J* =7.5 Hz, 2H), 1.20 (s, 6H), 0.91 (t, *J* =7.5 Hz, 3H).

^{13}C NMR (100 MHz, $CDCl_3$). δ 166.3, 159.0, 134.3, 131.49, 131.45, 125.6, 114.1, 61.7, 55.5, 32.0, 27.4, 9.4.

HRMS (+EI). Calculated: 247.1572 ($C_{15}H_{21}NO_2$). Observed: 247.1577.

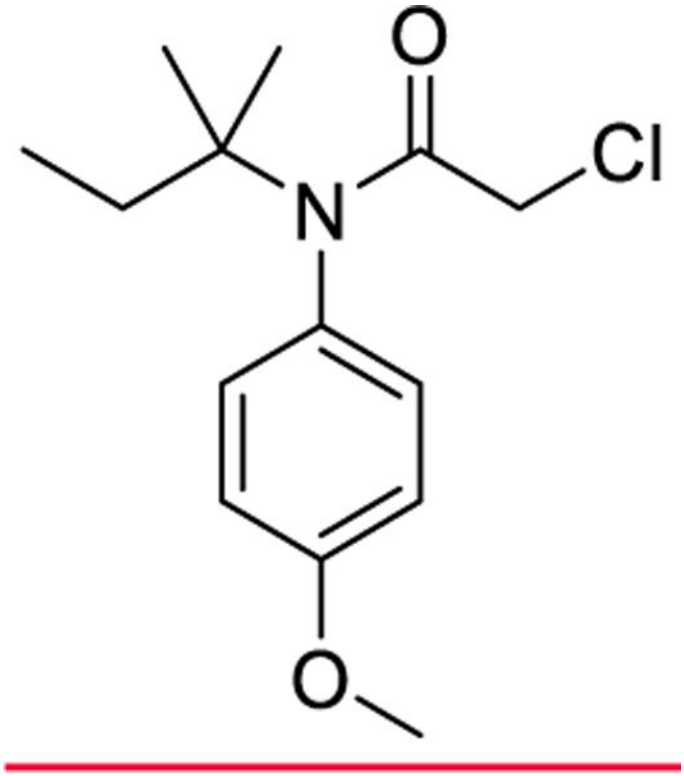

2-Chloro-N-(4-methoxyphenyl)-N-(tert-pentyl)acetamide (TRH-1–171): To a solution 4-methoxy-*N*-(*tert*-pentyl)aniline (95 mg, 0.5 mmol) in dichloromethane (5 mL) was added chloroacetyl chloride (0.05 mL, 0.6 mmol) followed by triethylamine (0.085 mL, 0.6 mmol) at 0°C under N_2 atmosphere. After stirring for 15 minutes, the reaction mixture was allowed to warm to room temperature and was stirred overnight. The solution was washed with saturated sodium bicarbonate solution and brine, dried with magnesium sulfate, and the resulting crude was purified by silica gel chromatography (0 to 10% ethyl acetate in hexanes) to yield 99 mg of a yellow oil (74% yield).

^{1}H NMR (400 MHz, $CDCl_3$). δ 7.04 (d, *J* = 8.6 Hz, 2H), 6.87 (d, *J* = 8.6 Hz, 2H), 3.80 (s, 3H), 3.63 (s, 2H), 2.05 (q, *J* = 7.4 Hz, 2H), 1.16 (s, 6H), 0.90 (t, *J* = 7.4 Hz, 3H).

^{13}C NMR (100 MHz, $CDCl_3$). δ 166.0, 159.5, 133.2, 131.0, 114.5, 62.5, 55.5, 44.8, 31.8, 27.1, 9.3.

HRMS (+ESI). Calculated: 270.1255 ($C_{14}H_{21}NO_2Cl$). Observed: 270.1254.

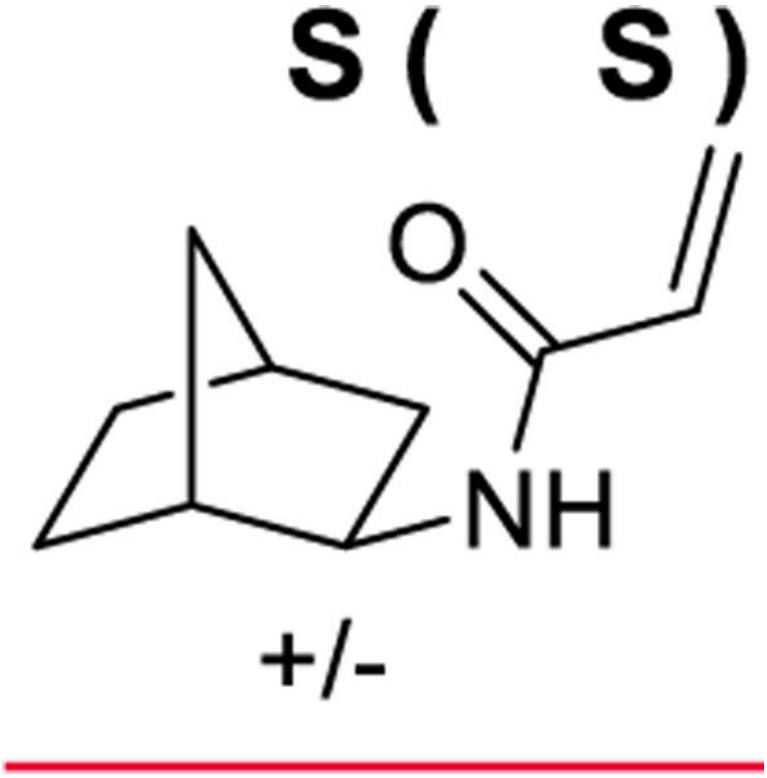

N-(exo-norborn-2-yl)acrylamide (TRH-1–176): To a solution of exo-2-aminonorbornane (0.24 mL, 2 mmol) in dichloromethane (10 mL) was added acryloyl chloride (0.20 mL, 2.4 mmol) followed by triethylamine (0.33 mL, 2.4 mmol) at 0°C under N_2 atmosphere. After stirring for 20 minutes, the reaction mixture was allowed to warm to room temperature and was stirred for 18 hours. The solution was washed with a saturated solution of sodium bicarbonate followed by brine, dried with magnesium sulfate, and the resulting crude was purified by silica gel chromatography (30% ethyl acetate in hexanes) to yield 271 mg of a white solid (82% yield).

^{1}H NMR (400MHz, $CDCl_3$). δ 6.42 (s, 1H), 6.25 (dd, *J* = 2.3,17.0 Hz, 1H), 6.18 (dd, *J* = 9.5,17.0 Hz, 1H), 5.58 (dd, *J* =2.3, 9.5 Hz, 1H), 3.8–3.77 (m, 1H), 2.27–2.24 (m, 2H), 1.78 (ddd, *J* =2.1, 8.1, 13.0 Hz, 1H), 1.55–1.38 (m, 3H), 1.30–1.10 (m, 4H).

^{13}C NMR (100 MHz, $CDCl_3$). δ 165.0, 131.4, 125.8, 52.9, 42.4, 40.0, 35.7, 35.6, 28.2, 26.6.

HRMS (+EI). Calculated:165.1154 ($C_{10}H_{15}NO$). Observed: 165.1155.

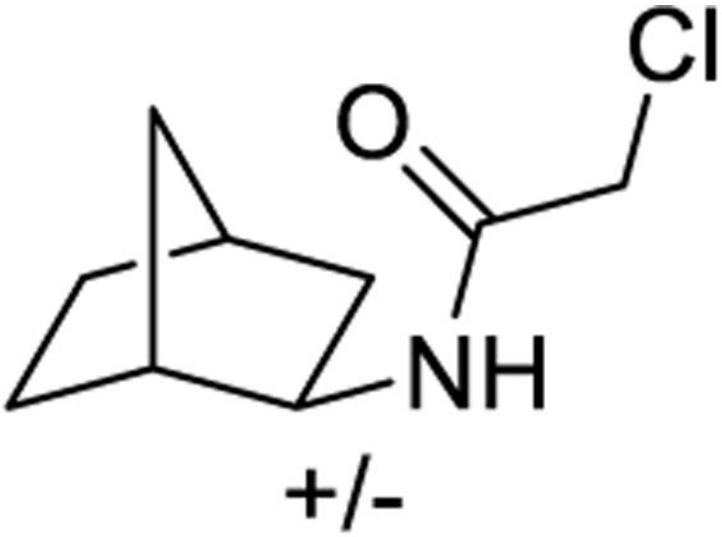

2-Chloro-N-(exo-norborn-2-yl)acetamide (TRH-1–177): To a solution of exo-2-aminonorbornane (0.24 mL, 2 mmol) in dichloromethane (10 mL) was added chloroacetyl chloride (0.19 mL, 2.4 mmol) followed by triethylamine (0.33 mL, 2.4 mmol) at 0°C under N_2 atmosphere. After stirring for 20 minutes, the reaction mixture was allowed to warm to room temperature and was stirred overnight. The solution was washed with saturated sodium bicarbonate solution and brine, dried with magnesium sulfate, and the resulting crude was purified by silica gel chromatography (20 to 40% ethyl acetate in hexanes) to yield 345 mg of a white solid (91% yield).

^{1}H NMR(400MHz, $CDCl_3$). δ 6.48 (s, 1H), 3.93 (s, 2H), 3.67–3.63 (m, 1H), 2.24–2.22 (m, 1H), 2.16–2.15(m,1H), 1.74 (ddd, *J* =1.9, 8.1, Hz, 1H), 1.50–1.36 (m, 2H), 1.30–1.26 (m, 1H), 1.21–1.14 (m, 3H), 1.09–1.03 (m, 1H).

^{13}C NMR (100 MHz, CDCl3). δ 165.0, 53.1, 42.6, 42.2, 40.0, 35.6, 35.5, 28.0, 26.3.

HRMS (+ESI). Calculated: 187.0764 ($C_9H_{14}NOCl$). Observed: 187.0765.

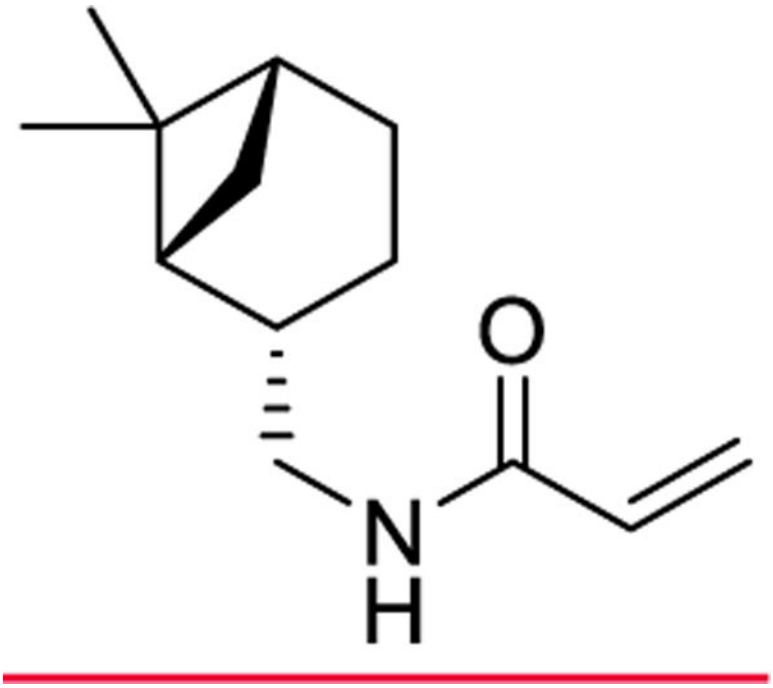

***N*-(((1 R,2S,5R)-6,6-dimethylbicyclo[3.1.1]heptan-2-yl)methyl)acrylamide (TRH-1–178):** To a solution of (−)-*cis*-myrtanylamine (0.34 mL, 2 mmol) in dichloromethane (10 mL) was added acryloyl chloride (0.20 mL, 2.4 mmol) followed by triethylamine (0.33 mL, 2.4 mmol) at 0°C under N_2 atmosphere. After stirring for 20 minutes, the reaction mixture was allowed to warm to room temperature and was stirred for 21 hours. The solution was washed with a saturated solution of sodium bicarbonate followed by brine, dried with magnesium sulfate, and the resulting crude was purified by silica gel chromatography (20 to 30% ethyl acetate in hexanes) to yield 369 mg of a white solid (89% yield).

^{1}H NMR (600 MHz, $CDCl_3$). δ 6.26 (dd, *J* =1.5,17.0 Hz, 1H), 6.11 (dd, *J* = 10.3,17.0 Hz, 1H) 5.85 (s, 1H), 5.61 (dd, *J* =1.5, 10.3 Hz, 1H), 3.39–3.29 (m, 2H), 2.38–2.34 (m, 1H), 2.26–2.21 (m, 1H), 1.98–1.90 (m, 4H), 1.88–1.83 (m, 1H), 1.53–1.47 (m, 1H), 1.19 (s, 3H), 1.04 (s, 3H), 0.89 (d, *J* = 9.6 Hz, 1H).

^{13}C NMR (150 MHz, $CDCl_3$). δ 165.7, 131.2, 126.2, 45.3, 43.9, 41.5, 38.8, 33.3, 28.1, 26.1, 23.3, 19.9.

HRMS (-ESI). Calculated: 206.1550 ($C_{13}H_{20}NO$). Observed: 206.1551.

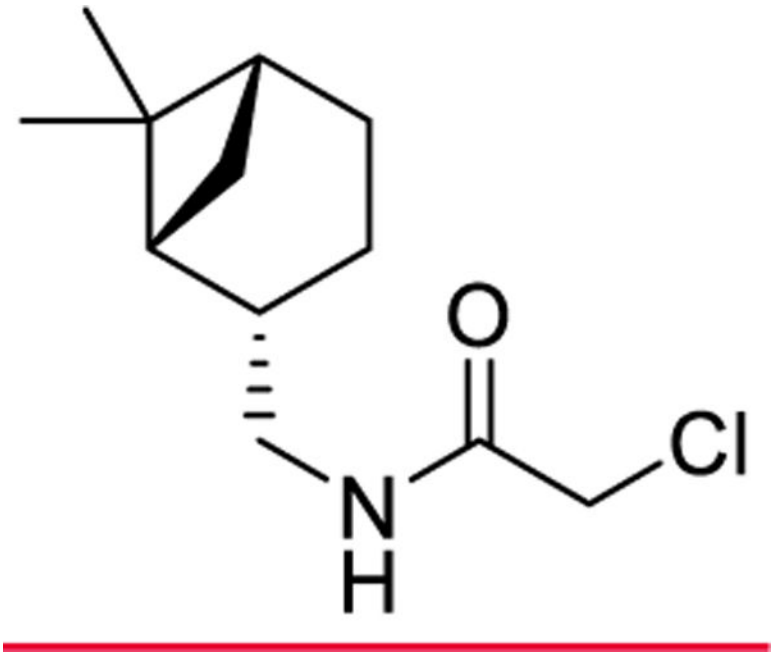

2-Chloro-N-(((1R,2S,5R)-6,6-dimethylbicyclo[3.1.1]heptan-2-yl)methyl)acetamide (TRH-1–179): To a solution of (−)-*cis*-myrtanylamine (0.34 mL, 2 mmol) in dichloromethane (10 mL) was added chloroacetyl chloride (0.19 mL, 2.4 mmol) followed by triethylamine (0.33 mL, 2.4 mmol) at 0°C under N_2 atmosphere. After stirring for 20 minutes, the reaction mixture was allowed to warm to room temperature and was stirred overnight. The solution was washed with saturated sodium bicarbonate solution and brine, dried with magnesium sulfate, and the resulting crude was purified by silica gel chromatography (0 to 20% ethyl acetate in hexanes) to yield 405 mg of an off-white solid (88% yield).

^{1}H NMR (600 MHz, $CDCl_3$). δ 6.61 (s, 1H), 4.05 (s, 2H), 3.33–3.30 (m, 2H), 2.40–2.36 (m, 1H), 2.27–2.21 (m, 1H), 1.99–1.83 (m, 5H), 1.53–1.46 (m, 1H), 1.20 (s, 3H), 1.05 (s, 3H), 0.90 (d, J = 9.7 Hz, 1H).

^{13}C NMR (150 MHz, $CDCl_3$). δ 165.8, 45.5, 43.8, 42.9, 41.4, 41.2, 38.8, 33.3, 28.0, 26.0, 23.3, 19.8.

HRMS (-ESI). Calculated: 228.1161 ($C_{12}H_{19}NOCl$). Observed: 228.1162.

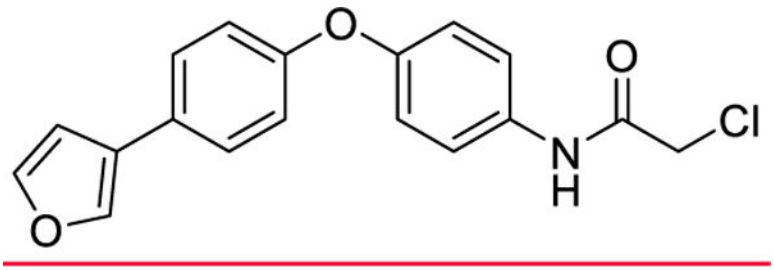

2-Chloro-N-(4-(4-(furan-3-yl)phenoxy)phenyl)acetamide (TRH-1–189): A reaction vial equipped with a stirbar was charged with 2-chloro-*N*-(4-(4-chlorophenoxy)phenyl)acetamide (**TRH-1–140**, 74 mg, 0.25 mmol), 3-furanylboronic acid (44 mg, 0.38 mmol), and XPhos-G3-palladacycle (4 mg, 2 mol%) and placed under a nitrogen atmosphere. THF (1 mL) and an aqueous solution of tribasic potassium phosphate (0.5M, 2 mL) that was freshly degassed by sparging with N_2 were sequentially added, and the reaction was stirred for 1 hour. The reaction mixture was diluted with water and extracted three times with diethyl ether. The combined organics were dried over magnesium sulfate, and the resulting crude was purified by silica gel chromatography (10% to 30% ethyl acetate in hexanes) to give 19 mg of a white solid (23% yield).

^{1}H NMR (400 MHz, $CDCl_3$). δ 7.50–7.47 (m, 2H), 7.43 (dt, *J* = 2.6, 9.8 Hz, 2H), 7.30–7.24 (m, 3H), 6.95 (dt, *J* = 2.6, 9.7 Hz, 2H), 6.90 (dt, *J* = 2.7, 9.7 Hz, 2H), 6.43 (s, 1H), 3.58 (s, 2H).

^{13}C NMR (100 MHz, $CDCl_3$). δ 168.5, 156.2, 153.3, 144.2, 141.2, 133.4, 129.7, 128.1, 121.8, 119.7, 119.6, 117.9, 111.2, 33.9.

HRMS (-ESI). Calculated: 326.0589 ($C_{18}H_{13}NO_3Cl$). Observed: 326.0594.

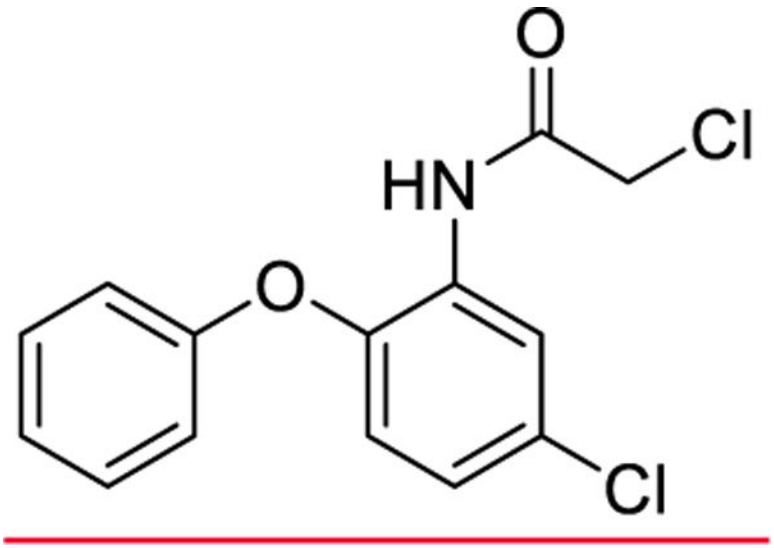

2-Chloro-N-(5-chloro-2-phenoxyphenyl)acetamide (TRH-1–191): To a solution of 2-amino-4-chlorophenyl phenyl ether (2.20 g, 10.0 mmol) in dichloromethane (30 mL) was added chloroacetyl chloride (0.96 mL, 12.0 mmol) followed by triethylamine (1.67 mL, 12 mmol) at 0°C under N_2 atmosphere. After stirring for 20 minutes, the reaction mixture was allowed to warm to room temperature and was stirred for 16 hours. The solution was diluted with DCM, washed with a saturated sodium bicarbonate solution and brine, dried with magnesium sulfate, and the resulting crude was recrystallized from hexanes to yield 1.84 g of light-brown solid (62% yield).

^{1}H NMR (400MHz, $CDCl_3$. δ 8.93 (s, 1H), 8.50 (d, *J* = 2.5 Hz, 1H), 7.40–7.35 (m, 2H), 7.19–7.15 (m, 1H), 7.04–7.01 (m,3H), 6.81 (d, *J* = 8.7 Hz, 1H), 4.16 (s, 2H).

^{13}C NMR (100 MHz, $CDCl_3$). δ 164.0, 156.0, 144.7, 130.2, 129.6, 129.2, 124.7, 124.5, 120.6, 118.71, 118.68, 43.1.

HRMS (-ESI). Calculated: 294.0094 ($C_{14}H_{10}NO_2Cl_2$). Observed: 294.0101.

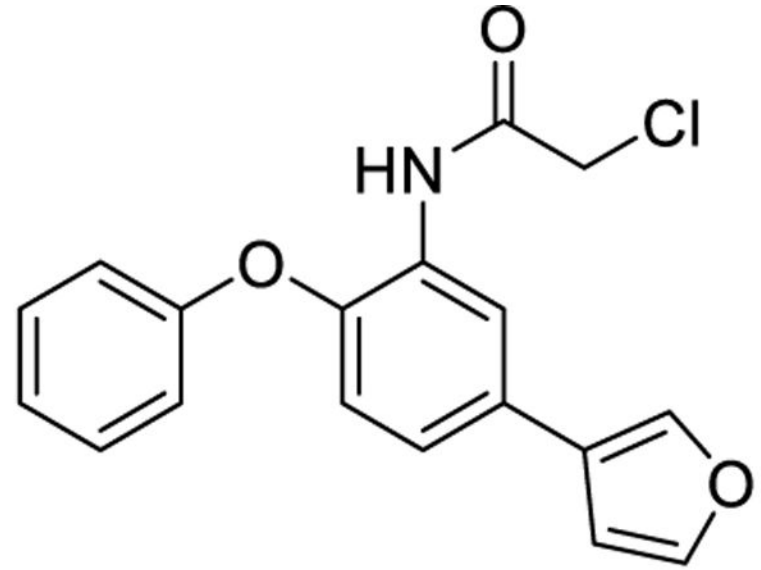

2-Chloro-N-(5-(furan-3-yl)-2-phenoxyphenyl)acetamide (TRH-1–194): A reaction vial equipped with a stirbar was charged with 2-chloro-N-(5-chloro-2-phenoxyphenyl)acetamide (**TRH-1–191**, 297 mg,

1.0 mmol), 3-furanylboronic acid (171 mg, 1.5 mmol), and XPhos-G3-palladacycle (17 mg, 2 mol%) and placed under a nitrogen atmosphere. THF (2 mL) and a freshly degassed aqueous solution of tribasic potassium phosphate (0.5M, 4 mL) were sequentially added, and the reaction was stirred for 6 hours. The reaction mixture was diluted with water and extracted three times with diethyl ether. The combined organics were dried over magnesium sulfate, and the resulting crude was purified by silica gel chromatography (10% to 15% ethyl acetate in hexanes) to give 120 mg of a yellow solid (37% yield).

^{1}H NMR (400 MHz, $CDCl_3$). δ 8.53 (d, J = 2.4 Hz, 1H), 7.93 (s, 1H), 7.33–7.25 (m, 4H), 7.12 (t, J = 7.4 Hz, 1H), 6.97 (dd, J = 2.5, 8.7 Hz, 1H), 6.84 (d, J = 7.8 Hz, 2H), 6.79 (d, J = 8.7 Hz, 1H), 6.23 (s, 6.23), 3.52 (s, 2H).

^{13}C NMR (100 MHz, $CDCl_3$). δ 168.6, 156.3, 144.0, 143.4, 141.1, 130.9, 130.1, 129.7, 124.0, 123.9, 120.7, 119.6, 117.5, 117.4, 111.0, 34.2.

HRMS (-ESI). Calculated: 326.0589 ($C_{18}H_{13}NO_3Cl$). Observed: 326.0585.

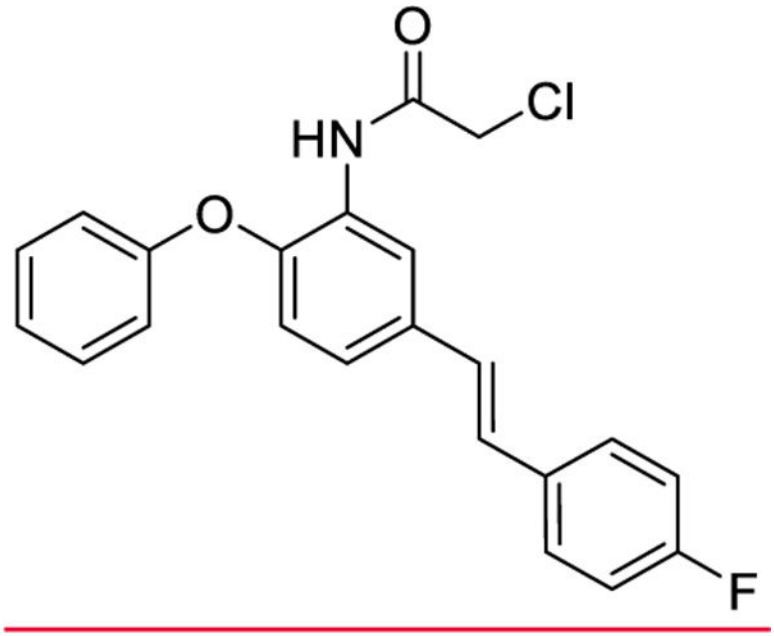

trans-2-Chloro-N-(5-(4-fluorostyryl)-2-phenoxyphenyl)acetamide (TRH-1–196): A reaction vial equipped with a stirbar was charged with 2-chloro-*N*-(5-chloro-2-phenoxyphenyl)acetamide (**TRH-1–191**, 296 mg, 1.0 mmol), frans-2-(4-fluorophenyl)vinylboronic acid (253 mg, 1.5 mmol), and XPhos-G3-palladacycle (17 mg, 2 mol%) and placed under a nitrogen atmosphere. THF (2 mL) and a freshly degassed aqueous solution of tribasic potassium phosphate (0.5M, 4 mL) were sequentially added, and the reaction was stirred for 21 hours. The reaction mixture was diluted with water and extracted three times with diethyl ether. The combined organics were dried over magnesium sulfate, and the resulting crude was purified by silica gel chromatography (5% to 15% ethyl acetate in hexanes) to give 256 mg of a yellow solid (67% yield).

^{1}H NMR (400 MHz, $CDCl_3$). δ 8.54 (d, *J* = 2.4 Hz, 1H), 8.00 (s, 1H), 7.27–7.20 (m, 4H), 7.10–7.06 (m, 1H), 6.99–6.93 (m, 3H), 6.84–6.79 (m, 3H), 6.47 (d, *J* =15.9 Hz, 1H), 6.17–6.10 (m, 1H), 3.27 (dd, *J* = 1.1, 7.3 Hz, 2H).

^{13}C NMR (100 MHz, $CDCl_3$). δ 168.8, 163.8, 161.3, 156.2, 143.5, 134.6, 132.59, 132.56, 130.9, 130.1, 129.6, 128.1, 128.0, 123.98, 123.96, 121.20, 121.18, 120.7, 119.5, 117.6, 115.7, 115.4, 41.8.

HRMS (+ESI). Calculated: 404.0824 ($C_{22}H_{17}NO_2ClFNa$). Observed: 404.0828.

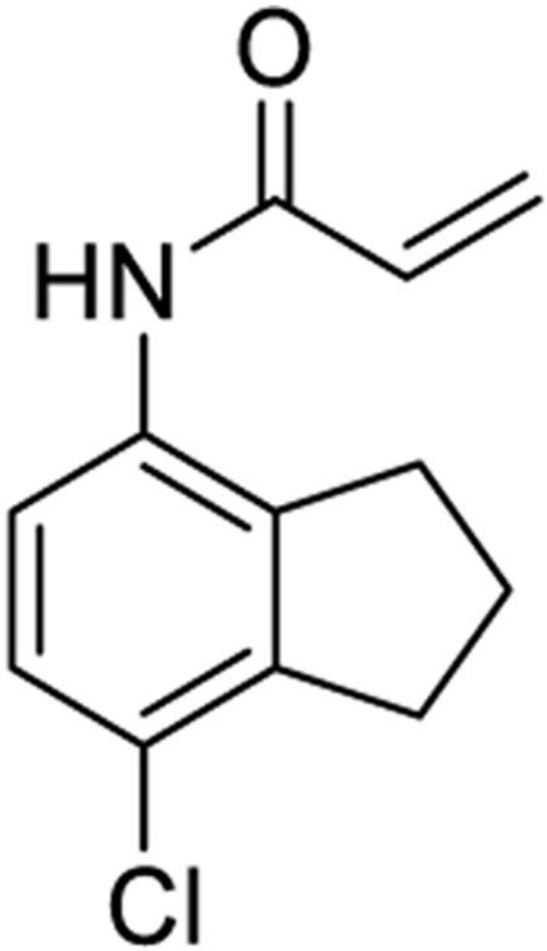

N-(7-chloro-2,3-dihydro-1H-inden-4-yl)acrylamide (YP-1–1): A solution of N-(2,3-dihydro-1H-inden-4-yl)acrylamide (187 mg, 1.0 mmol) in PEG 400 (5.2 mL) was cooled to 0°C. To the solution was added *N*-chlorosuccinimide (140 mg, 1.0 mmol). The solution was allowed to warm to room temperature after 30 min and stirred overnight. The solution was diluted with ethyl acetate and washed two times with brine and dried with magnesium sulfate. The crude product was purified via silica gel chromatography (30% ethyl acetate in hexanes). The obtained mixture of isomers was separated by recrystallization to afford the product in 22% yield as a white solid (47 mg).

^{1}H NMR (400MHz, $CDCl_3$). δ 7.78 (d, *J*=8.8 Hz, 1H), 7.15–7.11 (m, 2H), 6.42 (dd, *J*= 1.4, 16.8 Hz, 1H), 6.26 (dd, *J*=10.2, 16.8 Hz, 1H), 5.77 (dd, *J*= 1.4, 10.2 Hz, 1H), 2.98 (t, *J*=7.6 Hz, 2H), 2.87 (t, *J*= 7.5 Hz, 2H), 2.12 (quint, *J*= 7.5 Hz, 2 H).

^{13}C NMR (100MHz, $CDCl_3$). δ 163.4, 143.1, 136.1, 132.2, 131.0, 128.0, 127.2, 126.7, 120.9, 32.7, 31.1, 24.0.

HRMS (+ESI). Calculated: 220.0535 ($C_{12}H_{11}ClNO$). Observed: 220.0533.

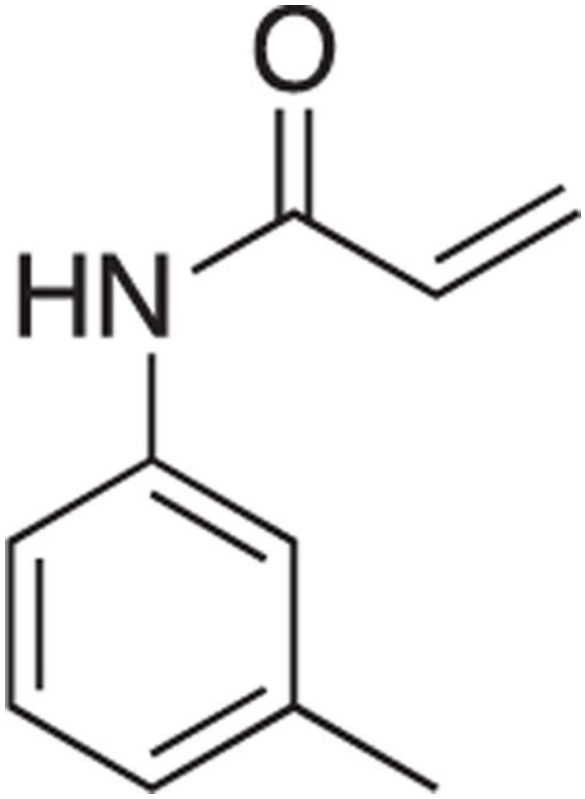

N-(m-tolyl)acrylamide (YP-1–16): A solution of o-toluidine (107 mg, 1.0 mmol) in DCM (10 mL) was cooled to 0°C. To the solution was added acryloyl chloride (109 mg, 1.2 mmol) followed by triethylamine (121 mg, 1.2 mmol). The solution was allowed to warm to room temperature after 40 min and stirred overnight. The solution was washed two times with brine and dried with magnesium sulfate. The crude product was purified via silica gel chromatography (20% to 40% ethyl acetate in hexanes) to afford the product in 86% yield as a white solid (139 mg).

^{1}H NMR (400MHz, $CDCl_3$). 5 7.82 (d, *J* = 7.9 Hz, 1H), 7.32 (s, 1H), 7.21–7.17 (m, 2H), 7.10–7.06 (m, 1H), 6.43–6.38 (m, 1H), 6.29 (dd, *J* = 10.2, 17.1 Hz, 1H), 5.75–5.72 (m, 1H), 2.25 (s, 1H).

^{13}C NMR (100MHz, $CDCl_3$). δ 135.5, 131.2, 130.5, 127.5, 126.8, 125.5, 123.4, 17.8.

HRMS (+ESI). Calculated: 162.0913 ($C_{10}H_{12}NO$). Observed: 162.0912.

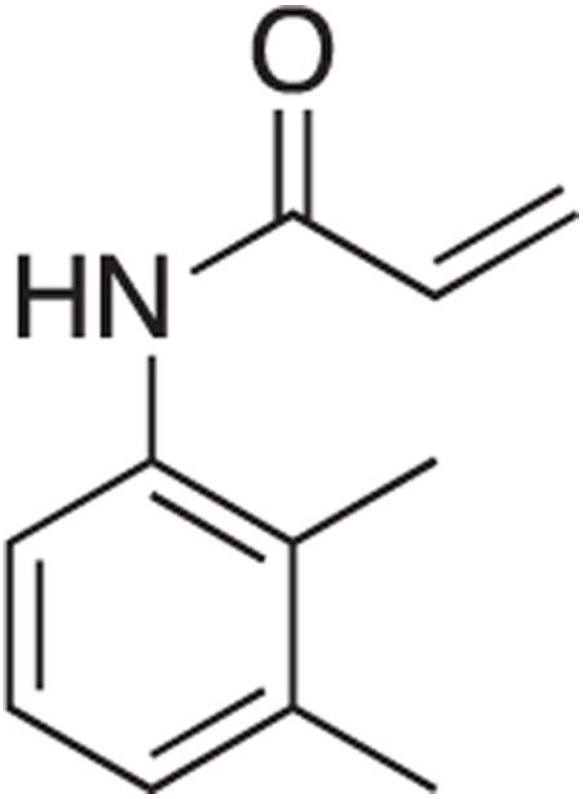

N-(2,3-dimethylphenyl)acrylamide (YP-1–18): A solution of 2,3-dimethylaniline (121 mg, 1.0 mmol) in DCM (10 mL) was cooled to 0°C. To the solution was added acryloyl chloride (109 mg, 1.2 mmol) followed by triethylamine (121 mg, 1.2 mmol). The solution was allowed to warm to room temperature after 29 min and stirred overnight. The solution was washed two times with brine and dried with magnesium sulfate. The crude product was purified via silica gel chromatography (30% to 40% ethyl acetate in hexanes) to afford the product in 88% yield as a white solid (154 mg).

^{1}H NMR (400MHz, $CDCl_3$). δ 7.49 (d, *J* = 7.9 Hz, 1H), 7.29 (s, 1H), 7.11–7.07 (m, 1H), 7.01 (d, *J* = 7.7,1H) 6.40 (d, *J* =17.1, 1H), 6.30 (dd, *J* =7.3, 17.1 Hz, 1H), 5.74 (d, *J* =10.1 Hz, 1H), 2.29 (s, 1H), 2.13 (s, 1H).

^{13}C NMR (100MHz, $CDCl_3$). δ 135.1, 131.2, 127.6, 127.3, 125.9, 122.3, 20.6, 13.9.

HRMS (+ESI). Calculated: 176.1070 ($\hat{C}H_{14}NO$). Observed: 176.1068.

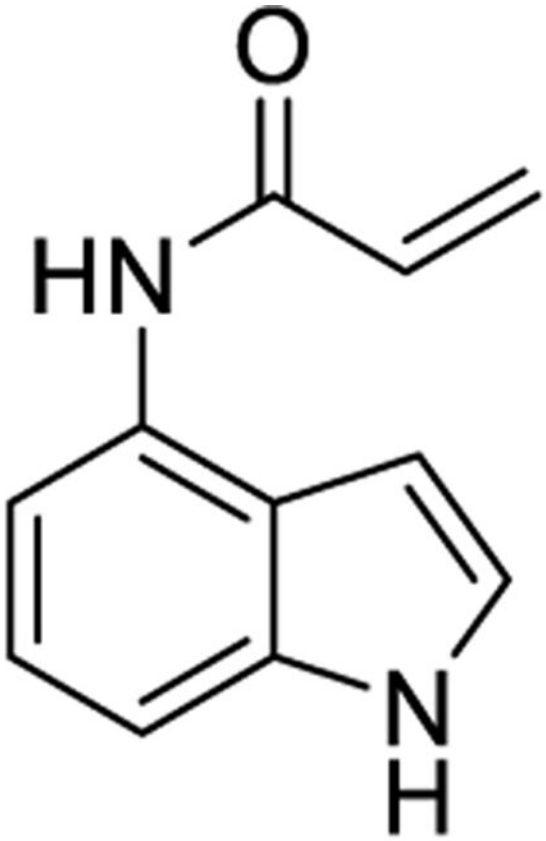

N-(1H-indol-4-yl)acrylamide (YP-1–19): A solution of 4-aminoindole (132 mg, 1 mmol) in DCM (5 mL) and DMF (5 mL) was cooled to 0°C. To the solution was added acryloyl chloride (109 mg, 1.2 mmol) followed by triethylamine (121 mg, 1.2 mmol). The solution was allowed to warm to room temperature after 26 min and stirred overnight. The solution was washed two times with brine and dried with magnesium sulfate. The crude product was purified via basic alumina chromatography (60% to 75% ethyl acetate in hexanes) to afford the product in 30% yield as a white-grey solid (56 mg).

^{1}H NMR (600MHz, MeOD). δ 7.51 (d, *J* = 7.6 Hz, 1H), 7.24–7.22 (m, 2H), 7.08 (t, *J* = 7.6 Hz, 1H), 6.64 (dd, *J* = 10.1, 16.7 Hz, 2H), 6.38 (dd, *J* =1.7, 16.9 Hz, 1H), 5.78 (dd, *J* =1.7, 10.3 Hz, 1H), 4.6 (s, 1H).

^{13}C NMR (150MHz, MeOD). δ 165.0, 137.2, 131.1, 129.2, 126.0, 123.8, 121.5, 120.9, 112.2, 108.4, 98.5.

HRMS (+ESI). Calculated: 187.0866 ($C_{11}H_{11}O$). Observed: 187.0865.

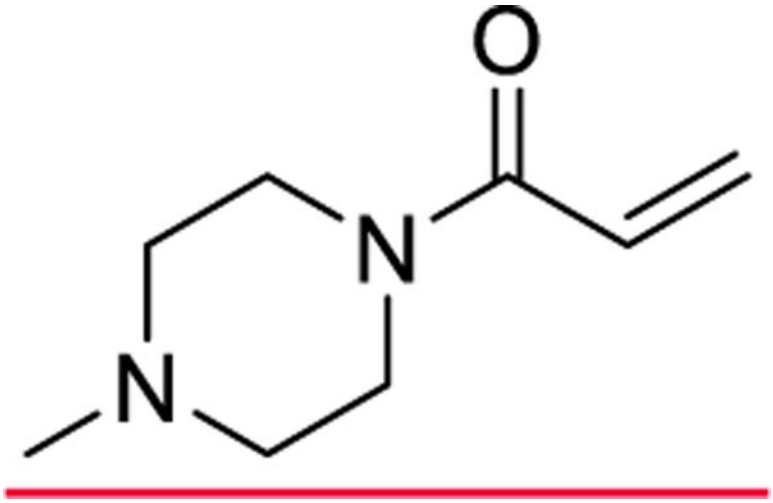

1-(4-Methylpiperazin-1-yl)prop-2-en-1-one (YP-1–22): A solution of 1-methylpiperazine (100 mg, 1.0 mmol) in DCM (10 mL) was cooled to 0°C. To the solution was added acryloyl chloride (109 mg, 1.2 mmol) followed by triethylamine (121 mg, 1.2 mmol). The solution was allowed to warm to room temperature after 30 min and stirred overnight. The solution was washed two times with brine and dried with magnesium sulfate. The crude product was purified via silica gel chromatography (85% to 100% ethyl acetate in hexanes) to afford the product in 29% yield as a yellow gel (44 mg).

^{1}H NMR (400MHz, $CDCI_3$). δ 6.56 (dd, *J* = 10.6, 16.9 Hz, 1H), 6.29 (dd, *J* =2.0, 16.8 Hz, 1H), 5.69 (dd, *J* = 2.0, 10.6 Hz, 1H), 3.71 (s, 2H), 3.58 (s, 2H), 2.42 (t, *J* = 5.1 Hz, 4H), 2.32 (s, 3H).

^{13}C NMR (100MHz, CDCI3). δ 165.4, 127.8, 127.5, 55.2, 54.6, 46.0, 45.7, 41.9.

HRMS (+ESI). Calculated: 155.1179 ($C_8H_{15}N_2O$). Observed: 155.1178.

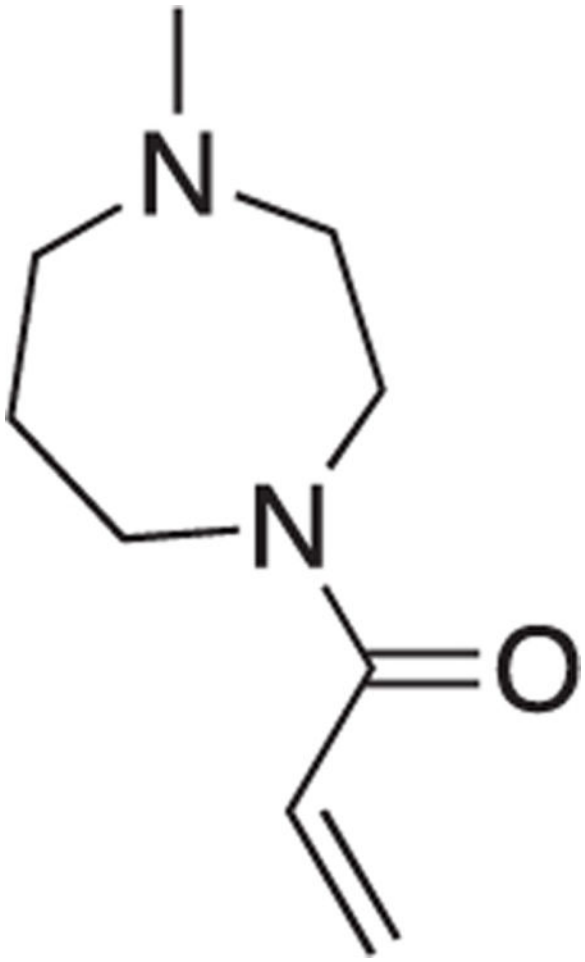

1-(4-methyl-1,4-diazepan-1-yl)prop-2-en-1-one (YP-1–23): A solution of 1-methylhomopiperazine (114 mg, 1.0 mmol) in DCM (10 mL) was cooled to 0°C. To the solution was added acryloyl chloride (109 mg, 1.2 mmol) followed by triethylamine (121 mg, 1.2 mmol). The solution was allowed to warm to room temperature after 32 minutes and stirred overnight. The solution was washed two times with brine and dried with magnesium sulfate. The crude product was purified via silica gel chromatography (1% to 10% methanol in DCM) to afford the product in 51% yield as a yellow oil (58 mg).

^{1}H NMR (400MHz, $CDCl_3$). δ 6.61–6.53 (m, 1H), 6.35–6.29 (m, 1H), 5.70–5.66 (m, 1H), 3.74–3.72 (m, 1 H), 3.69 (t, *J* = 6.4 Hz, 1H), 3.65–3.61 (m, 2H), 2.66–2.63 (m, 2H), 2.59–2.54 (m, 2H), 2.37 (s, 3H), 1.94 (quint, *J* = 6.2 Hz, 2H).

^{13}C NMR (100MHz, $CDCl_3$). δ 166.4, 166.3, 128.0, 127.9, 127.8, 127.6, 59.1, 58.0, 57.1, 56.8, 47.4, 47.1, 46.7, 46.6, 45.3, 44.8, 28.1, 26.9.

HRMS (+ESI). Calculated: 169.1335 ($C_9H_{17}N_2O$). Observed: 169.1333.

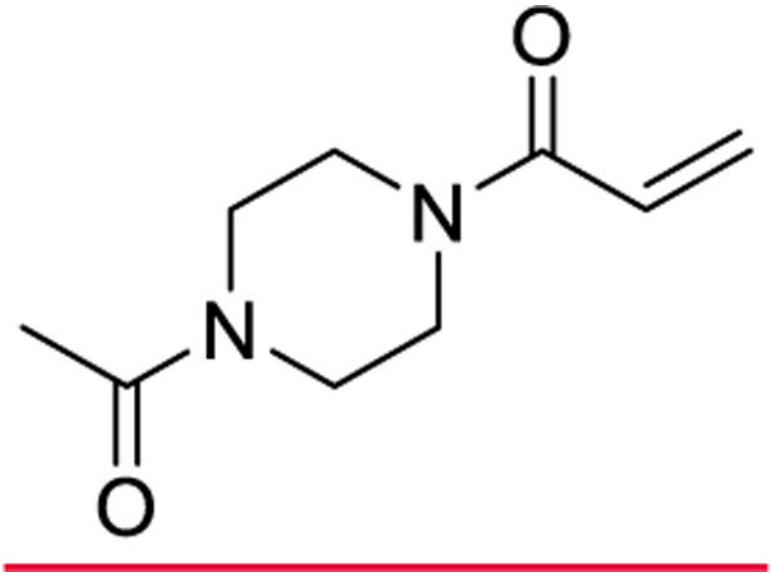

1-(4-acetylpiperazin-1-yl)prop-2-en-1-one (YP-1–24): A solution of 1-acetylpiperazine (128 mg, 1.0 mmol) in DCM (10 mL) was cooled to 0°C. To the solution was added acryloyl chloride (109 mg, 1.2 mmol) followed by triethylamine (121 mg, 1.2 mmol). The solution was allowed to warm to room temperature after 23 minutes and stirred for two hours. The solution was washed two times with brine and dried with magnesium sulfate. The crude product was purified via silica gel chromatography (0% to 10% methanol in DCM) to afford the product in 18% yield as a yellow oil (40 mg).

^{1}H NMR (400MHz, $CDCl_3$). δ 6.57 (dd, *J*=10.5, 16.8 Hz, 1H), 6.33 (dd, *J* = 1.8, 16.8 Hz, 1H), 5.75 (dd, *J*=1.9, 10.5 Hz, 1H), 3.72 (s, 1H), 3.66–3.64 (m, 3H), 3.57 (s, 1H), 3.51–3.49 (m, 2H), 2.13 (s, 3H).

^{13}C NMR (100MHz, $CDCl_3$). δ 165.6, 128.7, 127.0, 41.9, 41.4, 21.4.

HRMS (+ESI). Calculated: 183.1128 ($C_9H_{15}N_2O_2$). Observed: 183.1126.

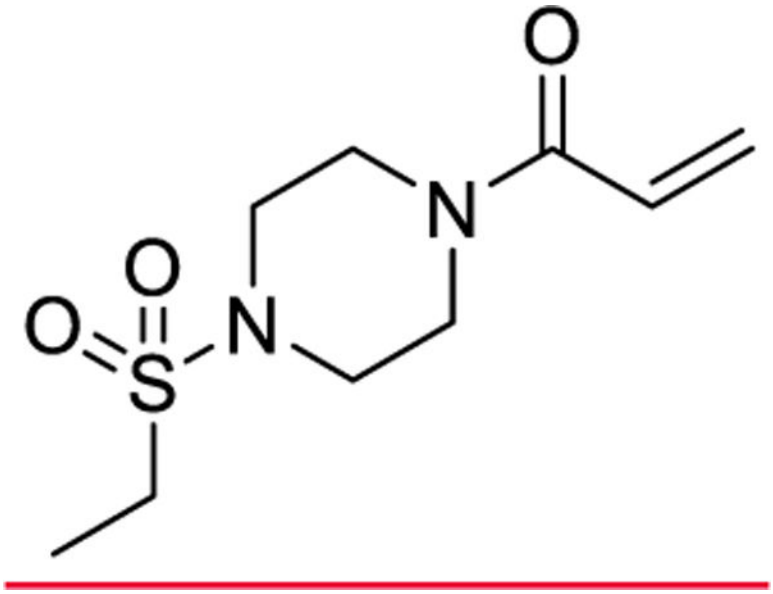

1-(4-(Ethylsulfonyl)piperazin-1-yl)prop-2-en-1-one (YP-1–25): A solution of 1-(ethanesulfonyl)piperazine (178 mg, 1.0 mmol) in DCM (10 mL) was cooled to 0°C. To the solution was added acryloyl chloride (109 mg, 1.2 mmol) followed by triethylamine (121 mg, 1.2 mmol). The solution was allowed to warm to room temperature after 27 min and stirred for two hours. The solution was washed two times with brine and dried with magnesium sulfate. The crude product was purified via silica gel chromatography (1% to 10% methanol in DCM) to afford the product in 70% yield as a white-yellow solid (163 mg).

^{1}H NMR (400MHz, $CDCl_3$). δ 6.57 (dd, *J* =10.5, 16.8 Hz, 1H), 6.32 (dd, *J* = 1.9, 16.8 Hz, 1H), 5.76 (dd, *J* =1.8, 10.5 Hz, 1H), 3.77 (s, 2H), 3.67 (s, 2H), 3.32 (t, *J* = 5.2 Hz, 4H), 2.98 (q, *J* = 7.5 Hz, 2H), 1.37 (t, *J* = 7.4, 3H).

^{13}C NMR (100MHz, $CDCl_3$). δ 165.5, 128.8, 127.0, 77.4, 45.9, 45.6, 44.2, 41.9, 7.8.

HRMS (+ESI). Calculated: 233.0954 ($C_9H_{17}N_2O_3S_1$). Observed: 233.0953.

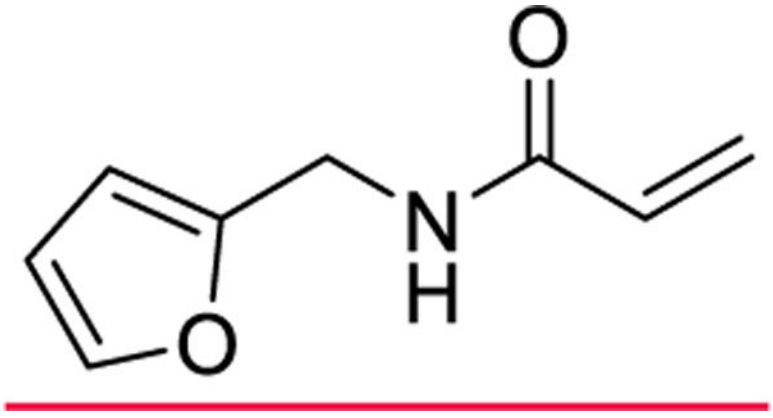

N-(Furan-2-ylmethyl)acrylamide (YP-1–26): A solution of furfurylamine (97 mg, 1.0 mmol) in DCM (10 mL) was cooled to 0°C. To the solution was added acryloyl chloride (109 mg, 1.2 mmol) followed by triethylamine (121 mg, 1.2 mmol). The solution was allowed to warm to room temperature after 17 min and stirred for two and a half hours. The solution was washed two times with brine and dried with magnesium sulfate. The crude product was purified via silica gel chromatography (35% to 70% ethyl acetate in hexanes) to afford the product in 86% yield as a white solid (132 mg).

^{1}H NMR (400MHz, $CDCl_3$). δ 7.33 (s, 1H), 6.60 (s, 1H), 6.31–6.22 (m, 3H), 6.15 (dd, *J* = 10.1,16.9 Hz, 1H), 5.63 (dd, *J* = 1.6,10.1 Hz, 1H), 4.48 (d, *J* = 5.6 Hz, 2H).

^{13}C NMR (100MHz, $CDCl_3$). δ 165.5, 151.2, 142.2, 130.6, 126.8, 110.5, 107.5, 36.5.

HRMS (+ESI). Calculated: 152.0706 ($C_8H_{10}O_2N_1$). Observed: 152.0706.

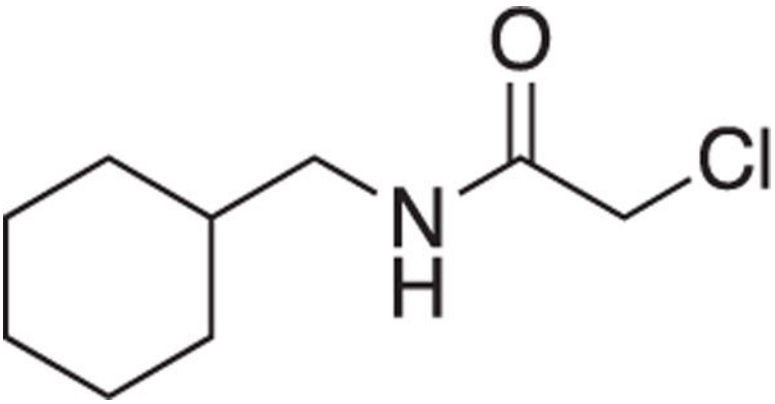

2-chloro-N-(cyclohexylmethyl)acetamide (YP-1–31): Following **General Procedure B** starting from cyclohexanemethylamine (113 mg, 1.0 mmol), product was obtained after silica gel chromatography (100% dichloromethane to 3% methanol in dichloromethane) in 60% yield as a white solid (112 mg).

^{1}H NMR (400MHz, $CDCl_3$). δ 6.70 (s, 1H), 4.06 (s, 2H), 3.15 (t, *J* = 6.47 Hz, 2H), 1.77–1.65 (m, 5H), 1.56–1.46 (m, 1H), 1.30–1.10 (m, 3H), 1.00–0.90 (m, 2H).

^{13}C NMR (100MHz, $CDCl_3$) δ 165.8, 58.1, 46.0, 42.8, 37.7, 30.7, 26.3, 25.7, 18.2.

HRMS (+ESI). Calculated: 190.0993 ($C_9H_{17}ONCl$). Observed: 190.0992.

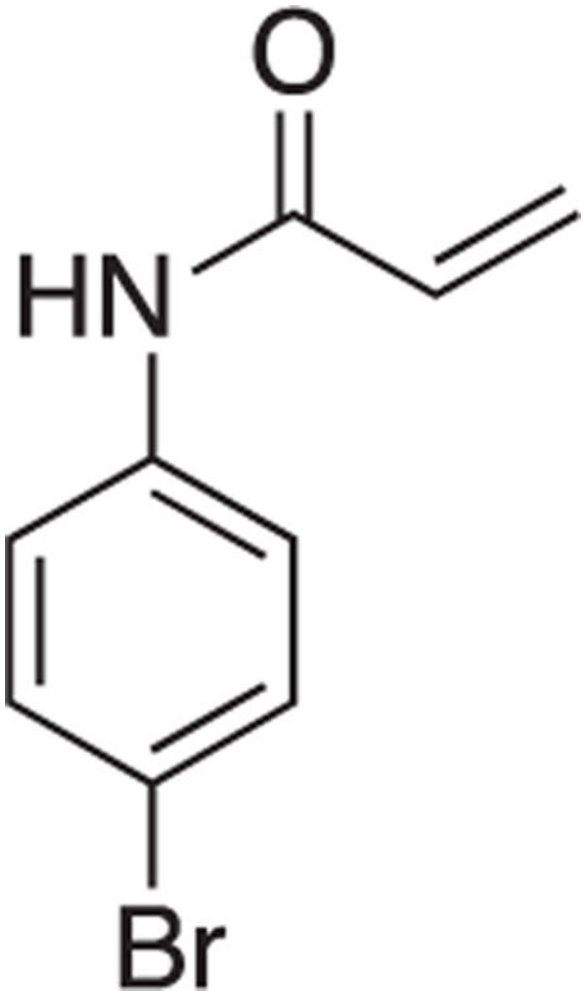

N-(4-bromophenyl)acrylamide (YP-1–36): Following **General Procedure A** starting from 4-bromoaniline (688 mg, 4.0 mmol), product was obtained after silica gel chromatography (30% to 60% ethyl acetate in hexanes) in 28% yield as a white solid (250 mg).

^{1}H NMR (400MHz, CD_3OD). δ 7.90 (s, 1H), 7.60–7.56 (m, 2H), 7.47–7.44 (m, 2H), 6.45–6.33 (m, 2H), 5.78 (dd, J = 2.8, 9.1 Hz, 1H).

^{13}C NMR (100MHz, CD_3OD). δ 164.7, 137.7, 131.4, 130.9, 126.7, 121.5, 116.3, 101.1, 78.1.

HRMS (+ESI). Calculated: 223.9716 (C_9H_7NOBr). Observed: 223.9719.

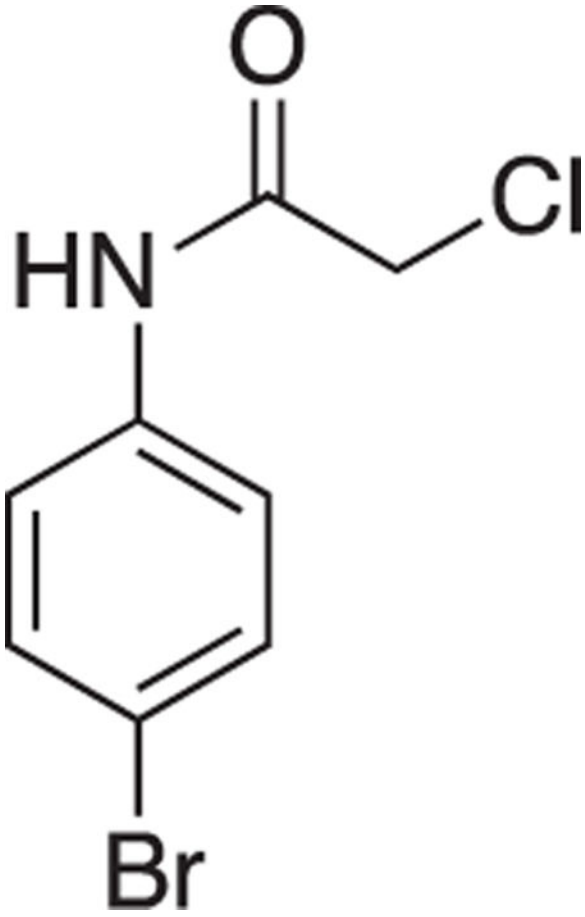

N-(4-bromophenyl)-2-chloroacetamide (YP-1–37): Following **General Procedure B** starting from 4-bromoaniline (688 mg, 4.0 mmol), product was obtained after silica gel chromatography (30% to 60% ethyl acetate in hexanes) in 49% yield as a white solid (491 mg).

^{1}H NMR (400MHz, CD_3OD). δ 7.9 (s, 1H), 7.57–7.53 (m, 2H), 7.50–7.47 (m, 2H), 4.17 (s, 2H).

^{13}C NMR (100MHz, CD_3OD). δ 166.0, 137.2, 131.5, 121.6, 116.7, 99.3, 78.1, 42.6.

HRMS (+ESI). Calculated: 245.9327 ($C_8H_6NOBrCl$). Observed: 245.9329.

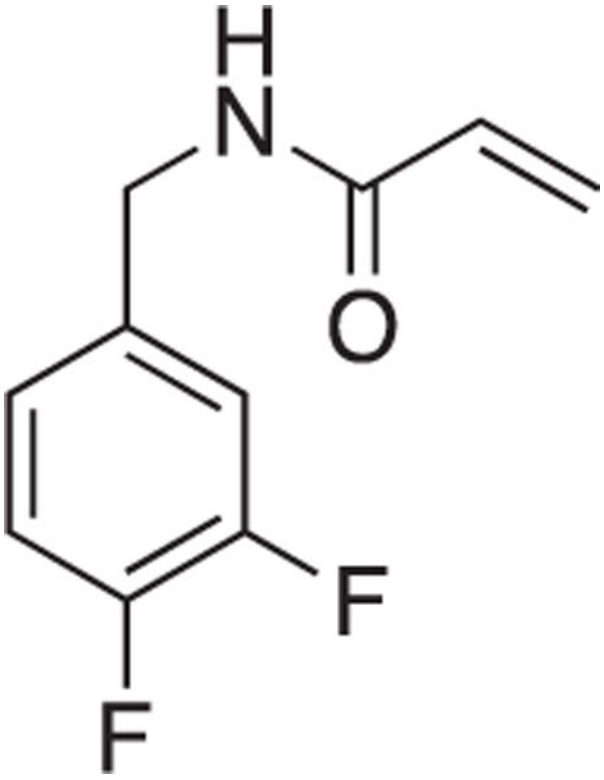

N-(3,4-difluorobenzyl)acrylamide (YP-1–38): Following **General Procedure A** starting from 3,4-difluorobenzylamine (286 mg, 2.0 mmol), product was obtained after silica gel chromatography (40% to 80% ethyl acetate in hexanes) in 61% yield as a white solid (239 mg).

^{1}H NMR (400MHz, $CDCl_3$). δ 7.56 (t, *J* = 6.2, 1H), 7.07–7.00 (m, 2H), 6.95–6.91 (m, 1H), 6.21–6.20 (m, 2H), 5.62–5.59 (m, 1H), 4.35 (d, *J* =6.1, 2H).

^{13}C NMR (100MHz, $CDCl_3$). δ 166.1, 151.4 (d), 150.7 (d), 148.9 (d), 148.2 (d), 135.5–135.4 (m), 130.5, 126.8, 123.5–123.4 (m), 117.2 (d), 116.3 (d), 42.4.

HRMS (+ESI). Calculated: 196.0579 ($C_{10}H_8NOF_2$). Observed: 196.0582.

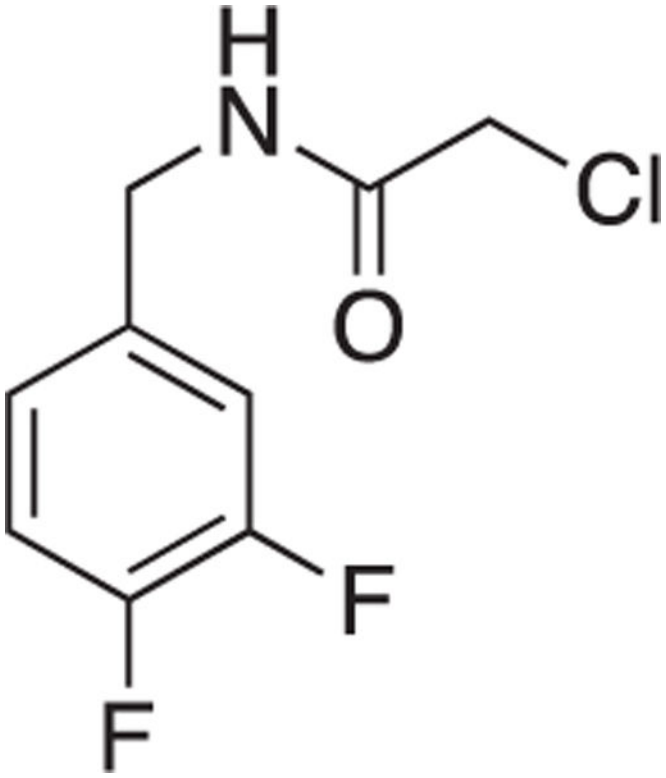

2-chloro-N-(3,4-difluorobenzyl)acetamide (YP-1–39): Following **General Procedure B** starting from 3,4-difluorobenzylamine (286 mg, 2.0 mmol), product was obtained after silica gel chromatography (40% to 50% ethyl acetate in hexanes) in 82% yield as a white solid (359 mg).

^{1}H NMR (400MHz, $CDCl_3$). δ 7.23 (s, 1H), 7.15–7.08 (m, 2H), 7.03–7.6.99 (m, 1H), 4.42 (d, J = 6.1 Hz, 2H), 4.08 (s, 2H).

^{13}C NMR (100MHz, $CDCl_3$). δ 166.3,151.5 (d), 151.0 (d), 149.1 (d), 148.5 (d), 134.7–134.6 (m), 123.7–123.6 (m), 117.5 (d), 116.6 (d), (d).

HRMS (+ESI). Calculated: 218.0190 ($C_9H_7NOClF_2$). Observed: 218.0192

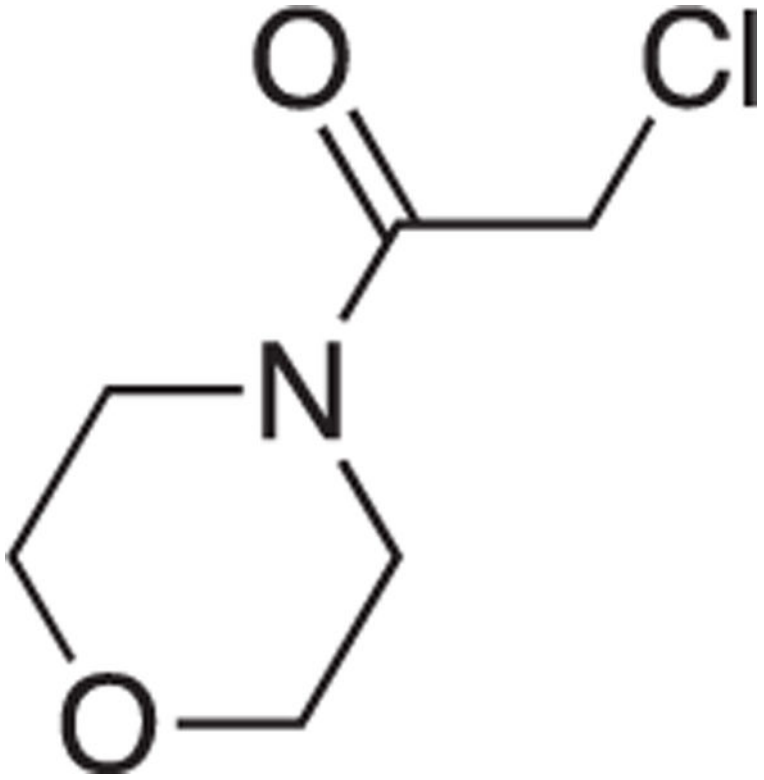

2-chloro-1-morpholinoethan-1-one (YP-1–40): Following **General Procedure B** starting from morpholine (174 mg, 2.0 mmol), product was obtained after silica gel chromatography (85% ethyl acetate in hexanes) in 61% yield as a white solid (200 mg).

^{1}H NMR (400MHz, $CDCl_3$). δ 4.01 (s, 2H), 3.65–3.59 (m, 4H), 3.55–3.52 (m, 2H), 3.45 (t, J = 4.8 Hz, 2H).

^{13}C NMR (100MHz, $CDCl_3$). δ 165.1, 66.5 (d), 46.6, 42.4, 40.7.

HRMS (+ESI). Calculated: 186.0292 ($C_6H_{10}O_2NClNa$). Observed: 186.0292.

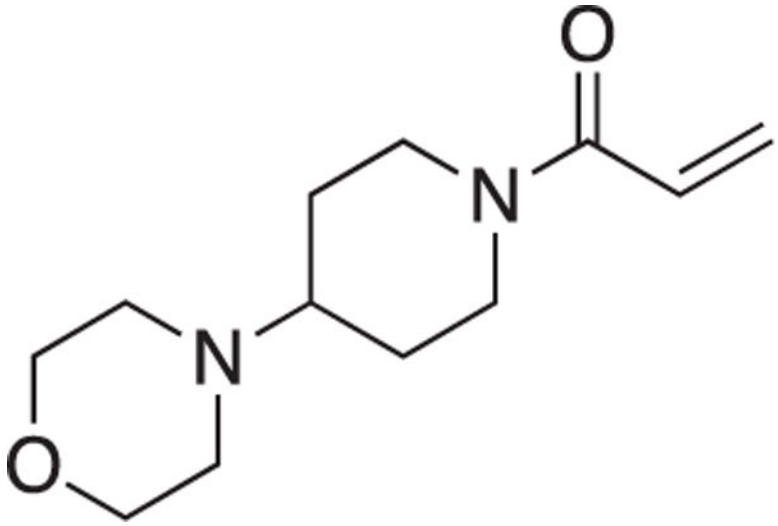

1-(4-morpholinopiperidin-1-yl)prop-2-en-1-one (YP-1–42): Following **General Procedure A** starting from 4-morpholinopiperidine (336 mg, 2.0 mmol), product was obtained after silica gel chromatography (1% methanol and 80% ethyl acetate in hexanes) in 58% yield as a colorless oil (259 mg).

^{1}H NMR(400MHz, $CDCl_3$). 5 6.42 (dd, *J*=10.6, 16.8 Hz, 1H), 6.06 (dd, *J* = 2.0,16.8 Hz, 1H), 5.49 (dd, *J* = 2.0,10.6Hz,1H),4.45(d, *J* = 12.8 Hz, 1H), 3.86 (d, *J* = 12.8 Hz, 1H), 3.52 (t, *J* = 4.7 Hz, 4H), 2.90 (t, *J* = 12.8 Hz, 1H),2.55–2.48 (m, 1H), 2.37–2.35 (m,4H), 2.26 (tt, *J* = 3.7, 11.0 Hz, 1H), 1.72 (d, *J* = 12.8 Hz, 2H), 1.30–1.20 (m, 2H).

^{13}C NMR (100MHz, $CDCl_3$). δ 165.0, 127.7, 127.3, 67.1, 61.6, 49.6, 44.9, 41.1, 28.9, 27.8.

HRMS (+ESI). Calculated: 225.1598 ($C_{12}H_{21}N_2O_2$). Observed: 225.1595.

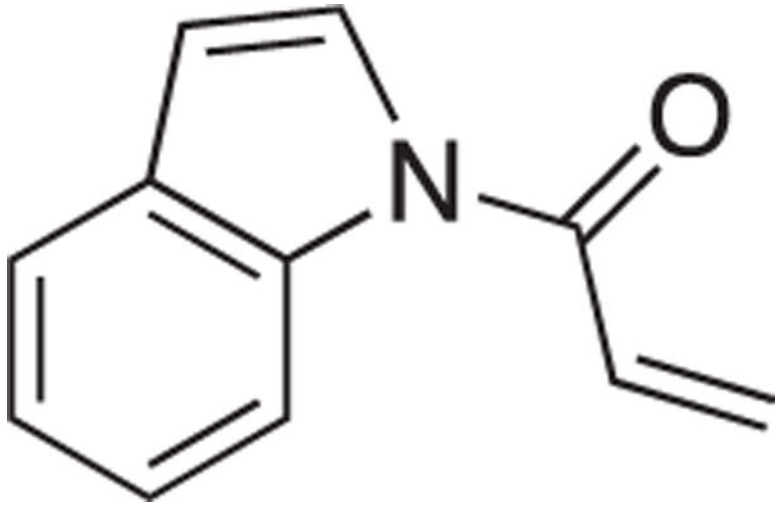

1-(1 H-indol-1-yl)prop-2-en-1-one (YP-1–44): A solution of indole (117 mg, 1.0 mmol) in 2-methyltetrahydrofuran (10 mL) was cooled to 0°C. To the solution was added sodium hydride (60 mg, 2.5 mmol). The resultant intermediate was subjected to **General Procedure**

A and product was obtained after alumina gel chromatography (10% to 40% ethyl acetate in hexanes) in 8% yield as a white solid (14 mg).

^{1}H NMR(400MHz, CD3OD). δ 8.48–8.46 (m,1H), 7.82 (d, *J* = 3.9 Hz,1H), 7.61–7.59 (m, 1H), 7.36–7.32 (m,1H),7.31–7.21(m, 2H),6.73 (dd, *J* =0.8, 3.8 Hz, 1H), 6.64 (dd, *J* =1.7, 16.7 Hz, 1H), 6.09 (dd, *J* =1.7, 10.5 Hz, 1H).

^{13}C NMR (100MHz, CD_3OD). δ 164.3, 135.7, 131.0, 130.9, 128.0, 125.0, 124.4, 123.6, 120.5, 116.2, 108.9.

HRMS (+ESI). Calculated: 172.0757 ($C_{11}H_{10}NO$). Observed: 172.0756.

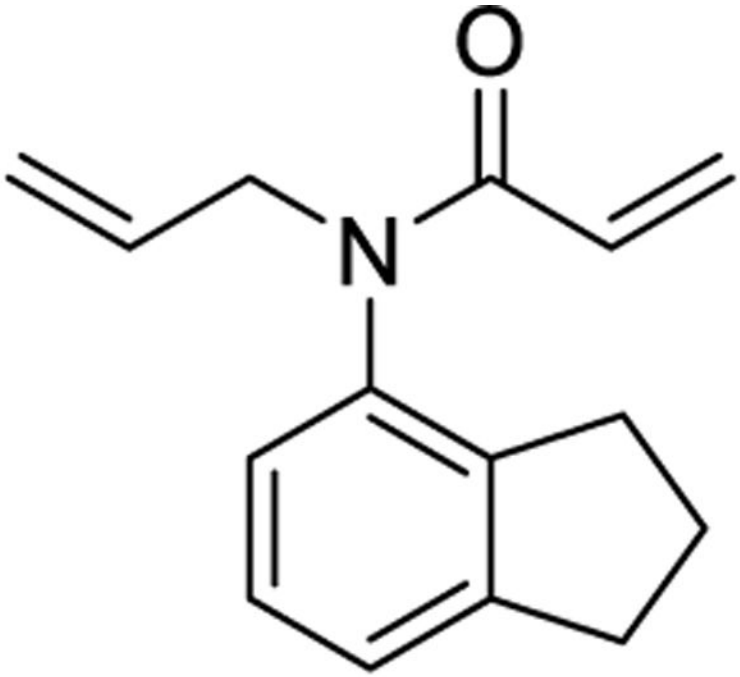

N-allyl-N-(2,3-dihydro-1H-inden-4-yl)acrylamide (IGA-1–12): A solution of sodium hydride (96 mg, 4.0 mmol) in tetrahydrofuran (8 mL) was put under nitrogen atmosphere. To the solution was added N-(2,3-dihydro-1H-inden-4-yl)acrylamide (187 mg, 1.0 mmol) in tetrahydrofuran (2 mL). The solution was cooled to 0°C and stirred. 3-bromoprop-1-ene (484 mg, 4.0 mmol) was added after 30 minutes, after which the solution was allowed to warm to room temperature and was stirred overnight. The solution was quenched with water and extracted with ethyl acetate. The crude product was purified via silica gel chromatography (20% ethyl acetate in hexanes) to afford the product in 67% yield as a yellow crystalline solid (151 mg).

^{1}H NMR (400MHz, $CDCl_3$). δ 7.06–7.18 (m, 2H), 6.80–6.88 (m, 1H), 6.26–6.37 (dd, *J* = 16.8, 2.0 Hz, 1H), 5.76–5.96 (m, 2H), 5.38–5.48 (dd, *J* = 10.3, 2.1 Hz, 1H), 4.98–5.08 (m, 2H), 4.40–4.52 (ddt, *J* = 14.5, 6.3, 1.3 Hz, 1H), 4.00–4.11 (ddt, *J* = 14.5, 6.8, 1.2 Hz, 1H), 2.822.98 (m, 2H), 2.59–2.79 (m, 2H), 1.92–2.07 (m, 2H).

^{13}C NMR (100MHz, CDCl$_3$). δ 165.1, 146.5, 142.4, 137.9, 133.0, 128.4, 127.8, 127.48, 126.1, 124.3, 118.1, 51.6, 33.3, 30.9, 25.0.

HRMS (+ESI). Calculated: 228.13 ($C_{15}H_{17}NO$). Observed: 228.1381.

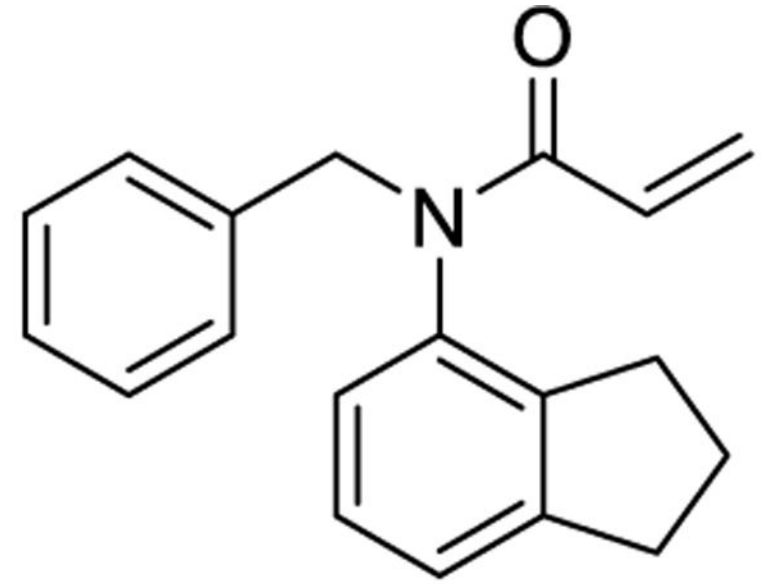

N-benzyl-N-(2,3-dihydro-1H-inden-4-yl)acrylamide (IGA-1–14): A solution of sodium hydride (96 mg, 4.0 mmol) in tetrahydrofuran (8 mL) was put under nitrogen atmosphere. To the solution was added N-(2,3-dihydro-1H-inden-4-yl)acrylamide (187 mg, 1.0 mmol) in tetrahydrofuran (2 mL). The solution was cooled to 0°C and stirred. Benzyl bromide (476 mg, 4.0 mmol) was added after 30 minutes, after which the solution was allowed to warm to room temperature and was stirred overnight. The solution was quenched with water and extracted with ethyl acetate. The crude product was purified via silica gel chromatography (20% ethyl acetate in hexanes) to afford the product in 63% yield as an orange oil (173 mg).

^{1}H NMR (400MHz, CDCI$_3$). δ 7.10–7.35 (m, 7H), 6.74–6.85 (dd, *J* = 7.8,1.1Hz, 1H), 6.40–6.55 (dd, *J* = 16.8, 2.1 Hz, 1H), 5.93–6.08 (dd, *J* = 16.8, 10.3 Hz, 1H), 5.49–5.62 (dd, *J* = 10.3, 2.1 Hz, 1H), 4.78–5.10 (m, 2H), 2.85–3.02 (m, 2H), 2.52–2.67 (m, 1H), 2.22–2.37 (m, 1H), 1.83–2.01 (m, 2H).

^{13}C NMR (100MHz, CDCIn). δ 146.4, 142.9, 137.7, 137.3, 129.3, 128.4, 128.3, 128.0, 127.5, 127.5, 126.0, 124.3, 52.3, 33.2, 30.6, 25.1.

HRMS (+ESI). Calculated: 278.15 ($C_{19}H_{19}NO$). Observed: 278.1538.

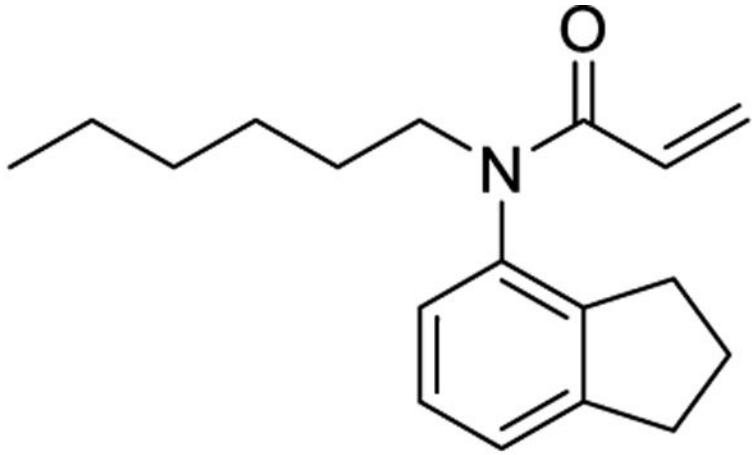

N-allyl-N-(2,3-dihydro-1H-inden-4-yl)acrylamide (IGA-1–15): A solution of sodium hydride (96 mg, 4.0 mmol) in tetrahydrofuran (8 mL) was put under nitrogen atmosphere. To the solution was added N-(2,3-dihydro-1H-inden-4-yl)acrylamide (187 mg, 1.0 mmol) in tetrahydrofuran (2 mL). The solution was cooled to 0°C and stirred. 1-bromohexane (660 mg, 4.0 mmol) was added after 30 minutes, after which the solution was allowed to warm to room temperature and was stirred overnight. The solution was quenched with water and extracted with ethyl acetate. The crude product was purified via silica gel chromatography (20% ethyl acetate in hexanes) to afford the product in 34% yield as a yellow oil (92 mg).

^{1}H NMR (400MHz, $CDCl_3$). δ 7.11–7.25 (m, 2H), 6.86–6.96 (dd, *J*=7.5, 1.2 Hz, 1H), 6.30–6.40 (dd, *J*=16.8, 2.1 Hz, 1H), 5.86–6.00 (m, 1H), 5.41–5.51 (dd, *J*= 10.3, 2.1 Hz, 1H), 3.82–3.96 (m, 1H), 3.42–3.56 (m, 1H), 2.90–3.04 (m, 2H), 2.65–2.85 (m, 2H), 1.98–2.16 (m, 2H), 1.47–1.63 (m, 2H), 1.20–1.36 (m, 6H), 0.80–0.90 (m, 3H).

^{13}C NMR (100MHz, $CDCl_3$). δ 165.16, 146.54, 142.38, 138.21, 128.59, 127.51, 127.35, 126.09, 124.13, 48.67, 33.26, 31.62, 30.85, 27.85, 26.72, 25.01, 22.59, 14.05.

HRMS (+ESI). Calculated: 272.19 ($C_{18}H_{25}NO$). Observed: 272.2007.

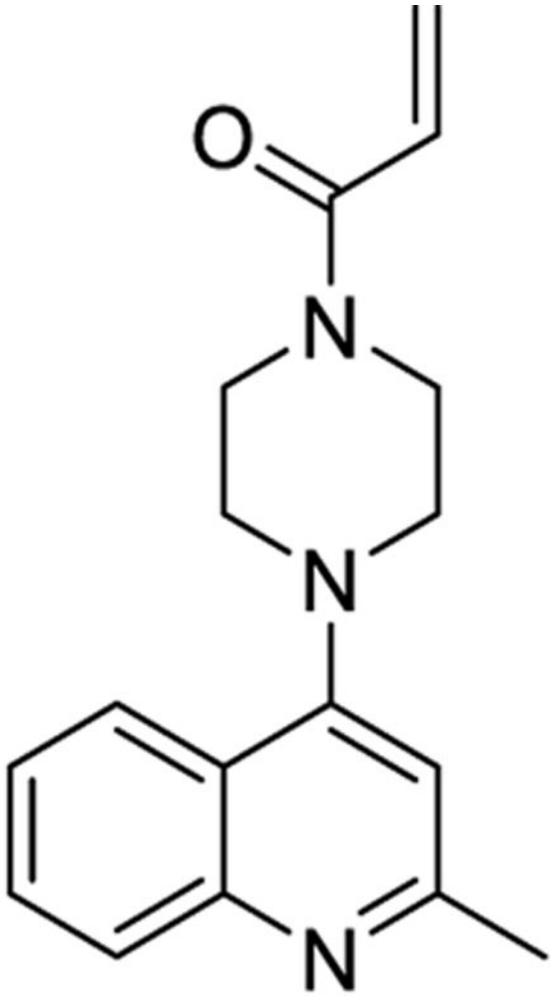

1-(4-(2-methylquinolin-4-yl)piperazin-1-yl)prop-2-en-1-one (IGA-1–26): A solution of 2-methyl-4-(piperazin-1-yl)quinolone (455 mg, 2.0 mmol) in DCM (20 mL) was cooled to 0°C. To the solution was added acryloyl chloride (217 mg, 2.4 mmol) followed by triethylamine (243 mg, 2.4 mmol). The solution was allowed to warm to room temperature and stirred overnight. The solution was washed with brine and the crude product was purified via basic alumina chromatography (100% ethyl acetate) to afford the product in 26% yield as a yellow oil (145 mg).

^{1}H NMR (400MHz, $CDCl_3$). δ 7.90–8.05 (m, 2H), 7.58–7.70 (ddd, *J* = 8.4, 6.8, 1.5 Hz, 1H), 7.40–7.50 (ddd, *J* = 8.2, 6.8, 1.3 Hz, 1H), 6.68–6.76 (s, 1H), 6.56–6.67 (dd, *J* = 16.8, 10.5 Hz, 1H), 6.30–6.40 (dd, *J* = 16.8, 2.0 Hz, 1H), 5.70–5.80 (dd, *J* = 10.5, 2.0 Hz, 1H), 3.70–4.06(d, *J* = 54.7 Hz, 4H), 3.10–3.30 (t, *J* = 5.0 Hz, 4H), 2.62–2.72 (s, 3H).

^{13}C NMR (100MHz, $CDCl_3$). δ 165.5, 159.4, 156.2, 149.2, 129.26, 129.24, 128.3,127.3, 124.9, 123.0, 121.6,109.8, 52.3, 51.9,45.8, 42.0 25.6.

HRMS (+ESI). Calculated: 282.17 ($C_{17}H_{19}N_3O$). Observed: 282.1597.

QUANTIFICATION AND STATISTICAL ANALYSIS

Unpaired Student's T-tests were used for statistical analyses. Where data were quantified, we report average ± standard error of mean (SEM). Significance is defined as *$p<0.05$ between described comparison groups. No data was excluded from analysis. More details of quantification and statistical analysis can be found in the figure legends.

DATA AND SOFTWARE AVAILABILITY

Datasets generated for isoTOP-ABPP data are provided in Table S1. Integrated Proteomics Pipeline (IP2) and PROLUCID was used for proteomic data analysis as described in Method Details. The IP2 platform can be obtained from: http://www.integratedproteomics.com.

Supplementary Material

Refer to Web version on PubMed Central for supplementary material.

ACKNOWLEDGMENTS

We thank the members of the Nomura Research Group for critical reading of the manuscript. This work was supported by the National Institutes of Health (NIH/NCI CA172667, NIH/NIEHS P42ES004705, R01ES028096, and R01GM116952), American Cancer Society Research Scholar award (RSG-14–242-01-TBE), the Novartis-Berkeley Center for Proteomics and Chemistry Technologies, and the Mark Foundation for Cancer Research ASPIRE award.

REFERENCES

Anderson KN, and Bejcek BE (2008). Parthenolide induces apoptosis in glioblastomaswithout affecting NF-kappaB. J. Pharmacol. Sci. 106, 318–320. [PubMed: 18277052]

Anderson KE, To M, Olzmann JA, and Nomura DK (2017). Chemoproteomics-enabled covalent ligand screening reveals a thioredoxin-caspase 3 interaction disruptor that impairs breast cancer pathogenicity. ACS Chem. Biol. 12, 2522–2528. [PubMed: 28892616]

Backus KM, Correia BE, Lum KM, Forli S, Horning BD, Gonzalez-Páez GE, Chatterjee S, Lanning BR, Teijaro JR, Olson AJ, et al. (2016). Proteome-wide covalent ligand discovery in native biological systems. Nature 534, 570–574. [PubMed: 27309814]

Banerjee R, Pace NJ, Brown DR, and Weerapana E (2013). 1,3,5-Triazine as a modular scaffold for covalent inhibitors with streamlined target identification. J. Am. Chem. Soc. 735, 2497–2500.

Bateman LA, Nguyen TB, Roberts AM, Miyamoto DK, Ku W-M, Huffman TR, Petri Y, Heslin MJ, Contreras CM, Skibola CF, et al. (2017). Chemoproteomics-enabled covalent ligand screen reveals a cysteine hotspot in reticulon 4 that impairs ER morphology and cancer pathogenicity. Chem. Commun. Camb. Engl. 53, 7234–7237.

Carlisi D, D'Anneo A, Angileri L, Lauricella M, Emanuele S, Santulli A, Vento R, and Tesoriere G (2011). Parthenolide sensitizes hepatocellular carcinoma cells to TRAIL by inducing the expression of death receptors through inhibition of STAT3 activation. J. Cell. Physiol. 226, 1632–1641. [PubMed: 21413021]

Carlisi D, Buttitta G, Di Fiore R, Scerri C, Drago-Ferrante R, Vento R, and Tesoriere G (2016). Parthenolide and DMAPT exert cytotoxic effects on breast cancer stem-like cells by inducing oxidative stress, mitochondrial dysfunction and necrosis. Cell Death Dis. 7, e2194. [PubMed: 27077810]

Coricello A, Adams JD, Lien E, Nguyen C, Perri F, Williams TJ, and Aiello F (2018). A walk in nature. sesquiterpene lactones as multi-target agents involved in inflammatory pathways. Curr. Med. Chem. 10.2174/0929867325666180719111123.

Curry EA, Murry DJ, Yoder C, Fife K, Armstrong V, Nakshatri H, O'Connell M, and Sweeney CJ (2004). Phase I dose escalation trial of feverfew with standardized doses of parthenolide in patients with cancer. Invest. New Drugs 22, 299–305. [PubMed: 15122077]

Dawson SJ, Provenzano E, and Caldas C (2009). Triple negative breast cancers: clinical and prognostic implications. Eur. J. Cancer 45 (Suppl 1), 27–40. [PubMed: 19775602]

Diamanti P, Cox CV, Moppett JP, and Blair A (2013). Parthenolide eliminates leukemia-initiating cell populations and improves survival in xenografts of childhood acute lymphoblastic leukemia. Blood 121, 1384–1393. [PubMed: 23264600]

Duan D, Zhang J, Yao J, Liu Y, and Fang J (2016). Targeting thioredoxin reductase by parthenolide contributes to inducing apoptosis of HeLa cells. J. Biol.Chem. 291, 10021–10031. [PubMed: 27002142]

Frame MC, Patel H, Serrels B, Lietha D, and Eck MJ (2010).The FERM domain: organizing the structure and function of FAK. Nat. Rev. Mol. Cell Biol. 11, 802–814. [PubMed: 20966971]

Ghantous A, Sinjab A, Herceg Z, and Darwiche N (2013). Parthenolide: from plant shoots to cancer roots. Drug Discov. Today 18, 894–905. [PubMed: 23688583]

Grossman EA, Ward CC, Spradlin JN, Bateman LA, Huffman TR, Miyamoto DK, Kleinman JI, and Nomura DK (2017). Covalent ligand discovery against druggable hotspots targeted by anti-cancer natural products. Cell Chem. Biol. 24, 1368–1376.e4. [PubMed: 28919038]

Hacker SM, Backus KM, Lazear MR, Forli S, Correia BE, and Cravatt BF (2017). Global profiling of lysine reactivity and ligandability in the human proteome. Nat. Chem. 9, 1181–1190. [PubMed: 29168484]

Helleday T, Petermann E, Lundin C, Hodgson B, and Sharma RA (2008). DNA repair pathways as targets for cancer therapy. Nat. Rev. Cancer 8, 193–204. [PubMed: 18256616]

Hu X, Xu S, and Maimone TJ (2017). A double allylation strategy for gramscale guaianolide production: total synthesis of (+)-mikanokryptin. Angew. Chem. Int. Ed. 56, 1624–1628.

Iwatani M, Iwata H, Okabe A, Skene RJ, Tomita N, Hayashi Y, Aramaki Y, Hosfield DJ, Hori A, Baba A, et al. (2013). Discovery and characterization of novel allosteric FAK inhibitors. Eur. J. Med. Chem. 61, 49–60. [PubMed: 22819505]

Jackson PA, Widen JC, Harki DA, and Brummond KM (2017). Covalent modifiers: a chemical perspective on the reactivity of α,β-unsaturated carbonyls with thiols via hetero-michael addition reactions. J. Med. Chem. 60, 839–885. [PubMed: 27996267]

Jafari N, Nazeri S, and Enferadi ST (2018). Parthenolide reduces metastasis by inhibition of vimentin expression and induces apoptosis by suppression elongation factor α−1 expression. Phytomedicine Int. J. Phytother. Phytopharm. 41, 67–73.

Jessani N, Humphrey M, McDonald WH, Niessen S, Masuda K, Gangadharan B, Yates JR, Mueller BM, and Cravatt BF (2004). Carcinoma and stromal enzyme activity profiles associated with breast tumor growth in vivo. Proc. Natl. Acad. Sci. U SA 101, 13756–13761.

Jeyamohan S, Moorthy RK, Kannan MK, and Arockiam AJV (2016). Parthenolide induces apoptosis and autophagy through the suppression of PI3K/Akt signaling pathway in cervical cancer. Biotechnol. Lett. 38, 1251–1260. [PubMed: 27099069]

Kim S-L, Trang KTT, Kim SH, Kim IH, Lee SO, Lee ST, Kim DG, and Kim S-W (2012). Parthenolide suppresses tumor growth in a xenograft model of colorectal cancer cells by inducing mitochondrial dysfunction and apoptosis. Int. J. Oncol. 41, 1547–1553. [PubMed: 22895542]

Kim SL, Park YR, Lee ST, and Kim S-W (2017). Parthenolide suppresses hypoxia-inducible factor-1 α signaling and hypoxia induced epithelial-mesenchymal transition in colorectal cancer. Int. J. Oncol. 51,1809–1820. [PubMed: 29075793]

Kwak SW, Park ES, and Lee CS (2014). Parthenolide induces apoptosis by activating the mitochondrial and death receptor pathways and inhibits FAK-mediated cell invasion. Mol. Cell. Biochem. 385, 133–144. [PubMed: 24065392]

Kwok BH, Koh B, Ndubuisi MI, Elofsson M, and Crews CM (2001). The anti-inflammatory natural product parthenolide from the medicinal herb Feverfew directly binds to and inhibits IkappaB kinase. Chem. Biol. 8, 759–766. [PubMed: 11514225]

Lesiak K, Koprowska K, Zalesna I, Nejc D, Duchler M, and Czyz M (2010). Parthenolide, a sesquiterpene lactone from the medical herb feverfew, shows anticancer activity against human melanoma cells in vitro. Melanoma Res. 20, 21–34. [PubMed: 19949351]

Lin M, Bi H, Yan Y, Huang W, Zhang G, Zhang G, Tang S, Liu Y, Zhang L, Ma J, et al. (2017). Parthenolide suppresses non-small cell lung cancer GLC-82 cells growth via B-Raf/MAPK/Erk pathway. Oncotarget 8, 23436–23447. [PubMed: 28423582]

Liu M, Xiao C, Sun M, Tan M, Hu L, and Yu Q (2018a). Parthenolide inhibits STAT3 signaling by covalently targeting Janus kinases. Molecules (Basel) 23, 10.3390/molecules23061478.

Liu W, Wang X, Sun J, Yang Y, Li W, and Song J (2017). Parthenolide suppresses pancreatic cell growth by autophagy-mediated apoptosis. Oncotargets Ther. 10, 453–61.

Liu Y-R, Cai Q-Y, Gao Y-G, Luan X, Guan Y-Y, Lu Q, Sun P, Zhao M, and Fang C (2018b). Alantolactone, a sesquiterpene lactone, inhibits breast cancer growth by antiangiogenic activity via blocking VEGFR2 signaling. Phytother. Res. 32, 643–650. [PubMed: 29210118]

Louie SM, Grossman EA, Crawford LA, Ding L, Camarda R, Huffman TR, Miyamoto DK, Goga A, Weerapana E, and Nomura DK (2016). GSTP1 is a driver of triple-negative breast cancer cell metabolism and pathogenicity. Cell Chem. Biol. 23, 567–578. [PubMed: 27185638]

Luo M, and Guan J-L (2010). Focal adhesion kinase: a prominent determinant in breast cancer initiation, progression and metastasis. Cancer Lett. 289, 127–139. [PubMed: 19643531]

Mathema VB, Koh Y-S, Thakuri BC, and Sillanpaa M (2012). Parthenolide, a sesquiterpene lactone, expresses multiple anti-cancer and anti-inflammatory activities. Inflammation 35, 560–565. [PubMed: 21603970]

Morel KL, Ormsby RJ, Bezak E, Sweeney CJ, and Sykes PJ (2017). Parthenolide selectively sensitizes prostate tumor tissue to radiotherapy while protecting healthy tissues in vivo. Radiat. Res. 187, 501–512. [PubMed: 28398879]

Quintana J, and Estevez F (2019). Recent advances on cytotoxic sesquiterpene lactones. Curr. Pharm. Des. 24, 4355–4361.

Ralstin MC, Gage EA, Yip-Schneider MT, Klein PJ, Wiebke EA, and Schmidt CM (2006). Parthenolide cooperates with NS398 to inhibit growth of human hepatocellular carcinoma cells through effects on apoptosis and G0-G1 cell cycle arrest. Mol. Cancer Res. 4, 387–399. [PubMed: 16778086]

Ren Y, Yu J, and Kinghorn AD (2016). Development of anticancer agents from plant-derived sesquiterpene lactones. Curr. Med. Chem. 23, 2397–2420. [PubMed: 27160533]

Roberts AM, Ward CC, and Nomura DK (2017a). Activity-based protein profiling for mapping and pharmacologically interrogating proteome-wide ligandable hotspots. Curr. Opin. Biotechnol. 43, 25–33. [PubMed: 27568596]

Roberts AM, Miyamoto DK, Huffman TR, Bateman LA, Ives AN, Akopian D, Heslin MJ, Contreras CM, Rape M, Skibola CF, et al. (2017b). Chemoproteomic screening of covalent ligands reveals UBA5 as a novel pancreatic cancer target. ACS Chem. Biol. 12, 899–904. [PubMed: 28186401]

Shin M, McGowan A, DiNatale GJ, Chiramanewong T, Cai T, and Connor RE (2017). Hsp72 is an intracellular target of the a,p-unsaturated sesquiterpene lactone, parthenolide. ACS Omega 2, 7267–7274. [PubMed: 30023543]

Silva Castro E, da Alves Antunes LA, Revoredo Lobo JF, Ratcliffe NA, Borges RM, Rocha L, Burth PF, and Fonte Amorim LM (2017). Antileukemic properties of sesquiterpene lactones: a systematic review. Anticancer Agents Med. Chem. 18, 323–334.

Spradlin JN, Hu X, Ward CC, Brittain SM, Ou L, Bussiere DE, Thomas JR, Tallarico JA, McKenna JM, Schirle M, et al. (2018). Harnessing the anti-cancer natural product nimbolide for targeted protein degradation. BioRxiv, 436998, https://doi.org/10.110¼36998.

Sulzmaier FJ, Jean C, and Schlaepfer DD (2014). FAK in cancer: mechanistic findings and clinical applications. Nat. Rev. Cancer 14, 598–610. [PubMed: 25098269]

Sun Y, St Clair DK, Fang F, Warren GW, Rangnekar VM, Crooks PA, and St Clair WH (2007). The radiosensitization effect of parthenolide in prostate cancer cells is mediated by nuclear factor-kappaB inhibition and enhanced by the presence of PTEN. Mol. Cancer Ther. 6, 2477–2486. [PubMed: 17876045]

Sweeney CJ, Mehrotra S, Sadaria MR, Kumar S, Shortle NH, Roman Y, Sheridan C, Campbell RA, Murry DJ, Badve S, et al. (2005). The sesquiterpene lactone parthenolide in combination with docetaxel reduces metastasis and improves survival in a xenograft model of breast cancer. Mol. Cancer Ther. 4, 1004–1012. [PubMed: 15956258]

Tabb DL, McDonald WH, and Yates JR (2002). DTASelect and Contrast: tools for assembling and comparing protein identifications from shotgun proteomics. J. Proteome Res. 1, 21–26. [PubMed: 12643522]

Tian C, Sun R, Liu K, Fu L, Liu X, Zhou W, Yang Y, and Yang J (2017). Multiplexed thiol reactivity profiling for target discovery of electrophilic natural products. Cell Chem. Biol. 24, 1416–1427.e5. [PubMed: 28988947]

Wang C, Weerapana E, Blewett MM, and Cravatt BF (2014). A chemoproteomic platform to quantitatively map targets of lipid-derived electrophiles. Nat. Methods 11, 79–85. [PubMed: 24292485]

Ward CC, Kleinman JI, Chung CYS, Kim K, Petri Y, Lee PS, Thomas JR, Tallarico JA, McKenna JM, Schirle M, et al. (2018). Covalent ligand screening uncovers a RNF4 E3 ligase recruiter for targeted protein degradation applications. BioRxiv, 439125, https://doi.org/10.110¼439125.

Weerapana E, Wang C, Simon GM, Richter F, Khare S, Dillon MBD, Bachovchin DA, Mowen K, Baker D, and Cravatt BF (2010). Quantitative reactivity profiling predicts functional cysteines in proteomes. Nature 468, 790–795. [PubMed: 21085121]

Xu T, Park SK, Venable JD, Wohlschlegel JA, Diedrich JK, Cociorva D, Lu B, Liao L, Hewel J, Han X, et al. (2015). ProLuCID: an improved SEQUEST-like algorithm with enhanced sensitivity and specificity. J. Proteomics 129, 16–24. [PubMed: 26171723]

Yen-Pon E, Li B, Acebron-Garcia-de-Eulate M, Tomkiewicz-Raulet C, Dawson J, Lietha D, Frame MC, Coumoul X, Garbay C, Etheve-Quelquejeu M, et al. (2018). Structure-based design, synthesis, and characterization of the first irreversible inhibitor of focal adhesion kinase. ACS Chem. Biol. 13, 2067–2073. [PubMed: 29897729]

Zhang X, Chen Q, Liu J, Fan C, Wei Q, Chen Z, and Mao X (2017). Parthenolide promotes differentiation of osteoblasts through the Wnt/β-catenin signaling pathway in inflammatory environments. J. Interferon Cytokine Res. 37, 406–414. [PubMed: 28829282]

Highlights

- Parthenolide covalently reacts with C427 of FAK1 to inhibit FAK1 activity
- Parthenolide impairs FAK1 signaling in breast cancer cells
- Other sesquiterpene lactone natural products also target FAK1

SIGNIFICANCE

Previous studies have shown that parthenolide and other sesquiterpene lactone natural products inhibit the FAK1 signaling pathway, but the mechanism through which parthenolide inhibited this pathway was poorly understood. In this study, we use chemoproteomic platforms to identify C427 within FAK1 as a functional site targeted by multiple sesquiterpene lactone natural products, including parthenolide, to impair FAK1-dependent signaling pathways and breast cancer cell proliferation, survival, and motility.

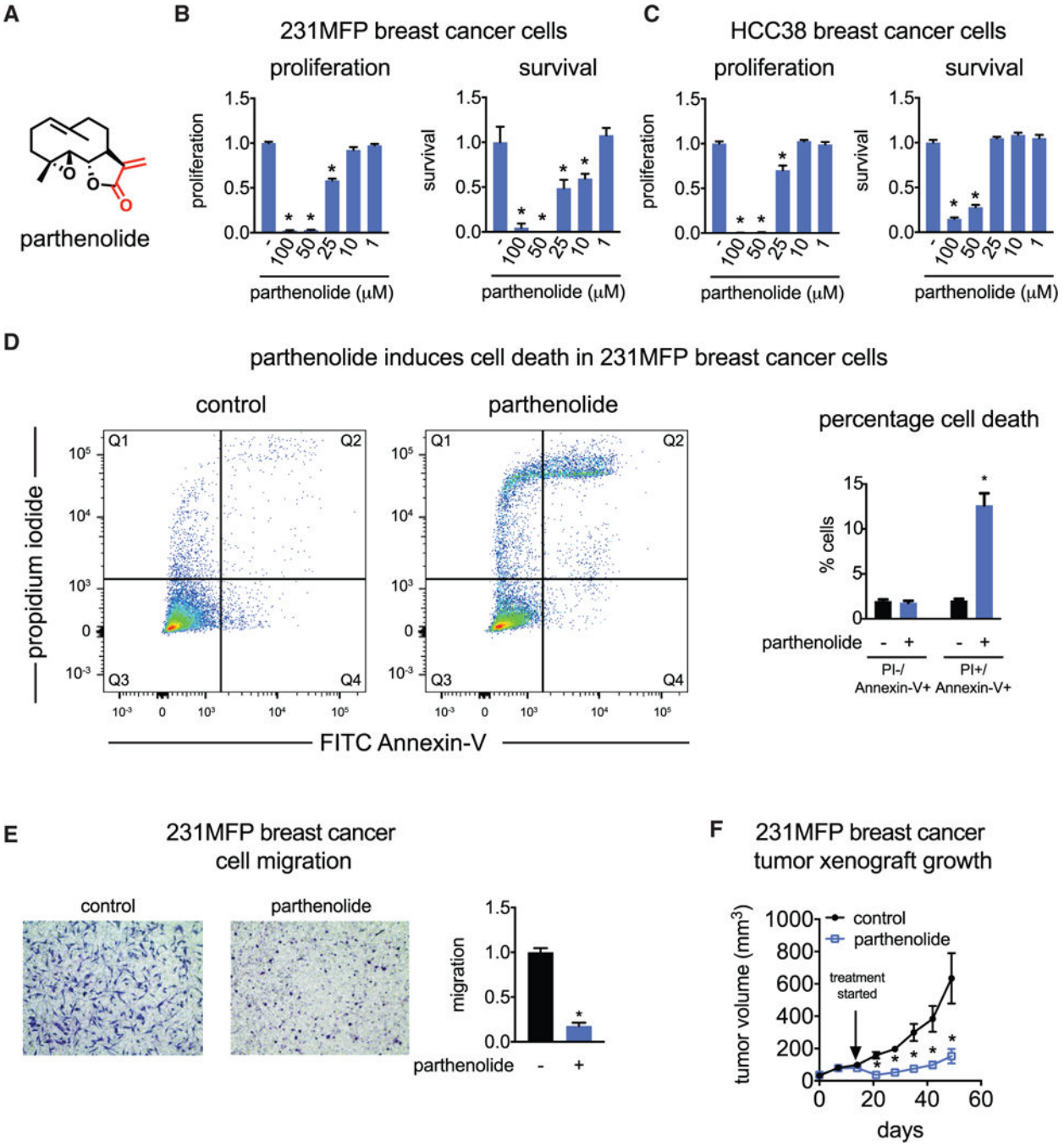

Figure 1. Parthenolide Impairs TNBC Pathogenicity

(A) Structure of parthenolide (red denotes cysteine-reactive enone).

(B and C) 231MFP (B) and HCC38 (C) breast cancer cell 48 h survival and proliferation from cells treated with DMSO control or parthenolide assessed by Hoechst stain.

(D) Percent early-stage and late-stage apoptotic cells assessed by flow cytometry after treating cells with DMSO control or parthenolide (50 mM)for2 h. Shown on the left panels are representative FACS data. On the right bar graph are percentage early apoptotic cells

defined as fluorescein isothiocyanate $(FITC)^+$/propidium iodide $(PI)^-$ and late apoptotic cells defined as $FITC^+/PI^+$.

(E) Migration of 231MFP cells treated with DMSO control or parthenolide (50 μM) for 6 h. Representative images of migrated cells are shown. (F) 231MFPtumorxenograft growth in immune-deficient SCID mice treated with vehicle (18:1:1 saline/ethanol/polyethylene glycol 40) or parthenolide (30 mg/kg intraperitoneally) daily once per day with treatment initiated after tumor establishment 14 days after tumor implantation.

Images shown in (E) are representative of n = 3 biological replicates/group. Data shown in (B) to (F) are average ± SEM, n = 3–6 biological replicates/group. Significance is expressed as $*p < 0.05$ compared with vehicle-treated controls. See also Figure S1.

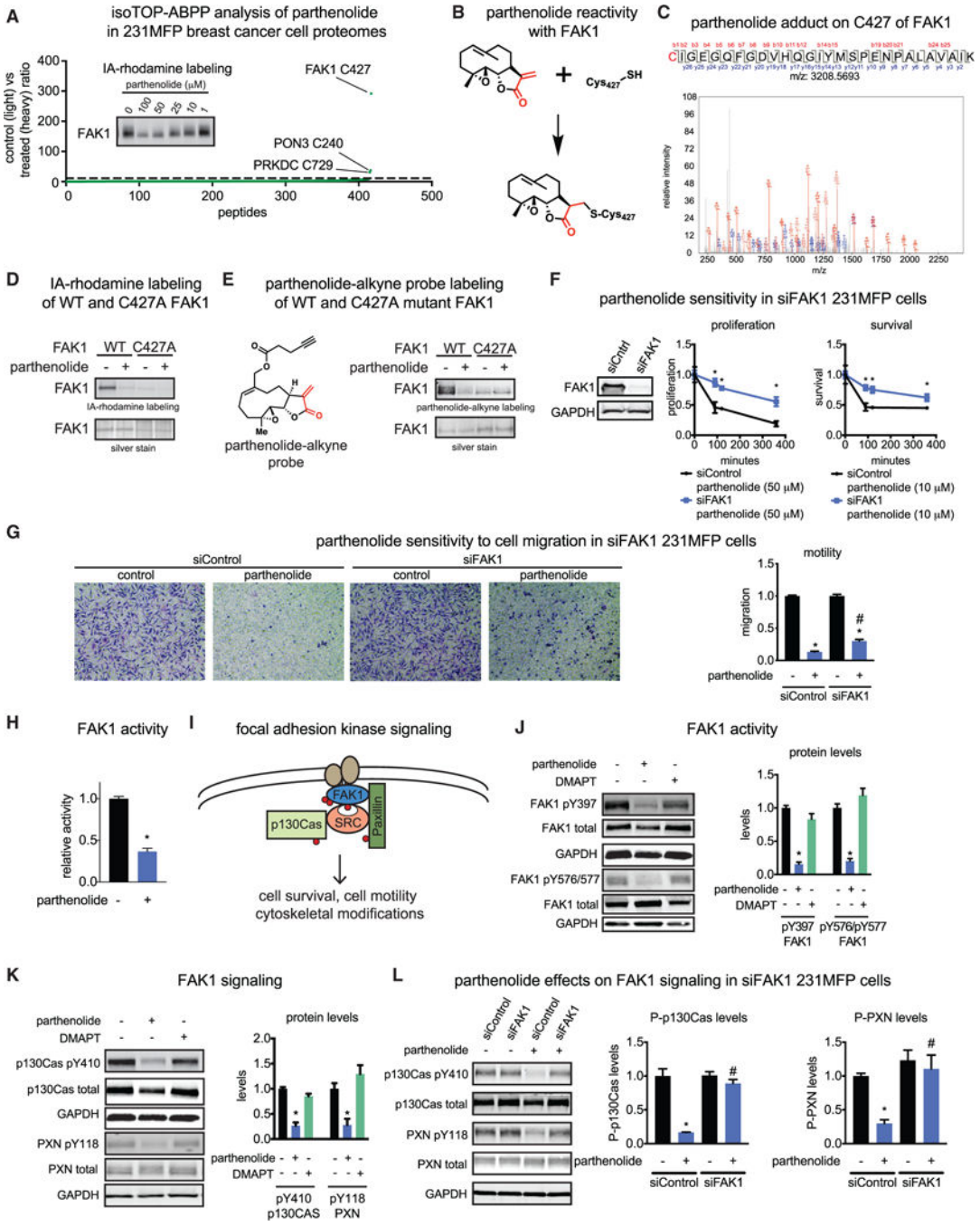

Figure 2. Parthenolide Targets an Allosteric Cysteine in FAK1 to Inhibit FAK1 Activity and Signaling

(A) iso TOP-ABPP analysis of parthenolide in 231MFPcell lysate. 231MFP proteomes were pre-treated with DMSO vehicle or parthenolide (50 μM) for 30 min prior to lA-alkyne (100 μM) labeling for 1 h. Shown are probe-modified peptides detected in at least two of out four biological replicates and the control (isotopically light) versus parthenolide-treated (isotopically heavy) ratios for each peptide. Those probe-modified peptides showing ratios >10are peptides that were observed in three out of four biological replicates. Shown in the

inset is gel-based ABPP analysis of parthenolide competition against lA-rhodamine labeling of pure human FAK1 kinase domain.

(B) Proposed reactivity of parthenolide with C427 of FAK1.

(C) Mass spectrometry data of covalent parthenolide adduct on C427 of human FAK1 protein. Pure human FAK1 kinase domain was labeled with parthenolide (100 μM) for 30 min and subsequently digested with trypsin for LC-MS/MS proteomic analysis.

(D) Gel-based ABPP analysis of recombinant human wild type and C427A mutant FAK1 kinase domain protein pre-incubated with parthenolide (50 μM) for 30 min prior to lA-rhodamine labeling (1 μM)for 1 h. Proteins were separated by SDS-PAGE and visualized by in-gel fluorescence. Also shown is silver staining of the gel as a loading control.

(E) Parthenolide-alkyne probe labeling of recombinant human wild type and C427A mutant FAK1 kinase domain protein pre-incubated with parthenolide (50 μM) for 30 min prior to parthenolide-alkyne labeling (50 μM)for 1 h. Rhodamine-azide was appended to probe-labeled protein by CuAAC, and proteins were separated by SDS-PAGE and visualized by in-gel fluorescence. Also shown is silver staining of the gel as a loading control.

(F) FAK1 knockdown in 231MFP cells using siControl or siFAK1 oligonucleotides confirmed by western blotting. Serum-containing cell proliferation and serum-free cell survival in siControl or siFAK1 231MFP cells treated with parthenolide (10 μM) for the reported time period.

(G) Cell migration in siControl or siFAK1 231MFP cells treated with parthenolide (10 μM) for 4 h.

(H) FAK1 activity with pure human FAK1 protein pre-treated with vehicle DMSO or parthenolide (100 μM)for30 min before addition of peptide substrate and ATP. Activity was assessed by substrate peptide phosphorylation reading out ADP release using an ADP-Glo kinase assay.

(I) FAK1 signaling pathways.

(J and K) FAK1 signaling assessed by western blotting in 231MFP cells treated with vehicle DMSO or parthenolide (50 μM) for 2 h.

(L) FAK1 signaling assessed by western blotting in siControl and siFAK1 cells treated with vehicle DMSO or parthenolide (50 μM) for 2 h.

Gels shown in (A), (D), (E), (F), (J), (K), and (L) are representative images from n = 3 biological replicates/group. Data shown in (F), (G), (H), (J), (K), and (L) are average ± SEM, n = 3–6 biological replicates/group. Significance is expressed as *$p < 0.05$ compared with vehicle-treated controls, #$p < 0.05$ comparing parthenolide-treated siFAK1 cells with parthenolide-treated siControl cells.

See also Tables S1 and S2; Figures S2 and S3.

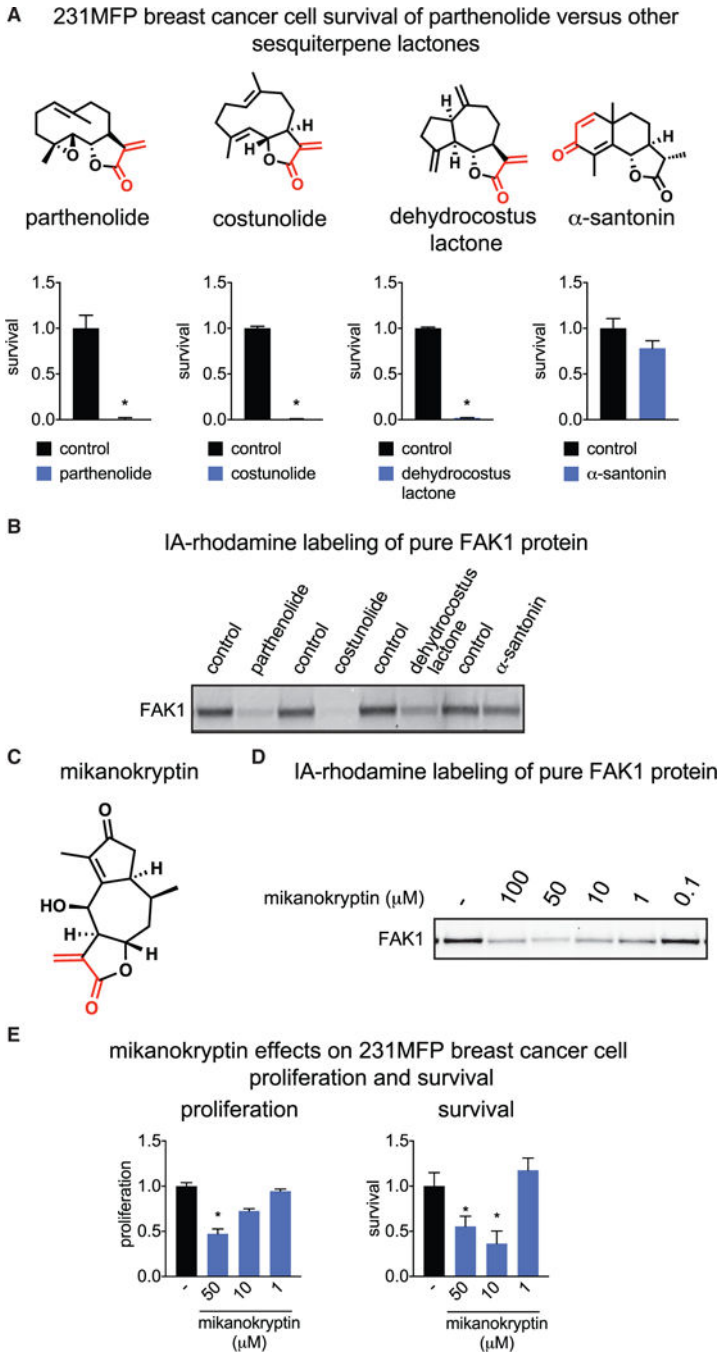

Figure 3. Other Sesquiterpene Lactones Also Interact with FAK1 and Impair TNBC Cell Viability

(A) 231MFP cell survival (48 h) after treatment with DMSO vehicle or parthenolide, and other sesquiterpene lactones (50 μM) assessed by Hoechst stain.

(B) Gel-based ABPP analysis of parthenolide and other sesquiterpene lactones. Pure human FAK1 kinase domain was pre-treated with DMSO vehicle or natural products (50 μM) for 30 min prior to IA-rhodamine labeling (1 μM) for 1 h and then analyzed by in-gel fluorescence.

(C) Structure of mikanokryptin. Cysteine-reactive enone is highlighted in red.

(D) Gel-based ABPP analysis of mikanokryptin analyzed as described in (B).

(E) 231MFP breast cancer cell proliferation and survival (48 h) after treatment of cells with DMSO vehicle or mikanokryptin.

Gels shown in (B) and (D) are representative of n = 3. Data shown in (A) and (E) are average ± SEM, n = 6 biological replicates/group. Significance is expressed as *$p < 0.05$ compared with vehicle-treated controls.

KEY RESOURCES TABLE

REAGENT or RESOURCE	SOURCE	IDENTIFIER
Antibodies		
Akt (pan) Mouse mAb	CST	2920
GAPDH (D16H11) XP ® Rabbit mAb	CST	5174
IRDye 800CW Goat anti-Mouse IgG (H + L), 0.5mg	LICOR	926–32210
IRDye 800CW Goat anti-Rabbit IgG (H + L), 0.5mg	LICOR	926–32211
NF-kappaB p65 XP Rabbit mAb	CST	8242
P-Akt (T308) Rabbit Ab	CST	9275
P-FAK (Y397) Rabbit Ab	CST	3283
P-FAK (Y576/577) Rabbit Ab	CST	3281
P-NF-kappaB p65 (S536) Rabbit mAb	CST	3033
P-p130 Cas (Y410) Rabbit Ab	CST	4011
P-Paxillin (Y118) Rabbit Ab	CST	2541
p130 Cas Rabbit mAb	CST	13846
Paxillin Rabbit mAb	CST	12065
Chemicals, Peptides, and Recombinant Proteins		
2-iodoacetamid	Millipore Sigma	8047440100
a-santonin	Millipore Sigma	S1250
AcTEV protease	Invitrogen	12575015
Aqua 5uM C18 125A	Phenomenex	04A-4299
Biotin-TEV-azide	(Weerapana et al., 2010)	
calyculin A	Millipore Sigma	208851
Copper (II) sulfate	Millipore Sigma	209198
Costunolide	Millipore Sigma	SML0417
dehydrocostus lactone	Millipore Sigma	42575
DharmaFECT 1 Transfection Reagent	GE	T-2001
Dimethylaminoparthenolide	Cayman chemical	20436
Dithiothreitol	Millipore Sigma	D9779
Formic acid	Millipore Sigma	695076
Hoechst 33342 dye	Invitrogen	H3570
Iodoacetamide −13C2, 2d2	Millipore Sigma	721328
Luna 5um SCX 100A	Phenomenex	04A-4398
Mikanokryptin	(Hu etal., 2017)	
N-Hex-5-ynyl-2-iodo-acetamide (IAyne)	Chess Organics	3187
Parthenolide	Cayman chemical	70080
Pierce Protease Inhibitor Mini Tablets, EDTA-Free	Thermo	A32599
ProteaseMAX Surfactant, Trypsin Enhancer	Promega	V2072
Sequencing grade trypsin (porcine)	Promega	V5111
Tetramethylrhodamine-5-Iodoacetamide Dihydroiodide (5-TMRIA)	Thermo	T6006

REAGENT or RESOURCE	SOURCE	IDENTIFIER
tris(2-carboxyethyl) phosphine	Strem Chemicals	15–7400
tris[(1-benzyl-1H-1,2,3-triazol-4-yl)methyl]amine	Millipore Sigma	678937
Urea	Fisher	U15
Sequencing grade trypsin (porcine)	Promega	V5111
Critical Commercial Assays		
ADP-Glo Kinase Assay	Promega	V6930
CellEvent Caspase-3/7 Green Flow Cytometry Assay Kit	Thermo	C10427
Diff-Quik	Dade Behring	b4132–1A
FAK Kinase Enzyme System	Promega	V1971
FITC Annexin V Apoptosis Detection Kit I	BD Biosciences	556547
Gibson Assembly Cloning Kit	New England Biosciences	E5510S
Q5 site-directed mutagenesis kit	New England Biosciences	E0554s
Experimental Models: Cell Lines		
231MFP	(Jessani et al., 2004)	
HCC38	ATCC	CRL-2314
HEK293T/17	ATCC	CRL-11268
Experimental Models: Organisms/Strains		
C.B17 SCID	Taconic	CB17SC-F
Oligonucleotides		
FAK1 SMARTPOOL siRNA	GE	L-003164–00
ON-TARGETplus Non-targeting Pool	GE	D-001810–10-05
CTGCCGCCGCGATCGCCatggaaacagatgattatgctgagatt ataga	ElimBio	N/A
TCGAGCGGCCGCGTACGCGTtcttctggactccatcctcatgcg ctcttcttgct	ElimBio	N/A
ACGCGTACGCGGCCG	ElimBio	N/A
GGCGATCGCGGCGG	ElimBio	N/A
ACTTGGACGAGCTATTGGAGAAGGC	ElimBio	N/A
TCTATTCTTTCTCTTT GAATCTC	ElimBio	N/A
Recombinant DNA		
FAK1 Expression Vector for sequence NM 005607.4	VectorBuilder	N/A
pCMV6-entry	Origene	PS100001
Software and Algorithms		
DTASelect	(Tabb et al., 2002)	N/A
FlowJo	FlowJo LLC	N/A
ImageJ	NIH	N/A
IP2 proteomics pipeline	Integrated Proteomics Applications	N/A
Raw Extractor	Scripps Research Institute	N/A

REAGENT or RESOURCE	SOURCE	IDENTIFIER
Other		
Amicon centrifugal filtration device	Amicon	UFC501008
Anti-DYKDDDDK G1 affinity resin	genescript	100432
MicroTee PEEK 360 mm fitting	Thermo	#p-888
Midi-PROTEAN TGX SDS/PAGE gel	BioRad	5671094
Streptavadin agarose beads	Thermo	20349
Transwell chambers	Costar	3422